

Identification of novel polysialic acid interacting partners and functional relevance of their interaction for peripheral nerve regeneration after injury in *Mus musculus* (Linnaeus, 1758).

Dissertation

Zur Erlangung des Grades eines Doktors der
Naturwissenschaften

- Dr. rer. Nat. -

des Department Biologie der Fakultät für Mathematik, Informatik
und Naturwissenschaften an der Universität Hamburg vorgelegt

von Bibhudatta Mishra
aus Bhawanipatna, Indien

Februar 2010

Hamburg, Februar 2010

Diese Arbeit wurde am im Institut für Biosynthese Neuraler Strukturen des
Zentrums für Molekulare Neurobiologie Hamburg angefertigt.

Gutachter: Prof. Dr. Melitta Schachner
Prof. Dr. Lothar Renwrantz

Genehmigt vom Department Biologie
der Fakultät für Mathematik, Informatik und Naturwissenschaften
an der Universität Hamburg
auf Antrag von Frau Professor Dr. M. SCHACHNER
Weiterer Gutachter der Dissertation:
Professor Dr. L. RENWRANTZ
Tag der Disputation: 22. Januar 2010

Hamburg, den 08. Januar 2010



Professor Dr. Jörg Ganzhorn
Leiter des Departments Biologie



University of Connecticut Health Center
School of Medicine

Department of Neuroscience

October 21, 2009

As a native English speaker I hereby confirm that the PhD thesis of Bibhudatta Mishra, titled "Identification of novel polysialic acid interacting partners and functional relevance of their interaction for peripheral nerve regeneration after injury in *Mus musculus* (Linnaeus, 1758)" is written in good English grammar and comprehensible style.

Sincerely,

Nicole Mayer

An Equal Opportunity Employer

63 Farmington Avenue
Farmington, Connecticut 06030-3401

Telephone: (860) 679-8787

Facsimile: (860) 679-8766

Web: <http://neuroscience.uchc.edu/>

*This project was supervised and guided by
Drs. Gabriele Loers and Ralf Kleene
at the Centre for Molecular Neurobiology (ZMNH), Hamburg.*

I. SUMMARY.....	7
II. INTRODUCTION.....	11
<i>II.1. Neural cell adhesion molecule.....</i>	<i>11</i>
II.1.1. Polysialylation of NCAM.....	14
II.1.2. Developmental Regulation of NCAM polysialylation.....	16
<i>II.2. Polysialic acid.....</i>	<i>17</i>
II.2.1. Structure of PSA.....	18
II.2.2. Phylogeny of PSA.....	20
II.2.3. Biosynthesis of PSA.....	21
<i>II.3. PSA functions.....</i>	<i>24</i>
II.3.1. PSA as a biophysical regulator of cell interactions.....	24
II.3.2. PSA serves as a permissive regulator in axon path finding and targeting..	26
II.3.3. PSA in cell migration.....	27
II.3.4. PSA in synaptic plasticity.....	28
<i>II.4. Anti-idiotypic approach to screen novel PSA binding partners</i>	<i>28</i>
II.4.1. Histone H1	30
II.4.2. Myristoylated alanine-rich C kinase substrate	32
III. RATIONALE AND AIMS OF THE STUDY	35
IV. MATERIALS AND METHODS	37
<i>IV.1. Materials.....</i>	<i>37</i>
IV.1.1. List of chemicals, commercial reagents and kits used.....	37
IV.1.2. Molecular weight standards.....	45
IV.1.2.A.Precision Plus Protein standard.....	45

IV.1.2.B.BenchMark™ Prestained Protein Ladder.....	45
IV.1.2.C.Ready-Load™ 1Kb Plus DNA Ladder	46
IV.1.3. List of buffers and solutions.....	47
IV.1.4. Primary antibodies.....	54
IV.1.5. Secondary antibodies.....	56
IV.1.6. Bacterial / Mammalian cell culture medium	56
IV.1.7. Bacterial strains.....	59
IV.1.8. Plasmids.....	60
IV.1.9. Mouse strains.....	60
IV.2. Methods.....	61
IV.2.1. Molecular biology.....	61
2.1.1. Maintenance of bacterial strains.....	61
2.1.2. Production of competent bacteria.....	61
2.1.3. Transformation of bacteria.....	62
2.1.4. Plasmid isolation.....	62
2.1.5. Enzymatic modification of DNA.....	62
2.1.5a. Restriction digestion of DNA.....	62
2.1.5b. De-phosphorylation of plasmid DNA.....	63
2.1.5c. Ligation of DNA fragments.....	63
2.1.5d. Polymerase chain reaction.....	64
2.1.6. DNA gel electrophoresis.....	65
2.1.7. Extraction of DNA fragments from agarose gels.....	65
2.1.8. Purification of DNA fragments after PCR.....	66
2.1.9. Determination of DNA concentration.....	66
2.1.10. Sequencing of DNA.....	66
IV.2.2. Protein biochemistry and conjugation procedures.....	67
2.2.1. Protein quantification by Bicinchoninic Acid (BCA) assay method.....	67

2.2.2. SDS-PAGE.....	67
2.2.3. Coomassie staining of polyacrylamide gels.....	68
2.2.4. Silver staining of polyacrylamide gels.....	68
2.2.5. Electrophoretic transfer of proteins.....	68
2.2.6. Immunochemical detection of electrophoretically transferred proteins.....	69
2.2.7. Enhanced chemiluminescence system.....	70
2.2.8. Stripping and re-probing of Western blots.....	70
2.2.9. Drying of polyacrylamide gels.....	70
IV.2.3. Expression of recombinant proteins in <i>Escherichia coli</i>	71
2.3.1. Lysis of bacteria using the French press.....	71
2.3.2. Protein purification.....	71
2.3.3. Brain homogenization.....	72
IV.2.4. Protein interaction detection methods.....	72
2.4.1. Enzyme-linked immunosorbent assay (ELISA).....	72
2.4.2. Co-immunoprecipitation.....	73
IV.2.5. Cell culture of primary neurons.....	74
2.5.1. Preparation and cultivation of dissociated cerebellar granule cells.....	74
2.5.2. Neuritogenesis of cerebellar granule cells.....	74
2.5.3. Cell surface biotinylation on cerebellar granule cells.....	76
2.5.4. Preparation and cultivation of dissociated hippocampal neurons.....	76
2.5.5. Schwann cell culture and analysis of process elongation.....	77
2.5.6. Schwann cell proliferation	79
2.5.7. Preparation and passage of neural stem cells	80
2.5.8. Neurosphere migration assay	80

IV.2.6. Immunocytochemistry.....	81
2.6.1. Immunocytochemistry of living cells.....	81
2.6.2. Immunocytochemistry of fixed cells	82
2.6.3. Immunocytochemistry of neurospheres	83
2.6.4. Confocal laser-scanning microscopy	83
IV.2.7. Femoral nerve injury and morphology.....	84
2.7.1. Animals.....	84
2.7.2. Femoral nerve injury and Histone H1 application.....	84
2.7.3. Analysis of motor function	86
2.7.4. Retrograde labelling and evaluation of motoneuron number and soma size.....	87
2.7.5. Analysis of degree of myelination	88
V. RESULTS.....	89
V.1. Histone H1 is a potential binding partner of PSA.....	89
V.2. Histone H1 is present at the surface of cultured cerebellar neurons.....	91
V.3. Histone H1 alters PSA induced neurite outgrowth of cerebellar neurons	93
V.4. Histone H1 and PSA influence process formation and proliferation of Schwann cells <i>in vitro</i>	94
V.5. Histone H1 and PSA alter migration of neural precursor cells <i>in vitro</i>	98
V.6. Histone H1 promotes functional recovery after femoral nerve injury in adult mice	100
V.7. Histone H1 promotes survival, regrowth and reinnervation of motoneurons	104
V.8. Cloning, expression and purification of MARCKS	106

V.9. Characterization of binding of MARCKS and PSA	107
V.10. Co-immunoprecipitation of MARCKS and PSA from brain homogenate	108
V.11. Confirmation intracellular localization of MARCKS and colocalization of MARCKS and PSA using imunocytochemistry of live and fixed hippocampal neurons.....	109
V.12. MARCKS and PSA alter neurosphere migration <i>in vitro</i>	111
VI. DISCUSSION.....	114
VI.1. Histone H1 is a novel binding partner of PSA	114
VI.2. Improvement of motor function by Histone H1.....	117
VI.3. Identification of MARCKS as a possible binding partner of PSA... ..	120
VI.4. Proposed working model indicating possible interaction between MARCKS and PSA	121
VII. REFERENCES.....	123
VIII. APPENDIX.....	143
1. Oligonucleotides.....	143
2. Abbreviations.....	143
IX. PUBLICATIONS.....	149
X. ACKNOWLEDGEMENTS.....	150

I. Summary

Traumatic peripheral nerve injuries are still underestimated and there is a major requirement for new therapies improving functional recovery after injury and to support microsurgery. In rodents, polysialylated NCAM (PSA-NCAM) was reported to be up-regulated in peripheral motor axons and Schwann cells after lesion. Based on this, it is hypothesized that polysialic acid (PSA) promotes preferential motor reinnervation (selective targeting) by enhancement of synapse formation. This makes PSA an interesting molecule for drug development and to support nerve repair. To make the positive effects of the PSA carbohydrate available for therapy of peripheral nerve injuries, potential binding partners of this carbohydrate have to be identified, since the carbohydrate itself is not useful for therapeutic approaches.

PSA has been shown to interact with extracellular molecules like heparan sulphate proteoglycans, the neurotrophic factor BDNF and the hormone estradiol. Histone H1 and myristoylated alanine-rich C kinase substrate (MARCKS) have been identified as potential binding partners of PSA using a PSA mimicking single chain variable fragment (scFv) antibody which is an anti-idiotypic antibody against a PSA antibody. Co-localization studies on live and fixed neuronal cells demonstrated that Histone H1 and MARCKS are co-expressed with PSA, although only a direct binding between PSA and Histone H1, but not between PSA and MARCKS using ELISA could be shown. Moreover, surface biotinylation of cerebellar granule cells confirmed the extracellular localization of Histone H1. Live staining of cerebellar neurons and Schwann cells confirmed that an extracellular pool of Histone H1 co-localizes with PSA in the extracellular matrix or on the cell surface. Staining of fixed hippocampal neurons showed that both MARCKS and PSA partially co-localize at the cell membrane. Furthermore, extracellular Histone H1 strongly stimulated process formation and proliferation of Schwann cells, neuritogenesis of cerebellar neurons and migration of neural stem cells from neurospheres via a PSA

dependent mechanism *in vitro*. These results indicate that Histone H1 is present in the extracellular matrix of neuronal cells, where it not only interacts with PSA but also regulates neurite outgrowth, cell migration and proliferation which are crucial during nervous system development.

To evaluate the function of Histone H1 during regeneration of the nervous system, *in vivo* femoral nerve lesion experiments were performed in adult mice. Application of Histone H1 improved the functional recovery, axon regrowth and the precision of reinnervation after femoral nerve injury, indicating that Histone H1 plays a functional role during regeneration in the peripheral nervous system in mice.

These results indicate that Histone H1 is present in the extracellular matrix of neural cells, where it interacts specifically with PSA and regulates neural cell migration and proliferation as well as neurite outgrowth; pointing out that the interaction between Histone H1 and PSA plays an important role during development and in regeneration of the nervous system.

Nach traumatischer Verletzung peripherer Nerven entstehende Funktionseinbußen werden bis heute unterschätzt und die Entwicklung neuer Therapien zur Verbesserung der Regeneration und zur Unterstützung der Mikrochirurgie ist dringend notwendig. In Nagetieren konnte gezeigt werden, dass polysialyliertes NCAM nach einer Läsion in Axonen peripherer Motoneurone und in Schwann'schen Zellen heraufreguliert wird. Basierend auf diesem Befund wird angenommen, dass Polysialinsäure (PSA) durch Erhöhung der Synapsenbildung eine verbesserte präferentielle Re-Innervierung (selektive „Zielerkennung“) von Motoneuronen stimuliert.

PSA ist deshalb ein interessanter Kandidat für die Medikamentenentwicklung und zum Einsatz zur Unterstützung der Reparatur von verletzten Nerven. Um die positiven Effekte des PSA Kohlenhydrats für die Therapien von peripheren Nervenverletzungen nutzbar zu machen, müssen die Bindungspartner dieses Kohlenhydrats identifiziert werden, da das Kohlenhydrat selbst nicht für therapeutische Anwendungen eingesetzt werden kann.

Es wurde gezeigt, dass PSA mit Molekülen der extrazellulären Matrix, wie Heparan-Sulfat-Proteoglykanen, dem neurotrophischen Faktor BDNF und dem Hormon Estradiol, interagiert. Es konnten unter Verwendung eines PSA mimikrierenden „single chain variable fragment“ (scFv) Antikörpers, der einen anti-idiotypischen Antikörper gegen einen PSA-Antikörper darstellt, Histon H1 und das myristoylierte Alanin-reiche C-Kinase Substrat (MARCKS) als neue potentielle PSA-Interaktionspartner identifiziert werden. Die Untersuchung der Lokalisation dieser Moleküle in lebenden und fixierten Zellen zeigte, dass Histon H1 und MARCKS mit PSA ko-lokalisiert vorliegen. Mittels ELISA konnte zudem eine direkte Interaktion zwischen PSA und Histon H1, aber nicht zwischen PSA und MARCKS nachgewiesen werden. Durch Oberflächenbiotinylierung von Körnerzellen aus dem Cerebellum konnte zudem nachgewiesen werden, dass Histon H1 auch extrazellulär lokalisiert vorkommt. Mit Hilfe von Immunfärbungen von Körnerzellen und von Schwann'schen Zellen ließ sich zeigen, dass

extrazelluläres Histon H1 mit PSA im Extrazellulärraum oder auf der Zelloberfläche ko-lokalisiert. Immunfärbung hippokampaler Neurone zeigte weiterhin, dass sowohl MARCKS als auch PSA teilweise auf der Zellmembran ko-lokalisiert vorliegen. Darüber hinaus konnte ich zeigen, dass extrazelluläres Histon H1 die Bildung von Fortsätzen und die Proliferation von Schwann'schen Zellen, die Neuritogenese bei Körnerzellen und die Migration neuronaler Stammzellen *in vitro* stark fördert, und dass diese Prozesse PSA abhängig sind. Diese Resultate zeigen, dass Histon H1 in der extrazellulären Matrix neuronaler Zellen vorliegt, wo es mit PSA interagiert und für die Entwicklung des Nervensystems wichtige Prozesse wie Neuritenwachstum, Zellmigration und Proliferation reguliert.

Um die Funktion von Histon H1 während der Regeneration des Nervensystems zu untersuchen, wurde der Femoralis Nerv in adulten Mäusen läsiert, und die Regeneration *in vivo* untersucht. Applikation von Histon H1 verbesserte die funktionelle Regeneration, das Wiederauswachsen von Axonen und die Präzision bei der Reinnervation nach Verletzung des Femoralis Nervs. Diese Ergebnisse zeigen, dass Histon H1 eine wichtige Rolle bei der Regeneration im peripheren Nervensystem der Maus spielt.

In meiner Arbeit konnte ich zeigen, dass Histon H1 in der extrazellulären Matrix von neuronalen Zellen vorkommt und dort spezifisch mit PSA interagiert um Migration neuronaler Zellen, Proliferation und Auswachsen von Neuronen zu induzieren. Diese Daten zeigen, dass der Interaktion zwischen Histon H1 und PSA während der Entwicklung und der Regeneration des Nervensystems nach Verletzung eine wichtige Funktion zukommt.

II. Introduction

II.1 Neural cell adhesion molecule

The neural cell adhesion molecule (NCAM) was identified as a cell surface glycoprotein more than 30 years ago (Rutishauser et al., 1976). Early studies demonstrated that NCAM interacts with other NCAM molecules in the same (cis-interactions) or in opposing cell membranes (trans-interactions) (Rutishauser et al., 1982) and thereby identifying NCAM as a key mediator of cell adhesion in the central nervous system (CNS). NCAM is produced by a single gene that contains 20 major exons plus 6 additional small exons in the mouse (Walmod et al., 2004). There are at least 27 alternatively spliced NCAM mRNAs produced giving a wide diversity of NCAM isoforms, named according to their apparent molecular weight (**Figure 1**). NCAM-180 is a single pass transmembrane protein generated from exons 0–19; NCAM-140 differs from NCAM-180 only in exon 18 and it is also a transmembrane protein which cytoplasmic domain is considerably shorter; NCAM-120 is a GPI anchored protein resulting from the transcription of exons 0–15. NCAM also exists in a secreted form produced when one of the small exons located between exons 12 and 13 is included in the mRNA. This small exon contains a stop codon and gives rise to a truncated form of NCAM (Walmod et al., 2004). Soluble forms of NCAM can also be generated by the enzymatic excision of NCAM-120 from the GPI anchor (He et al., 1986) or by the proteolytic cleavage of the extracellular part of the NCAM molecule (Hinkle et al., 2006; Kalus et al., 2006).

The presence of extracellular immunoglobulin (Ig) domains defines NCAM as a member of the immunoglobulin superfamily of cell adhesion molecules (for general reviews on cell adhesion molecules and their classification, refer to Chothia and

Jones, 1997; Elangbam et al., 1997). Although NCAM was initially characterized as a cell adhesion molecule, its role in cell signaling pathways classifies it more accurately as a signal transducing receptor molecule. NCAM is also expressed in non-neuronal cells like glial cells and myofibrils (Rieger et al., 1985). NCAM is a highly conserved molecule throughout the evolution of vertebrates (Hall and Rutishauser, 1985). In invertebrates, Fasciculin II is considered as the drosophila homologue and SAX-3 (Sensory Axon guidance family member protein) is the nematode homologue of NCAM (Mendoza and Faye, 1999).

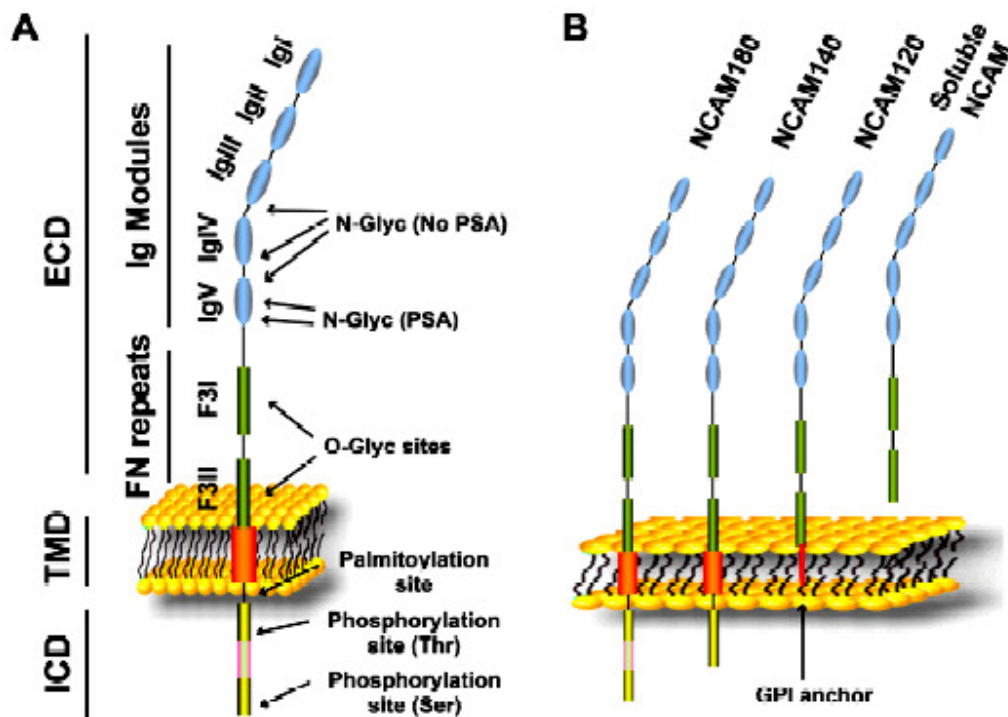


Figure 1. Schematic representation of NCAM and its main isoforms (Gascon et al., 2007).

(A) The highly conserved extracellular domain (ECD) mediates cell adhesion while the intracellular region (ICD) interacts with several proteins. The different post-translational modification sites including glycosylation, palmitoylation and phosphorylation are indicated.

(B) NCAM 140 and NCAM 180 differ in 261 amino acids in the ICD. NCAM 120 contains the extracellular domain linked to the membrane through a GPI anchor. Soluble NCAM results either from an alternative splicing or from the enzymatic removal of the extracellular domain of the transmembrane NCAM isoforms.

[Abbreviations: TMD: transmembrane domain, FN3I/II: fibronectin type 3 homology domain I and II, Ig I-V: immunoglobulin like domain I-V.]

The extracellular domain of NCAM consists of five immunoglobulin-like (Ig) domains followed by two fibronectin type III (FNIII) domains. The different domains of NCAM have been shown to have different roles with the Ig domains being involved in homophilic binding to NCAM and the FNIII domains being involved in signalling leading to neurite outgrowth. There is much controversy as to how exactly NCAM homophilic binding is arranged both in *trans*- and *cis*-interactions. The *cis*-interactions depend on aromatic residues located in the Ig-I module that are buried in a hydrophobic pocket formed in the Ig-II module (Soroka et al., 2003). On the other hand, *trans*-interactions require first the formation of NCAM *cis*-dimers. Two kinds of *trans*-interactions have been proposed for these dimers. The first one, known as “flat zipper”, involves Ig-II to Ig-III mediated *trans*-interaction reflecting an interaction between NCAM molecules on opposing cells whereas the second, referred to as “compact zipper”, implicates the interaction between Ig-I to Ig-III and IgII/IgII *trans*-interactions (Soroka et al., 2003; Walmod et al., 2004). Both *cis*- and *trans*-NCAM homophilic binding have been shown to be important in NCAM “activation” leading to neurite outgrowth.

NCAM is also capable to interact with a number of molecules in a heterophilic manner. Thus, it has been shown that NCAM can bind other members of the Ig family of adhesion molecules such as L1 or TAG-1 (Brummendorf and Rathjen, 1995). In addition, NCAM interacts with several members of the extracellular matrix (ECM) including the glycosaminoglycan heparin (Cole and Glaser, 1986), chondroitin sulfate proteoglycans such as phosphacan or neurocan (Milev et al., 1995; Retzler et al., 1996) and heparin sulfate proteoglycans (Storms et al., 1996) and the fibroblast growth factor receptor (FGFR) (Doherty and Walsh, 1996).

II.1.1 Polysialylation of NCAM

Proper temporal and spatial control of cellular interactions is essential for neural development and particularly important for nervous system wiring and plasticity. Among the numerous cell adhesion molecules of the immunoglobulin superfamily involved in this process, the neural cell adhesion molecule NCAM is developmentally regulated in its pattern of glycosylation (Hildebrandt et al., 2008). Glycosylation is a common modification of membrane and secreted proteins and carbohydrate residues have often a major impact on the three-dimensional folding, stability and function of native proteins (Varki, 1993). NCAM undergoes extensive glycosylation in the ER and Golgi compartments (Kiss and Rougon, 1997). N-glycosylation is largely the most important post-translational modification of the NCAM molecule, although O-glycans can also be found on certain muscle specific isoforms (Walsh et al., 1989). At least 6 potential N-glycosylation sites (Asn 203, 297, 329, 415, 441 and 470) have been identified in the extracellular domain of NCAM (Albach et al., 2004).

The process of glycosylation fundamentally alters its biophysical properties and, as a consequence, its homophilic and heterophilic binding abilities. The glycan responsible for the conversion of different NCAM isoforms from an interactive to an anti-adhesive state is a linear homopolymer of α -2, 8-linked N-acetylneuraminic acids which is popularly known as polysialic acid or PSA (Hildebrandt et al., 2008) (**Figure 2**). The term “polysialylation” has been used for the process of glycosylation in this thesis to emphasize PSA post-translational modification of NCAM.

The process of polysialylation increases the intermembrane space and disrupts the adhesive properties of NCAM and also of other cell adhesion molecules. It is because of the structure of PSA, which is highly negatively charged, and a hydrated one (Rutishauser et al., 1998).

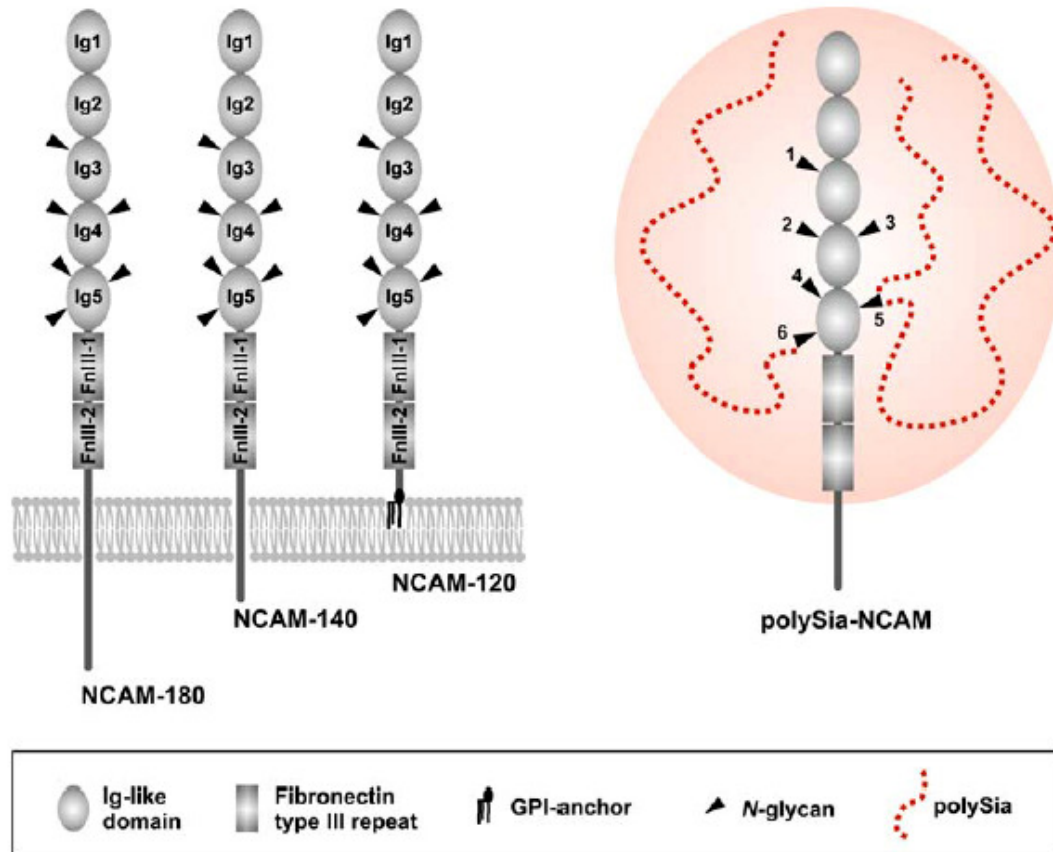


Figure 2. Scheme of the three major NCAM isoforms showing N-glycan sites (left) and the polysialylated form of NCAM (right) (Hildebrandt et al., 2008).

The extracellular part of NCAM is composed of five immunoglobulin (Ig)-like domains and two-fibronectin type III (FnIII) repeats. NCAM-180 and NCAM-140 are transmembrane proteins, which differ in the length of their intracellular part, whereas NCAM-120 is attached to the plasma membrane by a glycosylphosphatidylinositol (GPI) anchor. NCAM is a glycoprotein containing 6 N-glycosylation sites. In the polysialylated form of NCAM (PSA-NCAM), the N-glycans located at the 5th and 6th N-glycosylation site are modified by one or more PSA chains. The hydrodynamic radius of PSA is depicted as a shaded sphere.

PSA is a prominent regulator of neural cell migration and differentiation during nervous system development, and tightly associated with neurogenesis and synaptic plasticity in the adult brain (Fujimoto et al., 2001; Kleene and Schachner, 2004; Johnson et al., 2005).

II.1.2 Developmental Regulation of NCAM polysialylation

The entire process of NCAM polysialylation is tightly regulated during development. Although PSA is transiently expressed in mesodermal and endodermal derivatives during organogenesis, NCAM does not carry PSA by the time of its first appearance. On embryonic day 8–8.5 in the mouse it appears first, but shortly thereafter polysialylated NCAM becomes predominant reaching a maximum in the perinatal phase (Probstmeier et al., 1994; Kurosawa et al., 1997; Galuska et al., 2006). Until day 9 of postnatal development, PSA expression keeps pace with the rapid increase in brain weight and almost all of the NCAM is polysialylated (Oltmann-Norden et al., 2008). Subsequently, PSA drops rapidly by approximately 70% within one week accompanied by the first occurrence of PSA-free NCAM-140 and NCAM-180, the two transmembrane isoforms that are the major PSA carriers in mouse brain. In contrast, glycosylphosphatidylinositol anchored NCAM-120, the characteristic isoform of mature oligodendrocytes, is devoid of PSA during its massive up-regulation in the early postnatal brain, which is associated with the onset of myelination (Oltmann-Norden et al., 2008). Thus, the time-course of PSA down-regulation and the dramatic increase of PSA-free NCAM coincide with the completion of major morphogenetic events within the first 3 weeks of postnatal brain development. Expression of polysialylated NCAM persists into adulthood and is maintained at sites of ongoing neurogenesis or plasticity (Seki et al., 1993; Bonfanti, 2006). In the absence of any known PSA specific-degrading enzyme to modulate PSA on the surface of vertebrate cells, the state of NCAM polysialylation depends predominantly on the biosynthetic pathway.

II.2 Polysialic acid

The term polysialic acid (PSA) denotes polymers of derivatives of the nine carbon sugar neuraminic acid. More than 36 such derivatives, known as sialic acids, have been identified (Kelm and Schauer, 1997) but only a small number of these variants are found as a building unit in PSAs. In **Figure 3**, the three major building units of PSA, 5-N-acetylneuraminic acid (Neu5Ac), 5-N-glycolylneuraminic acid (Neu5Gc) and 5-deamino-3, 5-dideoxyneuraminic acid (2-keto-3-deoxynonulosonic acid, Kdn), are shown.

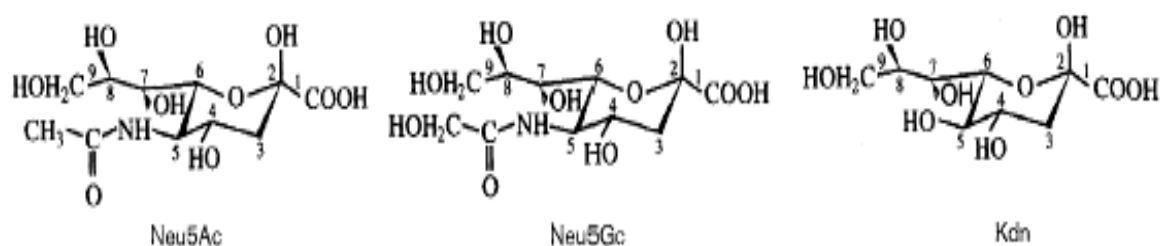


Figure 3. The structure of the three major building units of PSA (Mühlenhoff, 1998). 5-N-acetylneuraminic acid (Neu5Ac), 5-N-glycolylneuraminic acid (Neu5Gc) and 5-deamino-3, 5-dideoxyneuraminic acid (Kdn).

PSA in mammals is an exclusively homopolymeric structure of sialic acids joined by α -2, 8-glycosidic bonds. The predominant building units of PSA in mammals are 5-N-acetylneuraminic acid (Neu5Ac) and 5-deamino-3, 5-dideoxyneuraminic acid (Kdn). PSA chains form large negatively charged and highly hydrated structures and the expression of these carbohydrate chains attenuates cellular interactions and increases motility. Some pathogenic bacteria are surrounded by thick polysialylated coat structures that help to control and evade the host immune system.

II.2.1 Structure of PSA

As a linear homopolymer ($n = 8$ to over 100) of α -2, 8-linked sialic, PSA is a remarkably simple macromolecule (**Figure 4**) (Finne et al., 1983). The minimum chain length reflects characteristic formation of a helical conformation (Michon et al., 1987).

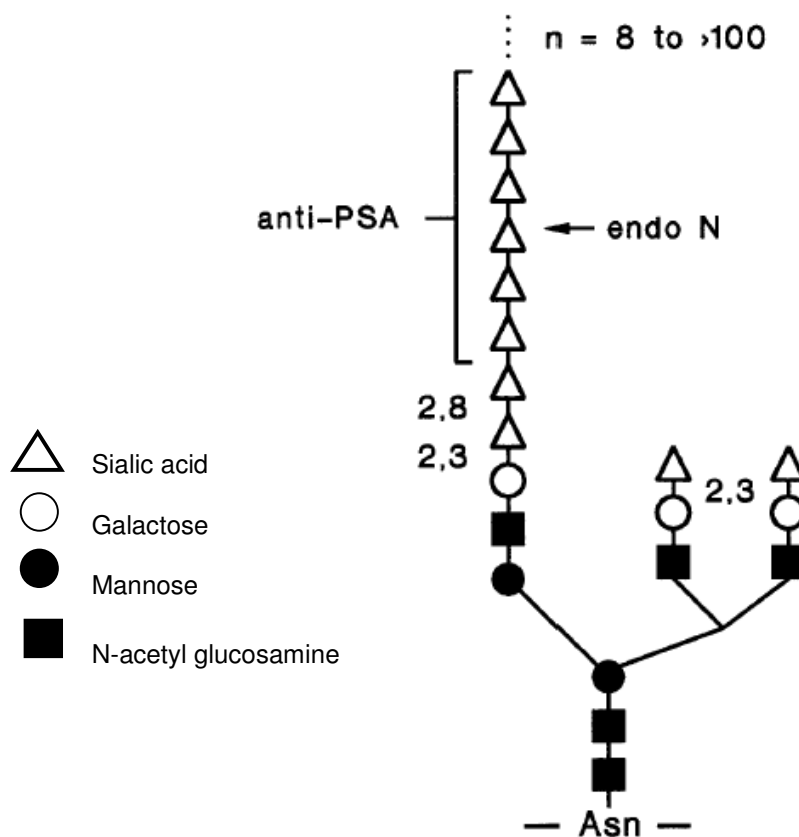


Figure 4. Proposed structure of PSA attached to NCAM via typical N-linked core glycosylation (Finne et al., 1983).

PSA is found on di- and triantennary *N*-glycan chains attached to two *N*-glycosylation sites within the fifth Ig-like domain of all three NCAM isoforms. A large number of α 2, 8-linked sialic acid residues were found attached to one antenna through α 2,3-linked sialic acid. The unique structure of the α -2, 8-linked polymer allows for its specific recognition by monoclonal antibodies (anti-PSA) and by a phage-derived endoneuraminidase (endo N).

Biosynthesis of PSA starts from the attachment of an initial α -2, 8-linked sialic acid residue to a sialic acid moieties in α -2, 3-linkage present on N-glycan backbone and continues with consecutive attachment of up to 100 α -2, 8-linked sialic acid residues (Gagneux P et al., 1999). The formation of extended helical segments explains the unusual immunological properties of PSA. Monoclonal antibodies directed against poly α -2, 8-linked sialic acids require a minimum of nine to ten residues for binding (Häyrynen et al., 1995) and a PSA-degrading enzyme endoneuraminidase N, derived from the *Escherichia coli* K1-specific bacteriophage PK1, requires a minimum of eight α -2, 8-linked sialic acids for binding and cleaves PSA into oligomers of two to seven residues (Finne et al., 1985).

The immunological properties of α -2, 8-linked PSA have been rationalized in terms of the presence of an epitope situated on a unique extended helical segment ($n \sim 9$) of the polymer. The presence of identical helices on the α -2, 8-linked PSA and poly (A) were also proposed (Brisson et al., 1992) to explain their cross-reactivity with a human monoclonal antibody (IgMNoV) (Kabat et al., 1988). In the extended helical structure, the carboxylate and acetamido groups of PSA are aligned (**Figure 5**). ¹³C and ¹H NMR chemical shift and potential energy calculations are used to compare the conformations of N-propionyl, N-butanoyl, N-isobutanoyl, N-pentanoyl, N-hexanoyl and N-glycolyl derivatives of α -2, 8-linked PSA (Brisson et al., 1992). Despite their bulkiness, none of these substituents disrupts the extended helical conformation. Hence the negatively charged carboxylate groups play a significant role in determining the conformational behaviour of α -2, 8-linked PSA (Samuel et al., 2004).

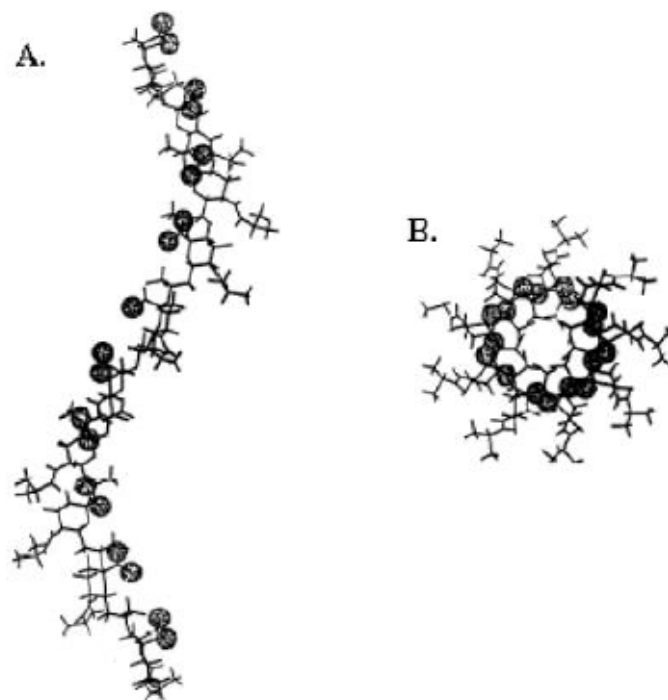


Figure 5. Extended helical structure of PSA. A: side view, B: top view.

The carboxylate and acetamido groups of PSA are aligned. Despite of the bulkiness of all the substituents of PSA, none of them disrupts the extended helical conformation. A: side view, B: top view; (Samuel et al., 2004).

II.2.2 Phylogeny of PSA

A peculiar phylogenetic distribution of PSA could be observed, being a component of the surface coat of Gram-negative bacteria (the natural target of the phage-derived endo N) (Troy et al., 1982), the zona pellucida of some vertebrate eggs (Kitajima et al., 1986), the sodium channel in the electric organ of electroplax (James and Agnew, 1987), and an abundant component of many developing vertebrate tissues. Surprisingly, this structure appears to be absent (Rutishauser, unpublished results) or at least much more restricted (Roth et al., 1992) in invertebrates, whose cells can exhibit similar phenomena found in vertebrates like cell migration, axon guidance and targeting, and neural plasticity. The attenuation of cell interactions does appear to be a feature of synaptic plasticity in *Aplysia*

(Nadja et al., 1994), except that in contrast to vertebrates, the decrease is accomplished through down-regulation of the adhesion receptors themselves rather than the up-regulation of an anti-adhesive mechanism. The human pathogens *E. coli* K1 and *Neisseria meningitidis* serogroup B (NmB) are the major causes of bacterial meningitidis (Bliss et al., 1996) express capsular polysaccharides that are chemically and immunologically identical to PSA expressed in the host organism. This capsular polysaccharides are hydrated, negatively charged and interfere with the activation of the humoral immune system and exhibit antiphagocytic activity (Vogel et al., 1997). Similarly, in *Drosophila* the over-expression of axon adhesion molecules produces aberrant axon pathfinding that resembles the effects produced by enzymatic removal of PSA in vertebrate (Lin and Goodman, 1994).

Thus it would appear that the evolution of PSA as a cell surface component on NCAM does not so much represent a fundamentally new process, but rather an improved mechanism for producing optimal levels of cell interactions. A possible driving force for this change in mechanism could well be the increase in the number of interaction receptors required for very large and complex tissues.

II.2.3 Biosynthesis of PSA

Biosynthesis of PSA is catalyzed by two Golgi-resident enzymes, the polysialyl-transferases ST8Sia-II and ST8Sia-IV (formerly named STX and PST, respectively) (**Figure 6**) (Eckhardt et al., 1995; Kojima et al., 1995; Nakayama et al., 1995; Scheidegger et al., 1995). Both enzymes show 59% identity on the amino acid sequence level and share the typical features of eukaryotic sialyl-transferases. Both ST8Sia-II and ST8Sia-IV are type II trans-membrane glycoproteins with a short N-terminal cytoplasmic tail, a trans-membrane domain, a stem region, and a large C-terminal catalytic domain that resides in the lumen of

the Golgi-apparatus. The catalytic domain includes three consensus sequences called sialyl-motifs large, small, and very small, which are found in all mammalian sialyl-transferases and are involved in substrate binding (Datta et al., 1995).

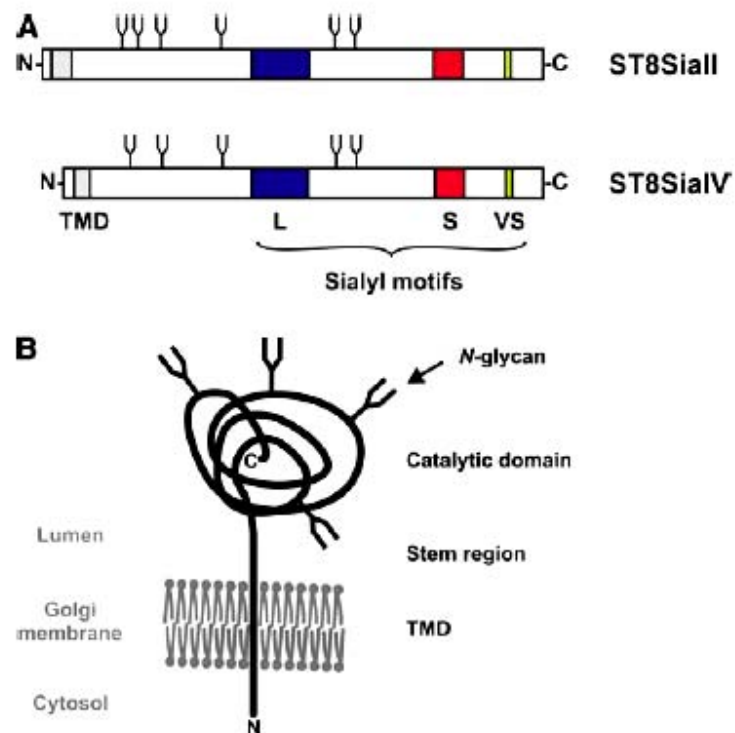


Figure 6. Schematic representation of the polysialyl transferases ST8Sia-II and ST8Sia-IV (Hildebrandt et al., 2008).

(a) The trans-membrane domain (TMD) and the sialyl motifs large (L), small (S), and very small (VS) of the catalytic domain. The relative positions of the N-glycans are indicated by Y-shaped symbols.

(b) Type II transmembrane topology of polysialyl transferases.

Although ST8Sia-II and ST8Sia-IV are typical members of the sialyl-transferase family, they are unique with respect to their catalytic ability to synthesize α -2,8-linked PSA polymers, which can exceed 50 residues (Inoue et al., 2000; Nakata et al., 2005; Galuska et al., 2006). The polysialyl-transferases ST8Sia-II and ST8Sia-IV are highly selective for NCAM, the carrier protein of PSA. Both enzymes catalyze the transfer of multiple α -2,8-linked sialic acid residues to terminally α -2,3- or α -2,6-sialylated galactose residues that are bound in α -1,4-linkage to N-acetyl glucosamine (Mühlenhoff et al., 1996; Angata et al., 1998). Although NCAM carries six N-glycosylation sites, the addition of PSA is restricted to N-glycans at the 5th and 6th site which are located in the 5th Ig-like domain (**Figure 2**) (Nelson et al., 1995; Liedtke et al., 2001; von der Ohe et al., 2002). *In vitro* studies demonstrated that both ST8Sia-II and ST8Sia-IV polysialylate N-glycans attached to NCAM with a much higher efficiency than isolated N-glycans released from NCAM (Kojima et al., 1996; Angata et al., 2000). The majority of polysialylated NCAM glycans in perinatal mouse brain was found to carry two PSA chains (Galuska et al., 2008). However, incomplete di-antennary N-glycans with only one PSA polymer as well as a small proportion of glycans that appeared to carry three or even four chains was also observed (Galuska et al., 2008). This highlights that the number of PSA chains per NCAM molecule can vary.

Transfection and *in vitro* experiments demonstrate that ST8Sia-II and ST8Sia-IV are individually able to synthesize PSA on NCAM (Eckhardt et al., 1995; Kojima et al., 1995; Nakayama et al. 1995; Scheidegger et al., 1995; Kojima et al., 1996; Mühlenhoff et al., 1996), provoking the question why NCAM polysialylation is mediated by two enzymes. *In vitro* analyses using soluble polysialyl-transferases lacking their transmembrane domain reveals distinct differences between ST8Sia-II and ST8Sia-IV. Under the experimental conditions used ST8Sia-II produced shorter PSA chains than ST8Sia-IV and appeared to be less efficient in NCAM polysialylation (Kitazume-Kawaguchi et al., 2001; Angata et al., 2002). When both enzymes work together, a synergistic effect is observed, yielding higher numbers

of PSA chains and a higher degree of polymerization (Angata et al., 2002) Using N-glycosylation site mutants of NCAM, it has been observed that ST8Sia-IV strongly preferred the 6th over the 5th N-glycosylation site, whereas this preference was only moderate for ST8Sia-II (Angata et al., 1998).

II.3 PSA functions

II.3.1 PSA as a biophysical regulator of cell interactions

PSA has the ability to decrease NCAM-mediated membrane-membrane adhesion *in vitro* (Sadoul et al., 1983). It is observed that a negative regulation of other cell interactions could also occur in the absence or independent of NCAM binding function (Rutishauser et al., 1988). Of greater biological relevance is the fact that, removal of PSA from cells can enhance the function of other cell adhesion molecules. This is particularly true for the L1/NgCAM class of adhesion molecules (Acheson et al., 1991). It has been proposed that PSA-mediated regulation of cell-cell interactions stems directly from its steric properties. Manipulations of ionic strength indicate that the steric properties of PSA directly underlie its effects on embryonic membrane adhesion (Yang et al., 1994). In considering mechanisms by which steric effects could act on cell adhesion molecules other than NCAM, two distinct modes are evident: those in which PSA impedes *trans* interactions between receptors on apposing cells, and those that involve a change in *cis* interactions between receptors on the same cell (**Figure 7**).

In the *trans* mode, an interference with overall membrane-membrane apposition affects other receptors as well as NCAM. This mechanism predicts two important things: (1) Enough space is influenced by PSA to affect overall membrane-membrane apposition, (2) intercellular space is actually changed upon removal of PSA. Furthermore, the distance between apposed cell membranes upon enzymatic removal of PSA decreases by 10–15 nm and this helps in receptor mediated

interactions (Yang et al., 1992). The *cis* mode is more complex, where PSA is involved in changes in an adhesion-promoting interaction of NCAM with other receptors on the same cell (Kadmon et al., 1990), or an indirect augmentation of interactions as a result of intracellular signaling (Doherty and Walsh, 1992) and/or clustering of NCAMs within the plane of the membrane (Doherty and Walsh, 1992).

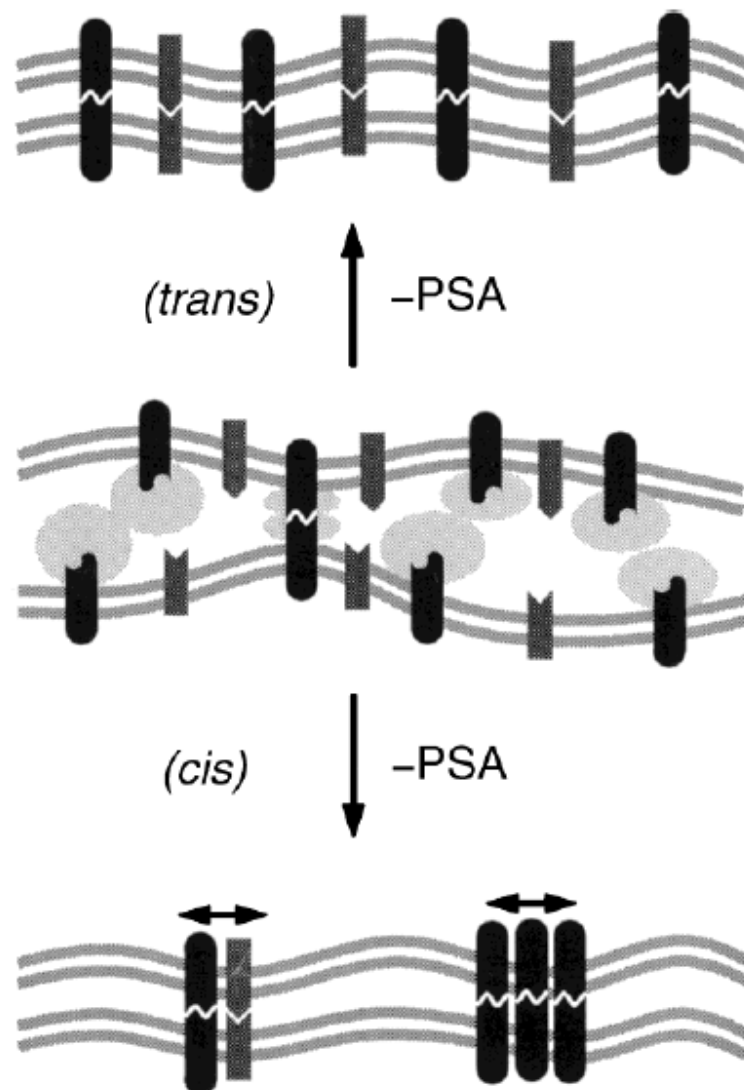


Figure 7. Steric mechanisms by which PSA could affect cell-cell interactions (Rutishauser, 1998).

In the *trans* mechanism, the highly hydrated polymer (shaded ellipses) attached to NCAM serves as an impediment to membrane-membrane contact, and therefore decreases the efficiency of encounter between complimentary receptors on apposing cells. In *cis* mechanisms, the steric action of PSA is more local, in that its presence affects cell-cell interactions via interference with a clustering of NCAMs (**right**) or by association of NCAM with other receptors on the same cells (**left**).

11.3.2 PSA serves as a permissive regulator in axon pathfinding and targeting

PSA plays a central role in the behavior of axons as they grow toward and innervate their specific targets. The patterns of motor neuron innervation are distinct for fast and slow muscle regions. Although the relative levels and distribution of the relevant adhesion molecules (NCAM and L1/NgCAM) are not different for fast and slow regions, there is considerably more PSA on axons in the fast region than in the slow (Landmesser et al., 1988). All axons grow towards the slow region when endoneuraminidase N (endo N) is used to remove the PSA. This implies that a high level of PSA serves to limit axon-axon interactions and thereby allows other environmental cues to attract fibers towards the fast region. Conversely, the lower levels of PSA on slow fibers produces thick fascicles that continue to grow along muscle fibers extending into the slow region. Similarly, PSA appears to be a critical factor in the establishment of specific motor-neuron pathways after they emerge from the neural tube (Tang et al., 1992). Motor neurons up-regulate their expression of PSA as their growth cones begin to enter the plexus region. When PSA is removed by endo N during this period of axonal outgrowth, errors in pathfinding are common, resulting in the innervation of inappropriate muscles. As in the fast/slow decision described above, the endo N-induced defect involved an inability of the axons to break away from fascicles to respond to environmental cues.

11.3.3 PSA in cell migration

Three modes of cell migration occur in the developing nervous system: 1) radial migration of neurons along glial fibers (gliophilic), 2) migration of neurons or glia along axon fibers (axophilic), and 3) co-operative streaming of neural precursors. PSA has been found to be a factor in axophilic and cooperative cell migration, but not in gliophilic migration (**Figure 8**). The migration of cells occurs by a mechanism in which the cells move forward in a stream by using each other as a substrate (Lois et al., 1994), and it has been suggested that the role of PSA is to enhance the cycles of adhesion and de-adhesion that would be required in such a 'leap-frog' type form of cell motility (Ono et al., 1994).

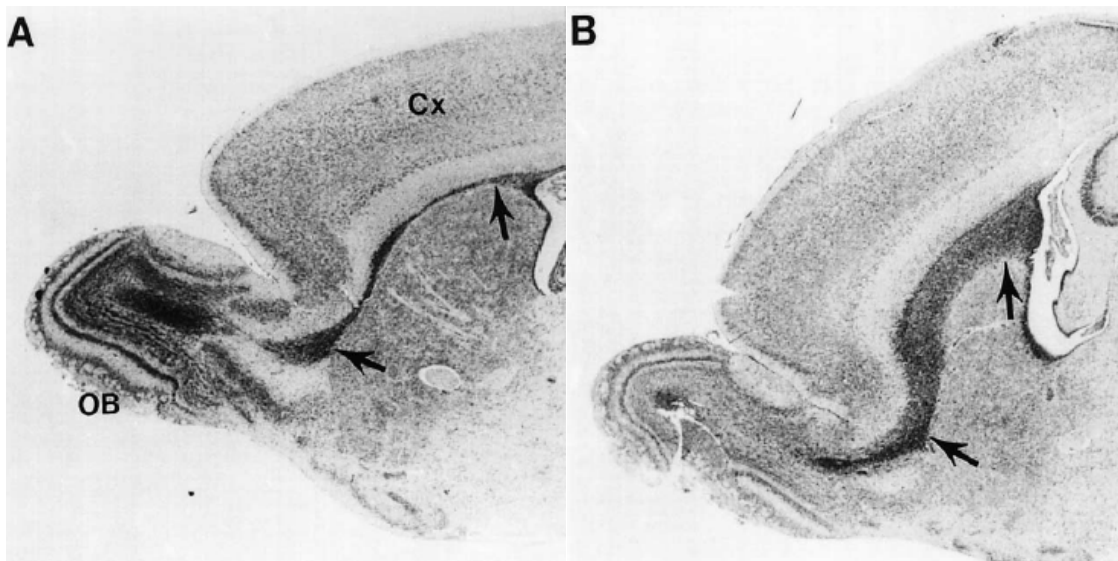


Figure 8. Effect of PSA on migration of olfactory bulb neural precursors in the subventricular zone of the neonatal mouse (Ono et al., 1994).

A. Precursors born in the subventricular zone below the cortex (Cx) follow a migratory path (arrows) toward the olfactory bulb (OB), where they become part of the characteristic layered structure of the OB.

B. When PSA is absent, either as a result of treatment with endo N or genetic deletion of NCAM, the precursors have difficulties in migrating and thus overpopulate the subventricular zone.

II.3.4 PSA in synaptic plasticity

Synaptic plasticity is the ability of the connection or synapse between two neurons to change in strength. There are several underlying mechanisms that work together to achieve synaptic plasticity, including changes in the quantity of neurotransmitter released into the synapse cleft and changes in response of cells to those neurotransmitters (Gaiarsa et al., 2002). Synaptic plasticity includes long term potentiation (LTP) and long term depression (LTD) an activity-induced lasting change in synaptic strength (Bliss and Collingridge, 1993).

PSA has an important functional role in the process of synaptic plasticity inducing long-term potentiation in acute hippocampal slices. But it is known that endo N treatment completely prevents the induction of LTP and LTD in the CA1 region of hippocampal slice cultures (Becker et al., 1996; Muller et al., 1996). However endo N treatment does not affect other cellular and synaptic parameters such as resting or action potentials. Importantly, the endo-N-induced blockade of LTP and LTD is entirely reversible by removing the enzyme from the culture, and the time course of recovery of LTP corresponds closely to the time course of re-expression of PSA as visualized by immunocytochemistry (Kiss and Rougon, 1997).

II.4 Anti-idiotypic approach to screen novel PSA binding partners

The possibility that PSA serves as a receptor for unknown potential interacting partners (ligands), raises an interest in identifying and characterizing the ligands for PSA. In order to identify novel potential binding partners of PSA, an anti-idiotypic approach was used by Maren von der Ohe and described in details in her Ph.D. thesis (von der Ohe, 2000).

An anti-idiotypic antibody is an antibody that treats another antibody as an antigen and suppresses its immunoreactivity. The idiotype represents the highly variable antigen-binding site of an antibody and is itself immunogenic. During the generation of an antibody-mediated immune response, antibodies are generated to the antigen as well as anti-idiotypic antibodies, whose immunogenic binding site (idiotype) mimics the antigen. Thus the anti-idiotypic antibodies may generate a strong immune response to antigens.

An antibody fragment (scFv, single chain variable fragment) which can mimic PSA was isolated from the Griffin.1 library (Griffiths et al., 1994) by using a standard panning methodology (Winter et al., 1994) and an immobilized monoclonal α -PSA 735 antibody as bait (**Figure 9**). To enlarge the quantity of the phages, α -PSA 735 antibody specific phages were recloned into a bacterial expression vector. After isolation and verification of scFv specificity, they were immobilized on an affinity chromatography column and both soluble brain proteins and Triton X-100 soluble brain membrane proteins were applied. Three proteins with apparent molecular weights of 80, 50 and 32 kDa were identified as potential binding partners of PSA by using mass spectrometry analysis. The first protein sequence revealed identity to myristoylated alanine-rich C kinase substrate (MARCKS), the second to the well known DNA binding nuclear protein Histone H1 and the third to the neuronal tissue-enriched acidic protein (NAP-22) (von der Ohe, unpublished data).

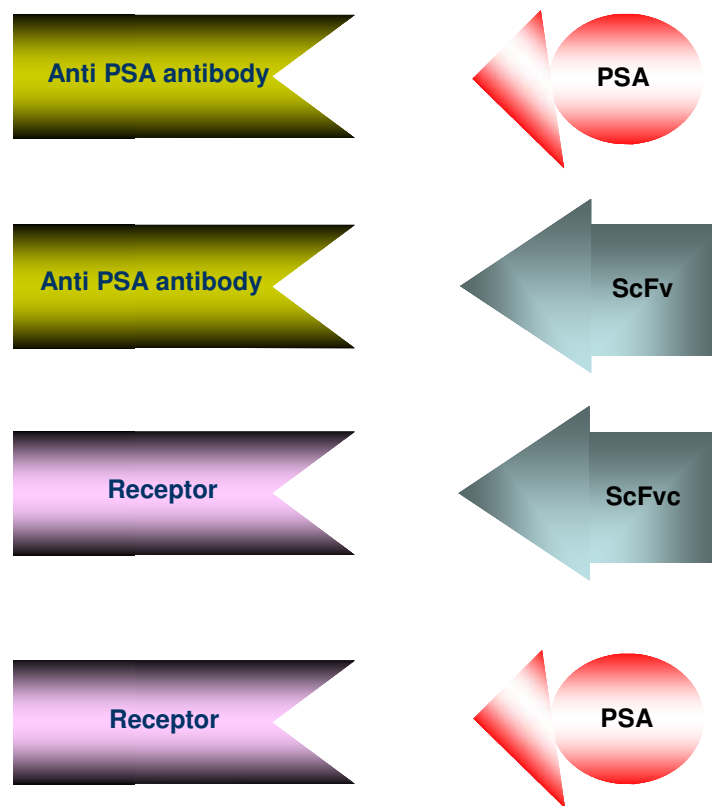


Figure 9. Schematic diagram showing working model of anti-idiotypic approach to screen novel PSA binding partners.

PSA mimicking antibody fragment (scFv, single chain variable fragment) was screened by an anti-idiotypic approach. The scFv was used to isolate PSA binding partners (receptors for PSA) from different brain homogenates of mice.

II.4.1 Histone H1

Histones are the chief protein components of chromatin. They act as spools around which DNA winds and they play a role in gene regulation. Without histones, the unwound DNA in chromosomes would be very long. Six major histone classes are known: H1 (sometimes called the linker histone, also related to histone H5), H2A, H2B, H3, H4 and archaeal histones. A variant of the Histone H1 protein is the histone H5, which has a similar structure and function, but is only found in avian erythrocytes. Histone H1 is one of the most abundant proteins in the nucleus and

present in half the amount of the other four histones. This is because unlike the other histones, H1 does not make up the nucleosome 'bead'. Instead, it sits on top of the structure, keeping in place the DNA that has wrapped around the nucleosome. Specifically, the Histone H1 protein binds to the linker DNA (approximately 80 nucleotides in length) at the point from which the DNA exits the nucleosome, and is required for higher order packing of chromatin (Alberts et al., 2002b) (**Figure 10**).

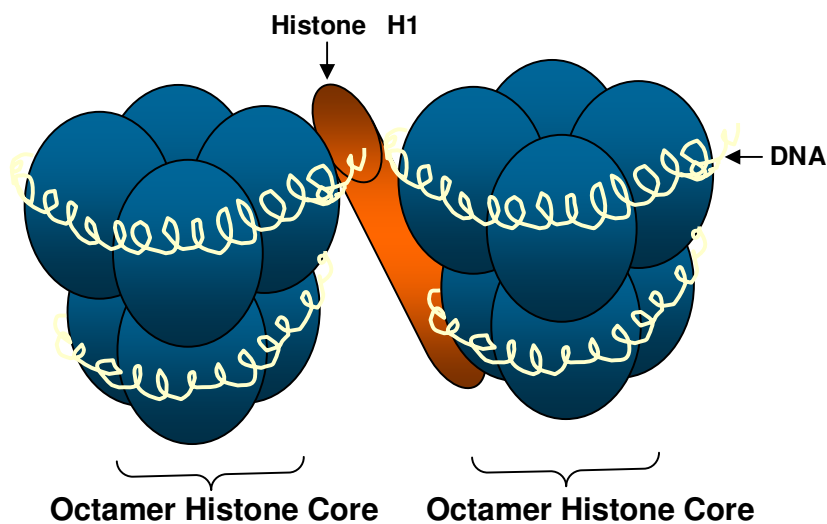


Figure 10. Schematic diagram showing Histone H1 binding to linker DNA and helping in chromatin fiber stabilization.

The nucleosome core is formed of two H2A-H2B dimers and a H3-H4 tetramer, forming two nearly symmetrical halves by tertiary structure. The 4 'core' histones (H2A, H2B, H3 and H4) that forms an octamer are relatively similar in structure. The linker Histone H1 binds the nucleosome and the entry and exit sites of the DNA, thus locking the DNA into place and allowing the formation of higher order structure.

There are six distinct subtypes of Histone H1: H1a–e and H1, that display both developmental and tissue specificities (Lennox, 1983). H1a and H1c can be considered as a separate subset to H1b, -d, and -e based on functional differences (Lennox, 1983). Histone H1 has been detected to be localized not only to the nucleus, but also at the membranes of neurones, using the anti-Histone H1 antibodies ANA108 (Bolton and Perry, 1997). Extranuclear functions of cytoplasmic

Histone H1 were firstly identified in 1985 by Reichhart et al.. Histone H1 revealed strong lipopolysaccharide (LPS) binding properties (Bolton and Perry., 1997) and it was suggested to be an acute phase protein like LPS-binding protein. Histone H1 is involved in host defence mechanisms against bacterial infections as it has been shown to exhibit antibacterial properties (Hiemstra et al., 1993). It is also known that non-nuclear histones act as cell surface receptors as T-cells express histones H2 and H3 on their cell surfaces, which bind to sulfated polysaccharides (Watson et al., 1999).

II.4.2 Myristoylated alanine-rich C kinase substrate (MARCKS)

The myristoylated alanine-rich C-kinase substrate (MARCKS) is rod-shaped, acidic protein that is unusually rich in alanine, glycine, proline, and glutamic acid and a protein kinase C (PKC) specific substrate. MARCKS is abundant [in the brain it constitutes 0.2% of total soluble protein (Albert et al., 1987)] and remarkably widely distributed in different tissues, and binds both calmodulin and actin (Graff et al., 1989b; Hartwig et al., 1992). MARCKS proteins possess three highly conserved regions: 1) The N-terminus represents a consensus sequence for myristoylation, a co-translational lipid modification attaching myristic acid, (C₁₄ saturated fatty acid) via an amide bond to the amino group of the N-terminal glycine residue. 2) The MH2-domain of unknown function resembles the cytoplasmic tail of the cation-independent mannose-6-phosphate receptor and is also the site of the only intron-splicing event. 3) The phosphorylation site domain contains all serine residues known to be PKC phosphorylation sites (Arbuzova et al., 2002). This domain has been shown to be central to the function of the MARCKS proteins, and is therefore called the effector domain (ED). The ED is highly basic (**Figure 11**), in contrast with the rest of the highly acidic protein.

The electrostatic interactions of the basic residues with acidic lipids and hydrophobic insertion of the myristate group into the core of the membrane helps

the MARCKS protein to bind to membranes. Neither of these two interactions on its own is sufficient for significant membrane binding (McLaughlin et al., 1995; Bhatnagar, 1997; Murray et al., 1997). MARCKS interacts with the plasma membrane of macrophages (Rosen et al., 1990; Allen 1995), neurons (Ouimet et al., 1990) and fibroblasts (Allen, 1995; Swierczynski, 1995). Phosphorylation by PKC, which attaches negatively charged phosphate groups to the serine residues, abrogates membrane binding of MARCKS in many cell types (Rosen et al., 1990; Swierczynski, 1995; Ohmori, 2000), it is because neutralization of the positive charges of the basic residues by the phospho-serine residues abolishes the electrostatic contribution of the ED to membrane binding, and myristoylation on its own is not sufficient to anchor the protein to the membrane. If the phosphoserine residues are subsequently dephosphorylated, MARCKS returns to the membrane (**Figure 11**). This molecular model explains the observed reversible translocation of MARCKS from the plasma membrane to the cytosol.

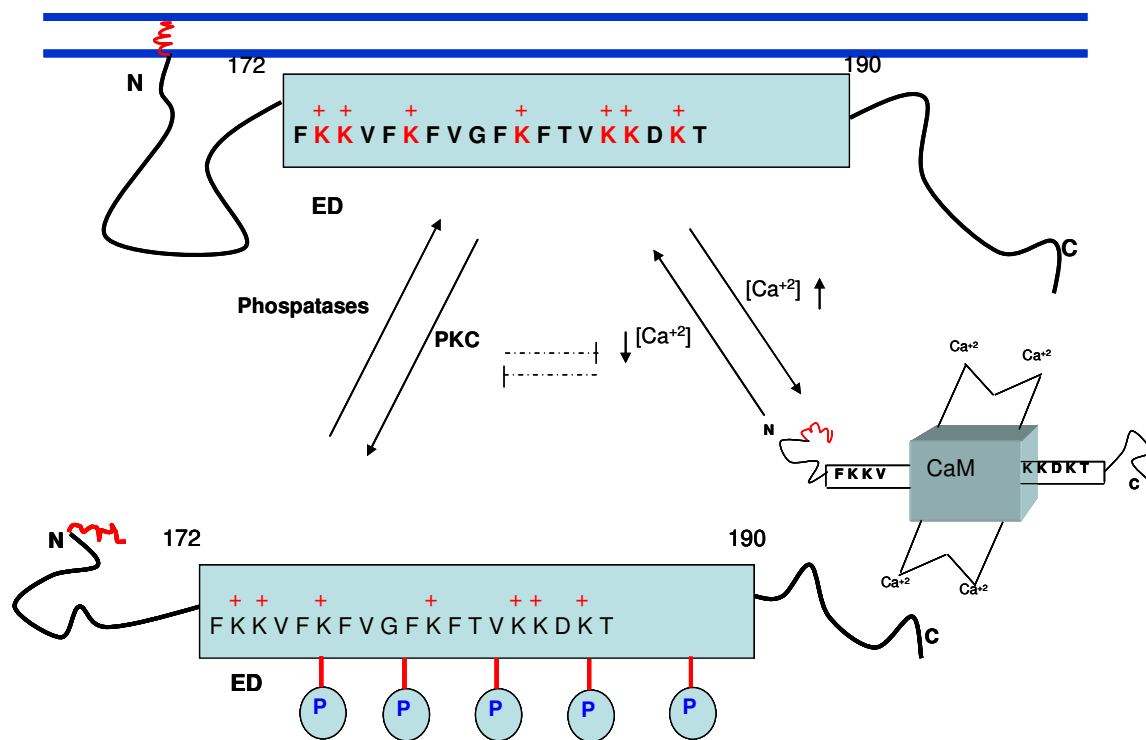


Figure 11. Schematic diagram showing the structure of the MARCKS protein and its reversible translocation into cytosol.

MARCKS bound to the plasma membrane through the N-terminal myristoyl moiety and the effector domain (ED) can translocate reversibly into the cytosol, either through cycles of phosphorylation by PKC and dephosphorylation, or through temporary increases in the intracellular calcium concentration ($[Ca^{2+}]_i$) leading to activation of calmodulin (CaM). The interactions of PKC and CaM with MARCKS are mutually exclusive (broken lines). Highlighted in red are the myristoyl moiety (myr) and the positive charges contributed by the basic residues within the ED (-), as well as the phosphate groups that are attached by PKC (P).

III. Rationale and aims of the study

Carbohydrate-carrying molecules in the nervous system have important roles during development, in regeneration and synaptic plasticity. Carbohydrates mediate interactions between recognition molecules, thereby contributing to the formation of a complex molecular meshwork at the cell surface and in the extracellular matrix. The tremendous structural diversity of glycan chains allows for immense combinatorial possibilities that might underlie the fine-tuning of cell–cell and cell–matrix interactions. The discovery of PSA as a component of vertebrate brains, and its unique association with the immunoglobulin superfamily neural cell-adhesion molecule NCAM, marked the beginning of seminal research on the functional interplay between carbohydrates and proteins in cell interactions in the nervous system. *In vitro*, PSA can promote or limit neurite outgrowth, depending on the environment. PSA appeared to be an important modulator of adhesive properties of NCAM and PSA itself has been shown to possess ligand-binding activity. Regarding to that, the identification of novel potential binding partners of PSA using structurally mimicking anti-idiotypic antibody was indeed important confirmation for the presence of still unknown PSA functions in the nervous system.

This study deals with characterization of the association between PSA and its novel binding partners Histone H1 and MARCKS using different binding assays. The aim was to verify the direct interaction of PSA with its ligands *in vitro* and then to perform functional analyses *in vitro* and *in vivo* in order to determine the involvement of these new interactions in regulation of neuroplasticity in the brain.

The main focuses of the thesis are as follows:

Rationale and aims of the study

- Determine if PSA directly interacts with Histone H1 and MARCKS using ELISA.
- Investigate whether Histone H1 expressed at the cell surface and colocalizes on cell surface with its interaction partners Histone H1 and MARCKS using immunochemical assays.
- Determine the functional consequences of the interaction between Histone H1 and PSA for neurite outgrowth, neuronal cell migration and proliferation *in vitro*.
- Investigate the role of Histone H1 on functional recovery, axon regrowth and the precision of reinnervation after femoral nerve injury in adult mice.

IV. Materials and methods

IV.1 Materials

IV.1.1 List of chemicals, commercial reagents and kits used

1. β -Mercaptoethanol	Sigma-AldrichChemie Deisenhofen, Germany
2. 2-propanol	Th.Geyer, Hamburg Germany
3. 4-(2-hydroxyethyl)-1-piperazineethanesulfonic acid (HEPES)	Sigma-Aldrich Chemie Deisenhofen, Germany
4. Accutase	Invitrogen Karlsruhe, Germany
5. Acetic acid 100%	Th. Geyer, Hamburg Germany
6. Acrylamide / Bis solution 29:1 30% W/V	SERVA Electrophoresis Heidelberg, Germany
7. Adenosine 5' – triphosphate (ATP)	Sigma-Aldrich Chemie Deisenhofen, Germany

8. Ammonium persulphate (APS)	Sigma-Aldrich Chemie Deisenhofen, Germany
9. Ammonium sulphate	Sigma-Aldrich Chemie Deisenhofen, Germany
10. BC (bicinchoninic acid) Assay	Uptima, INTERCHIM quantification kit, France
11. BenchMark™ Prestained Protein Ladder	Bio-Rad Laboratories Munich, Germany
12. Bovine serum albumin (BSA)	Sigma-Aldrich Chemie Deisenhofen, Germany
13. Bromophenol blue	Sigma-Aldrich Chemie Deisenhofen, Germany
14. Calcium chloride (CaCl ₂)	Sigma-Aldrich Chemie Deisenhofen, Germany
15. CHAPS	SERVA Electrophoresis Heidelberg, Germany
16. dATP, dCTP, dGTP, dTTP	Invitrogen Karlsruhe, Germany

17. Dimethyl sulfoxide (DMSO)	Sigma-Aldrich Chemie Deisenhofen, Germany
18. Dipotassium hydrogen phosphate	Sigma-Aldrich Chemie Deisenhofen, Germany
19. Dulbecco's modified Eagle's Medium (DMEM)	Invitrogen Karlsruhe, Germany
20. Enhanced chemiluminescence (ECL) western Blotting reagents	Amersham Pharmacia Biotech Europe, Freiburg, Germany
21. Ethanol absolute	Th. Geyer, Hamburg Germany
22. Ethanolamine	GE Healthcare Europe Freiburg, Germany
23. Ethidium bromide	Sigma-Aldrich Chemie Deisenhofen, Germany
24. Ethylene diamine tetra acetic acid (EDTA)	Sigma-Aldrich Chemie Deisenhofen, Germany
25. Ethylene glycol	Sigma-Aldrich Chemie Deisenhofen, Germany
26. Fluoromount-G	Southern Biotech Birmingham, UK

27. GC-RICH PCR system	Roche Diagnostics Roche Applied Science Mannheim, Germany
28. Glasgow MEM medium	Invitrogen Karlsruhe, Germany
29. Glucose	Sigma-Aldrich Chemie Deisenhofen, Germany
30. Glutathione agarose beads	Sigma-Aldrich Chemie Deisenhofen, Germany
31. Glycerol	Merck Biosciences Bad Soden/Ts, Germany
32. Glycine	Sigma-Aldrich Chemie Deisenhofen, Germany
33. Histone H1	Upstate, NY, USA
34. Hydrochloric acid (HCl)	Merck Biosciences Bad Soden/Ts, Germany
35. L-glutathione reduced	Sigma-Aldrich Chemie Deisenhofen, Germany
36. Magnabind streptavidin beads	Polysciences Europe Eppelheim, Germany

37. Magnesium chloride (MgCl ₂)	Sigma-Aldrich Chemie Deisenhofen, Germany
38. Methanol	Th. Geyer, Hamburg Germany
39. Neuroregulin	ImmunoTools, Friesoythe Germany
40. N, N, N', N'- tetramethylethylenediamine (TEMED)	SERVA Electrophoresis Heidelberg, Germany
41. Ni-NTA agarose beads	QIAGEN Hilden, Germany
42. NucleoSpin Plasmid mini prep	MACHEREY-NAGEL Düren, Germany
43. Orange G	Sigma-Aldrich Chemie Deisenhofen, Germany
44. OPD	Thermo Scientific Rockford, IL, USA
45. Penicillin/streptomycin solution (100X)	Invitrogen Karlsruhe, Germany
46. Phenylmethylsulfonyl fluoride (PMSF)	Sigma-Aldrich Chemie Deisenhofen, Germany
47. Phusion High-Fidelity DNA polymerase	New England Biolabs Frankfurt am Main, Germany,

48. Potassium chloride (KCl)	Sigma-Aldrich Chemie Deisenhofen, Germany
49. Precision plus protein all blue standard	Bio-Rad Laboratories Munich, Germany
50. Protein A/G plus agarose	Santa Cruz Biotechnology Heidelberg, Germany
51. Protran nitrocellulose membranes	VWR International Hannover, Germany
52. QIAfilter Plasmid Maxi kit	QIAGEN Hilden, Germany
53. QIAquick gel extraction kit	QIAGEN Hilden, Germany
54. QIAquick rapid PCR purification kit	QIAGEN Hilden, Germany
55. Restriction enzymes	New England Biolabs Frankfurt am Main, Germany
56. Ready Load 1kb Plus DNA ladder	Invitrogen GmbH Karlsruhe, Germany
57. Roti-Blue	Carl Roth Karlsruhe, Germany
58. Sodium chloride (NaCl)	Carl Roth Karlsruhe, Germany

59. Shrimp alkaline phosphatase (SAP)	New England Biolabs Frankfurt am Main, Germany
60. Sodium dodecyl sulfate (SDS)	Carl Roth Karlsruhe, Germany
61. Sodium fluoride (NaF)	Sigma-Aldrich Chemie Deisenhofen, Germany
62. Sodium orthovanadate (Na_3VO_4)	Sigma-Aldrich Chemie Deisenhofen, Germany
63. Sodium phosphate dibasic (Na_2HPO_4)	Sigma-Aldrich Chemie Deisenhofen, Germany
64. Sodium phosphate monobasic (NaH_2PO_4)	Sigma-Aldrich Chemie Deisenhofen, Germany
65. Sucrose	Sigma-Aldrich Chemie Deisenhofen, Germany
66. Sulfo-NHS-LC Biotin	Pierce, Rockford, IL, USA
67. SuperSignal West Dura	PerBio Science Bonn, Germany
68. T4 taq DNA polymerase	New England Biolabs Frankfurt am Main, Germany
69. Tris (hydroxymethyl) aminomethane	Carl Roth Karlsruhe, Germany

Materials and methods

70. Trypsin-EDTA (0.05% Trypsin with EDTA 4Na) Invitrogen
Karlsruhe, Germany
71. Tween. 20 Merck Biosciences
Bad Soden/Ts, Germany

IV.1.2 Molecular weight standards

IV. 1.2.A Precision Plus Protein Standard

10 µl of the Precision Plus Protein Standard (Bio-Rad) were loaded on SDS-PAGE gels.

Band No.	Apparent molecular weight (kDa)
1	250
2	150
3	100
4	75 *
5	50 *
6	37
7	25
8	20
9	15
10	10

*75kDa and 50 kDa proteins are more prominent for proper identification

IV. 1.2.B BenchMark™ Prestained Protein Ladder

10 µl of the Prestained Protein (Invitrogen) were loaded on SDS-PAGE gels.

Band No.	Apparent molecular weight (kDa)
1	182.9
2	113.7
3	80.9
4	63.8*

5	49.5
6	37.4
7	26.0
8	20.5
9	14.9
10	8.4

*Orientation band (pink in colour)

IV. 1.2.C Ready-Load™ 1Kb Plus DNA Ladder

1X of the 1Kb Plus DNA Ladder (Invitrogen) were loaded on agarose gels.

Band No.	Apparent molecular weight (Kb)
1	12,000
2	5,000
3	2,000
4	1,650
5	1,000
6	850
7	650
8	500
9	400
10	300
11	200
12	100

IV.1.3 List of buffers and solutions

Table 1: Solutions, buffers and their components

Name	Amount		Components
BCA-Reagent A	1	% (w/v)	Bicincholin (<i>BCA kit</i>) acid disodium salt
	1.7	% (w/v)	Na ₂ CO ₃ x H ₂ O
	0.16	% (w/v)	Natriumtartrat
	0.4	% (w/v)	NaOH
	0.95	% (w/v)	NaHCO ₃ (pH 11.25)
BCA-Reagent B (<i>BCA kit</i>)	4	% (w/v)	CuSO ₄ x 5H ₂ O
Blocking buffer (<i>ELISA</i>)	1	% (w/v)	BSA in PBS
Blocking buffer (<i>Immunoblotting</i>)	5	% (w/v)	Skim milk powder in PBS
Blocking buffer (<i>Immunocytochemistry</i>)	2	% (w/v)	BSA in PBS
Blotting buffer (<i>Western blotting</i>)	25	mM	Tris
	192	mM	Glycine
	10	% (v/v)	Methanol

Materials and methods

BSA cushion	4	% (w/v)	BSA
	12.5	ml	DMEM
	12.5	ml	F12
Cacodylate buffer	42.8	g	Sodium cacodylate in 500 ml distilled water
	0.4	M	HCl
	1	Lt (Up to)	Distilled water
Developing solution (Silver staining)	2	% (w/v)	Na ₂ CO ₃
	0.04	% (v/v)	Formaldehyde
Developing solution (ELISA)	0.1	% (w/v)	OPD in water
Destaining solution (Coomassie staining)	45	% (v/v)	Ethanol
	10	% (v/v)	Acetic acid
Digestion solution (Isolation of Primary hippocampal neurons)	136	mM	NaCl
	5	mM	KCl
	7	mM	Na ₂ HPO ₄
	25	mM	HEPES
	4	mM	NaHCO ₃
Digestion solution (Isolation of Schwann cells)	0.25	% (w/v)	Trypsin
	0.1	% (w/v)	Collagenase
	12.5	ml	DMEM
	12.5	ml	F12

Materials and methods

Dissection solution	500	ml	HBSS
<i>(Isolation of primary hippocampal neurons)</i>	3.5	mM	NaHCO ₃
	10	mM	HEPES
	33.3	mM	Glucose
	0.28	% (w/v)	BSA
	12	mM	MgSO ₄
	0.05	% (v/v)	Gentamycine
DNA sample buffer	5	% (v/v)	Glycerol
5X, <i>(For agarose gel for DNA)</i>	10	mM	Tris-HCl (pH 7.5)
	10	mM	EDTA
	0.05	% (w/v)	Bromophenol blue
	5	mM	NaCl
Ethidium bromide solution	0.05	% (w/v)	Ethidium bromide in
<i>(For agarose gel for DNA)</i>	1	X	TAE
Elution buffer	50	mM	NaH ₂ PO ₄
<i>(Ni-NTA purification of His tagged proteins)</i>	300	mM	NaCl
	250	mM	Imidazole
Fixation solution	50	% (v/v)	Methanol
<i>(Silver staining)</i>	5	% (v/v)	Acetic acid
	45	% (v/v)	Water

Materials and methods

Fixation solution	1	X	PBS
<i>(Immunocytochemistry)</i>	4	% (w/v)	Paraformaldehyde
Homogenization buffer	320	mM	Sucrose
<i>(Whole brain homogenization)</i>	1	mM	MgCl ₂
	1	mM	NaHCO ₃
	5	mM	Tris-HCl (pH 7.5)
IPTG stock solution	1	M	238 mg IPTG in 1 ml ddH ₂ O
Lysis buffer	50	mM	NaH ₂ PO ₄ , pH 8.0
<i>(Ni-NTA purification of</i>	300	mM	NaCl
<i>His tagged proteins)</i>	10	mM	Imidazole
Phosphate buffered saline/	1	X	PBS
<i>(PBS 2+)</i>	0.5	mM	CaCl ₂
<i>(Cell surface biotinylation)</i>	2	mM	MgCl ₂
Quenching buffer	1	X	PBS 2+
<i>(Cell surface biotinylation)</i>	20	mM	Glycine
RIPA buffer	50	mM	Tris, pH 7.5
<i>(Lysis of brain homogenates)</i>	150	mM	NaCl
	1	% (v/v)	Nonidet-P 40
	1	mM	Na ₄ P ₂ O ₇
	1	mM	NaF
	1	mM	EDTA
	2	mM	Na ₃ VO ₄
	1	mM	PMSF

Materials and methods

Roti-Blue staining solution	20	ml	Methanol
<i>(Colloidal coomassie Staining)</i>	20	ml	Roti-Blue 5X
	60	ml	H ₂ O
Resolving gel for SDS-PAGE	375	mM	Tris-HCl (pH 8.8)
	0.1	% (v/v)	SDS
	0.025	% (v/v)	APS
	X	ml	30% Acrylamide Bis, 29:1 (x = according to the percentage of gel required)
	0.001	% (v/v)	TEMED
Sample buffer for protein gels (2X)	125	mM	Tris-HCl (pH 6.8)
	4	% (w/v)	SDS
	10	% (w/v)	β-mercaptoethanol
	20	% (v/v)	Glycerol
	0.00625	% (w/v)	Bromophenol blue
SDS-PAGE running buffer	192	mM	Glycine
	25	mM	Tris
	0.1	% (v/v)	SDS
Sensitizing solution <i>(Silver staining)</i>	0.02	% (w/v)	Sodium thiosulfate
Stacking gel for SDS-PAGE	125	mM	Tris-HCl, pH 6.8
	0.1	% (v/v)	SDS
	0.06	% (v/v)	APS

Materials and methods

	X	ml	30% Acrylamide-Bis 29:1 (x = according to the percentage of gel required)
	0.025	% (v/v)	TEMED
Staining solution <i>(Coomassie staining)</i>	40	% (v/v)	Ethanol
	10	% (v/v)	Acetic acid
	0.1	% (w/v)	Brilliant blue R-250
Staining solution <i>(Silver staining)</i>	0.1	% (w/v)	AgNO ₃
Staining solution <i>(Neurite outgrowth assay)</i>	1	% (w/v)	Na-tetraborate
	1	% (w/v)	Toluidin blue
Stopping solution <i>(Silver staining)</i>	1	% (v/v)	Acetic acid
Stopping solution <i>(ELISA)</i>	2.5	M	Sulphuric acid
Storage solution <i>(Silver staining)</i>	1	% (v/v)	Acetic acid
Stripping buffer <i>(Western blotting)</i>	0.5	M	NaCl
	0.5	M	Acetic acid
Titration solution <i>(Isolation of Schwann cells)</i>	0.01	% (w/v)	DNase I
	12.5	ml	DMEM
	12.5	ml	F12
	10	% (v/v)	FCS

Materials and methods

Transfer buffer	192	mM	Glycine
<i>(For electrophoretic transfer of</i>	25	mM	Tris
<i>SDS-PAGE gels during western</i>	0.1	% (w/v)	SDS
<i>blotting)</i>	20	% (v/v)	Methanol
Tris-EDTA buffer	0.1	M	Tris-HCl, pH 7.5
10X <i>(Solvent for DNA)</i>	10	mM	EDTA
Tris-EDTA Acetate (TAE) buffer	2	mM	Tris-Acetate, pH 8.0
50X <i>(Buffer for running DNA agarose</i>	100	mM	EDTA
<i>gels)</i>			
TSS buffer in Luria-Bertani broth	10	mM	Tris-HCl, pH 8.0
<i>(To make chemically</i>	150	mM	NaCl
<i>competent bacteria)</i>	10	% (w/v)	PEG 300
	30	mM	MgCl ₂
	5	% (v/v)	DMSO
	Filter sterilized with 0.22 µm filter.		
Tween-20 (PBST)	0.05	% (v/v)	Tween-20
Phosphate buffered saline	1	X	PBS
Washing buffer	25	ml	Methanol
<i>(Coomassie staining)</i>	75	ml	H ₂ O
Wash buffer 1	50	mM	NaH ₂ PO ₄ , pH 8.0
<i>(Ni-NTA purification of</i>	600	mM	NaCl
<i>His tagged proteins)</i>	10	mM	Imidazole

Wash buffer 2	50	mM	NaH ₂ PO ₄ , pH 8.0
<i>(Ni-NTA purification of His tagged proteins)</i>	300	mM	NaCl
	20	mM	Imidazole
Wash buffer 3	50	mM	NaH ₂ PO ₄ , pH 8.0
<i>(Ni-NTA purification of His tagged proteins)</i>	300	mM	NaCl
	40	mM	Imidazole
Wash buffer 4	50	mM	NaH ₂ PO ₄ , pH 8.0
<i>(Ni-NTA purification of His tagged proteins)</i>	300	mM	NaCl
	60	mM	Imidazole

IV.1.4 Primary antibodies

Table 2: List of primary antibodies and their description

Name	Description	Reference
G3G4	Mouse monoclonal antibody against BrDU	Developmental Studies Hybridoma bank, University of Iowa, USA
GAPDH	Mouse monoclonal antibody against rabbit skeletal muscle GAPDH	Chemicon International Schwalbach, Germany

GST	Mouse monoclonal antibody against GST.	Novagen, Darmstadt, Germany
His6	Rabbit polyclonal antibody against His6 tag	Cell signalling, MA, USA
Histone H1	Rabbit polyclonal antibody against Histone H1	Santa Cruz, CA, USA
Histone H1	Mouse monoclonal antibody	Upstate, CA, USA
MARCKS	Rabbit polyclonal antibody against MARCKS	Lab of Perry J. Blackshear NIEHS, USA
NCAM 5b8	Mouse monoclonal IgG ₁	Developmental Studies, Hybridoma bank, University of Iowa, USA
NCAM D3	Mouse monoclonal IgG ₁	Developmental Studies, Hybridoma bank, University of Iowa, USA
PSA	Mouse monoclonal antibody against PSA clone 735	Provided by Rita Gerardy-Schahn Medizinische Hochschule, Hannover, Germany

IV.1.5 Secondary antibodies

All horseradish-coupled secondary antibodies were purchased from Dianova and used in a dilution of 1:10,000 or 1:5,000. For immunocytochemistry Cy2 and Cy3 secondary antibodies were obtained from Dianova and used in a dilution of 1:100. NeutrAvidin, horseradish peroxides conjugated was obtained from Pierce Biotechnology and used in a dilution of 1:10,000.

IV.1.6 Bacterial / Mammalian cell culture medium

IV. 1.6.A Bacterial cell culture media

Table 3: Bacterial cell culture media and their supplements

Name	Amount	Supplements
LB medium, pH 7.4	10 g/L	Bacto-tryptone
	10 g/L	NaCl
	5 g/L	Yeast extract
LB/Amp-medium	100 mg/L	Ampicilin in LB-medium
LB/Amp-plates	20 g/L	Agar in LB-medium
	100 mg/L	Ampicilin
LB/ Chloramphenicol plates	20 g/L	Agar in LB-medium
	50 mg/L	Chloramphenicol

IV. 1.6.B Mammalian cell culture media

Table 4: Mammalian cell culture media and their supplements

Name	Supplements
X-1 medium (<i>Cerebellar primary neurons</i>)	Neurobasal A medium 50 U/ml Penicillin 50 µg/ml Streptomycin 0.1% (w/v) BSA 10 µg/ml insulin 4 nM L-thyroxin 100 µg/ml transferrin 0.027 TIU/ml aprotinin 30 nM Na-selenite 1% (w/v) L-glutamine 1% (w/v) sodium pyruvate
Hippocampal culture medium (<i>First day</i>)	Neurobasal A medium 2 mM L-glutamine 5 µg/ml Gentamycin 10% Horse serum 1X B27 supplement 12.5 ng/ml FGF2
Hippocampal culture medium (<i>Third day</i>)	Neurobasal A medium 2 mM L-glutamine 5 µg/ml Gentamycin

Materials and methods

	1X B27 supplement
	5 μ M AraC
	12.5 ng/ml FGF2
Schwann cell culture medium	DMEM/F12 (1:1)
	60 ng/ml progesterone
	16 μ g/ml putrescine
	5 μ g/ml insulin
	400 ng/ml thyroxine
	160 ng/ml sodium selenite
	10.1 ng/ml tri-iodothyroxine
	38 ng/ml dexamethasone
	7.9 mg/ml glucose
	0.3 mg/ml bovine serum albumin
	100 IU/ml streptomycine
	2 mM L-glutamine
	15% FCS
Neural stem cell medium	DMEM/F12 (1:1)
	1X B27 suppliment
	0.02% sodium bicarbonate
	0.5 M HEPES
	16.6 mM glucose
	100 mM glutamine
	20 ng/ml EGF
	20 ng/ml FGF-2

IV.1.7 Bacterial strains

Table 5: Bacterial strains and their description

Name	Description	Genotype	Company
BL 21 (DE 3)	<i>Escherichia coli</i> strain for protein over-expression.	F ⁻ , <i>ompT</i> , <i>hsdSB</i> (rB ⁻ mB ⁻), <i>gal dcm</i> (DE3)	Novagene, VWR International, Darmstadt, Germany
DH5 α	<i>Escherichia coli</i> strain for cloning and sub-cloning.	F, ϕ 80d <i>lacZ</i> Δ M15, Δ (<i>lacZYA argF</i>)U169, <i>deoR</i> , <i>recA1</i> , <i>endA1</i> , <i>hsdR17</i> (rk ⁻ ,mk ⁺), <i>phoA</i> , <i>supE44</i> , λ -, <i>thi-1</i> , <i>gyrA96</i> , <i>relA1</i>	New England Biolabs, Frankfurt am Main, Germany, Roche Diagnostics, Mannheim, Germany

IV.1.8 Plasmids

Table 6: Plasmids and their description

Plasmid Name	Description	Reference
pET31F1P	prokaryotic expression plasmid for recombinant expression of proteins; ampicillin resistant; T7 Promoter	(Appel et al., 1993)
pOTB7	Contains full length cDNA clone of MARCKS	ImaGenes Berlin, Germany

IV.1.9 Mouse strains

C57BL/6J mice were used as control wild type mice in all experiments. For most of the biochemical experiments, when not indicated in the text, animals of postnatal day 2 to 7 were used. For *in vivo* experiment 3 months old mice were used.

IV.2 Methods

IV.2.1 Molecular biology

2.1.1 Maintenance of bacterial strains

Glycerol stocks (LB-medium, 15% (v/v) glycerol) of strains were prepared and stored at -80°C . An aliquot of the stock was streaked on a LB-plate containing the appropriate antibiotics and incubated overnight at 37°C . A single colony was picked up and inoculated into 2 ml of LB broth with the selection antibiotic and incubated at 37°C either for 4 hours for a starter culture or 8 hours for isolating plasmids.

2.1.2 Production of competent bacteria (Inoue et al., 1990)

An inoculum of DH5 α or BL21 bacteria from a glycerol stock was streaked on a LB plate to obtain a single colony. This single colony was used to obtain a 5 ml overnight culture in LB medium. This culture was diluted 100fold in LB medium. The diluted culture was grown to an OD_{600} of 0.3 - 0.5. The culture was split into two 50 ml falcon tubes and incubated on ice for 10 minutes. All subsequent steps were carried out at on ice or at 4°C in the cold room. The cells were pelleted down by centrifuging at $5,000 \times g$ for 10 minutes at 4°C . The supernatant was discarded. The pellet of cells was re-suspended in chilled 5 ml TSS buffer (refer to materials). The pellet was re-suspended thoroughly by vortexing gently to ensure that there are no lumps. The re-suspended cells were centrifuged again at $5,000 \times g$ for 10 minutes at 4°C and the pellet was re-suspended in 5 ml of pre-chilled TSS buffer. Aliquots of 100 μl of the re-suspended cells were made in pre-chilled microfuge tubes and immediately frozen in liquid nitrogen.

2.1.3 Transformation of bacteria (Sambrook, 1989)

To 100 µl of thawed competent DH5α or BL21 on ice, either 50-100 ng of plasmid DNA or 20 µl of DNA ligation mixture (refer to 2.1.5c) were added and incubated for 30 minutes on ice. After a heat shock (90 seconds, 42°C) and successive incubation on ice (3 minutes), 800 µl of LB medium without antibiotics was added to the bacteria and incubated at 37°C for 40 minutes. After transformation with a plasmid, then 100 µl of the transformation mixture was plated on LB plates with the selection antibiotic. If a ligation mixture was used for the transformation, then cells were centrifuged (5,000 x g, 1 minute, RT) and the supernatant removed. Cells were then re-suspended 100 µl LB medium and plated on LB plates containing the appropriate antibiotics. Plates were incubated at 37°C overnight.

2.1.4 Plasmid isolation

All plasmid isolations were done using kits mentioned in materials. Protocols followed were according to the manufacturer's instructions.

2.1.5 Enzymatic modification of DNA

2.1.5a Restriction digestion of DNA

All restriction digestions were made using restriction enzyme in accordance with the New England Biolabs catalogue and technical reference.

2.1.5b De-phosphorylation of plasmid DNA (Sambrook, 1989)

To prevent re-ligation of digested vector ends during ligation, the plasmid DNA was de-phosphorylated. After restriction digestion, the plasmid DNA was purified and 1 U of Shrimp alkaline phosphatase (SAP) buffer (Boehringer Ingelheim) and 1 U SAP per 100 ng plasmid DNA was added. The reaction was incubated at 37°C for 2 hours and terminated by incubation at 70°C for 10 minutes. The plasmid DNA was used for ligation without further purification.

2.1.5c Ligation of DNA fragments (Sambrook, 1989)

For the ligation, T4 DNA ligase (New England Biolabs) was used. The amount of PCR product, which has been taken for the ligation, was calculated as: (ng of vector x size of insert in kb) / size of vector in kb x ratio (insert / vector).

The reaction mixture for a ligation contained:

Component	Amount per reaction
Vector (x ng)	2 µl
Insert (x ng)	3 µl
10x buffer for T4 DNA ligase	1 µl
T4 DNA ligase	1 µl
Autoclaved, distilled water	up to 10 µl

The reaction mixture was incubated at 4°C for overnight. Finally, *E. coli* DH5α were

transformed with 5 μ l of ligation mixture and selected by an appropriate antibiotic. Positive clones were analysed by the restriction analysis and sequence analysis.

2.1.5d Polymerase chain reaction (Saiki et al., 1988)

Amplification of DNA fragments was performed in a 50 μ l reaction mix with thin-walled PCR tubes in PCR cyclers (MJ Research, MA, USA). GC rich PCR system was obtained from Roche.

The following reaction mixture was used for a standard PCR:

Component	Amount per reaction
DNA template	20 ng
Plus strand primer (5 pm/ μ l)	5 μ l
Minus strand primer (5 pm/ μ l)	5 μ l
dNTP mix (2 mM each dNTP)	5 μ l
GC rich resolution solution	10 μ l
5X GC rich PCR buffer containing 7.5mM MgCl ₂ and DMSO	10 μ l
GC rich enzyme mix	1 μ l
Autoclaved, distilled water	Up to 50 μ l

Cycling parameters:

Segment	Cycles	Temperature in °C	Time
1	1	98 °C	3 minutes
2	27	98 °C	30 seconds
		66 °C	30 seconds
		72 °C	50 seconds
3	1	72 °C	10 minutes
4		4 °C	Forever

2.1.6 DNA gel electrophoresis

DNA fragments were separated by horizontal electrophoresis in DNA electrophoresis chambers (Bio-Rad) using agarose gels. Agarose gels were prepared by heating 1-2% agarose (w/v) (depending on the size of DNA fragments) in 1xTAE buffer till all the agarose was dissolved and then poured onto DNA gel trays. After solidification the gel was covered with 1xTAE buffer, the DNA samples were mixed with DNA sample buffer and pipetted into the sample pockets. The gel was run at constant voltage (10 V/cm gel length) until the orange G dye had reached the end of the gel. Afterwards, the gel was stained with ethidium bromide staining solution for 20 minutes and documented using the E.A.S.Y. UV-light documentation system (Herolab, Wiesloh, Germany).

2.1.7 Extraction of DNA fragments from agarose gels

For isolation and purification of DNA fragments from agarose gels, ethidium bromide stained gels were illuminated shortly with UV-light and the appropriate

DNA band was excised from the gel with a clean scalpel and transferred into a microfuge tube. The fragment was isolated using the QIAquick gel extraction kit from Qiagen following the manufacturer's protocol.

2.1.8 Purification of DNA fragments after PCR

For purification of DNA fragments, the Rapid PCR Purification kit from QIAgen was used according to the manufacturer's protocol.

2.1.9 Determination of DNA concentration

DNA concentrations were determined spectroscopically. The absolute volume necessary for measurement was 10 μ l. For determining the concentration of DNA in case of large-scale plasmid preparations, the DNA was diluted appropriately with distilled water before taking the reading. Concentration was determined by measuring the absorbance at 260 nm and 280 nm. Absorbance at 260 nm had to be higher than 0.1 but less than 0.6 for reliable determinations. The concentration of DNA was calculated from the absorbance at 260nm (50 μ g/ml of double stranded DNA has an absorbance of 1 at 260nm). A ratio of A_{260}/A_{280} between 1.8 and 2 indicated sufficient purity of the DNA preparation for either transformation or further enzymatic modifications.

2.1.10 Sequencing of DNA

DNA sequencing was performed by the sequencing facility of the ZMNH, Hamburg. For preparation, 1 μ g of DNA was diluted in 7 μ l double distilled water along with the appropriate sequencing primer (10 pM).

IV.2.2 Protein biochemistry and conjugation procedures

2.2.1 Protein quantification by Bicinchoninic Acid (BCA) assay method

The protein concentration was determined using the BCA kit (Pierce, Rockford, USA). Solution A and B were mixed in a ratio of 1:50 to give the BCA solution. 10 μ l of the protein sample was applied to 200 μ l BCA solutions in microtiter plates and incubated for 30 minutes at 37°C. BSA standards ranging from 100 μ g/ml to 2 mg/ml were co-incubated. The extinction of the samples was determined at 560 nm in a microtiter plate by an ELISA reader.

2.2.2 SDS-polyacrylamide gel electrophoresis (SDS-PAGE)

Separation of proteins was performed by SDS-polyacrylamide gel electrophoresis (SDS-PAGE) using the Mini-Protean III system (Bio-Rad). The size of the stacking and running gels were followed:

Stacking gel:

Height 1 cm, thickness 1 mm

4% - 5% (v/v) acrylamide solution (depending on the molecular weight of the proteins to analyze)

Running gel:

Height 4.5 cm, thickness 1 mm

8-10% acrylamide solution (depending on the molecular weight of the proteins to analyze)

10 or 15-well combs

After complete polymerisation of the gel, the chamber was assembled as described

by the manufactures protocol. Samples were diluted with appropriate amount of 5X SDS sample buffer followed by boiling for 10 minutes at 100°C and up to 35 µl of sample were loaded in the pockets and the gel was run at constant voltage at 60 V for 20 minutes and then for the rest at 130V. The gel run was stopped when the bromophenol blue line had reached the end of the gel. Gels were then either stained (coomassie or silver) or subjected to Western blotting.

2.2.3 Coomassie staining of polyacrylamide gels (Ausrubel, 1996)

After SDS-PAGE, the gels were stained in staining solution (overnight) with constant agitation. The gels were then incubated in de-staining solution until the background of the gel appeared nearly transparent.

2.2.4 Silver staining of polyacrylamide gels

After SDS-PAGE, gels were fixed with acetic acid/methanol solution for 30 minutes, washed in distilled water for at least 30 min and quickly rinsed with freshly prepared sensitizing solution. Afterwards, gels were stained with silver staining solution for 30 minutes at 4°C, washed twice in water and developed with developing solution. When a sufficient degree of staining has been obtained, reaction was quenched with 1% acetic acid and the gels were replaced in a storage solution.

2.2.5 Electrophoretic transfer of proteins

Proteins were transferred after SDS-PAGE (see above) onto a Protran® nitrocellulose membranes using a MINI TRANSBLOT-apparatus (Bio-Rad). After equilibration of the polyacrylamide gels in transfer buffer for approximately 5

minutes, a blotting sandwich was assembled as described in the manufacturer's protocol. Proteins were transferred at 4°C in blot buffer at constant voltage (80V for 2 hours or 35 V overnight). Pre-stained protein markers from Bio-Rad Laboratories were used as a molecular weight marker and to monitor successful protein transfer after tank blotting.

2.2.6 Immunochemical detection of electrophoretically transferred proteins

After the electrophoretic transfer, membranes were removed from the sandwiches and placed protein-bound side-up in glass vessels. Membranes were washed once in PBST for 5 minutes and were subsequently blocked for 1 h in PBST with 5% skim milk powder under gentle shaking at room temperature. Incubation with an appropriate antibody diluted in PBST with 5% skim milk powder, was performed either for 90 minutes at room temperature or overnight at 4°C. The primary antibody solution was removed and membranes were washed 6 times by incubating with PBST with constant shaking and changing of the PBST at 5 minutes intervals. The appropriate horseradish peroxidase (HRP)-conjugated secondary antibody was applied at a concentration varying from 1:5,000 to 1:20,000 in PBST with 5% skim milk powder for 60 minutes at room temperature. The membranes were washed 6 times by incubating with PBST with constant shaking and changing of the PBST at 5 minutes intervals. Immunoreactive bands were visualized using the chemiluminescence detection reagents. The membranes were soaked for 5 minutes in detection solution (1:1 mixture of kit-supplied reagent I and II of enhanced chemiluminescence detection system). The detection solution was drained off and the blots were placed between plastic sheets. The membranes were exposed to BIOMAX ML films (Kodak) for several time intervals, starting with a 1-minute exposure to 12 hours. In case of weak signal detection of the desired protein, enhanced chemiluminescence solution with extended duration was used to amplify the signal.

2.2.7 Enhanced chemiluminescence system

The antibodies bound to the membranes were detected using the enhanced chemiluminescence detection system (SuperSignal West Dura or SuperSignal West Pico). The membranes were soaked for 5 minutes in detection solution (1:1 mixture of solutions I and II). The solution was removed and the blots were placed between transparent plastic sheets. The membranes were exposed to BIOMAX ML films (Kodak) for several time periods, starting with a 30 seconds exposure to 24 hours.

2.2.8 Stripping and re-probing of Western blots

For detection of an additional protein on the same immunoblot, the nitrocellulose membranes were stripped from bound antibodies by shaking blots in stripping buffer for 30 minutes at room temperature. Blots were neutralized by incubation for 1x5 minutes in 1 M Tris-HCl (pH 7.5) and again subjected to immunochemical detection as described above.

2.2.9 Drying of polyacrylamide gels

Polyacrylamide gels were dried using Gel Air Drying Frame (Bio-Rad). The gels were placed between two wet cellophane sheets, fixed using a metal frame and plastic clips and dried during 6 hours at 50°C with constant blowing.

IV.2.3 Expression of recombinant proteins in Escherichia coli

For recombinant expression of proteins in *E. coli*, the corresponding cDNA of the gene was cloned in frame with the purification tag of the corresponding expression plasmid. The appropriate *E. coli* strain was transformed with the expression plasmid and streaked on LB plates supplemented with the selection antibiotic (ampicillin, 100µg/ml). A single colony was inoculated in a 2 ml of LB culture with the selection antibiotic and incubated overnight at 37°C with constant agitation. The overnight culture was used as a starter inoculum at a ratio of 1:50 and incubated at 37°C under constant agitation until the culture had reached an optical density of 0.6. Protein expression was induced by adding IPTG (0.1-0.5 mM) to the culture with further incubation for 2-3 hours at 37°C. Bacteria were collected by centrifugation and stored at -20°C. Protein expression was monitored by Western blotting by removing small aliquots of the culture every hour after IPTG induction.

2.3.1 Lysis of bacteria using the French press

Bacteria were pelleted (8,000 x g, 4°C, 10 minutes) and re-suspended in native lysis buffer (20 ml lysis buffer per 500 ml culture). The suspension was transferred into a pre-cooled French-Pressure-20K-chamber (capacity: 40 ml; Spectronic Instruments/SLM Aminco). Bacteria were compressed (10,000 psi, 5 minutes) and lysed by opening the valve carefully. The procedure was repeated 3 times and then the suspension was centrifuged (15,000 x g, 10 minutes, 4°C) in a Beckman centrifuge.

2.3.2 Protein purification

Histidine tagged proteins were captured using Ni-NTA agarose beads (QIAGEN)

and the protein purified from the beads according to the manufacturer's protocol. Glutathione S transferase tagged proteins were captured using glutathione agarose beads (Sigma–Aldrich). The captured protein was purified from the beads according to the manufacturer's protocol.

2.3.3 Brain homogenization

Brains were prepared from wild-type mice of different ages varying from postnatal day 2 to day 7. Mice were decapitated; brains were removed from skulls and immediately transferred into a homogeniser (Teflon pestle, 0.1 µm) (Wheaton, Millville, USA). All following steps were carried out on ice. Each brain was homogenized applying 10-12 up-and-down strokes in 3 ml of homogenisation buffer containing the cocktail of protease inhibitors (Roche, Germany) diluted to the appropriate concentration. Then brain homogenate was subjected to immunoprecipitation or other experiments.

IV.2.4 Protein interaction detection methods

2.4.1 Enzyme-linked immunosorbent assay (ELISA)

Several proteins were coated into 384-well microtiter plate (non-treated surface; CORNING, NY, USA) in concentrations of 4 -100 µg/ml overnight at 4°C. Non-absorbed proteins were removed; the wells were washed 3 times for 5 minutes with PBS-T and blocked with 1% BSA in PBS for 1 hour at room temperature (RT). After washing wells were subsequently incubated with the putative binding partners (either proteins or carbohydrates) diluted in a wide range of 0.5 µg/ml to 2.5 µg/ml in PBS at RT. Non-bound interacting partners were removed and the wells were washed 3 to 5 times for 5 minutes at RT to remove non-specifically bound interacting partners. Specifically bound proteins/ carbohydrates were detected with

respective primary antibodies and appropriate HRP-linked secondary antibodies. Protein-protein or protein-carbohydrate binding was visualized by the detection reaction of HRP with OPD reagent that resulted into a coloured product. Optical density was measured using an ELISA reader (μ Quant, Bio-Tek Instruments, Winooski, VT, USA) and reading the absorption at 490 nm. All graphic results are presented in this study as the experiment values of absorbance, where the values of PBS control were subtracted, to the concentration of titrated proteins.

2.4.2 Co-immunoprecipitation

Polyclonal antibodies against MARCKS (Lab of Perry J. Blackshear, NIEHS, USA) was used to immunoprecipitate MARCKS from total brain homogenate. One mg of total protein of brain homogenate was incubated with 1 ml of ice-cold RIPA lysis buffer for 2 hours at 4°C with constant gentle shaking. Samples were centrifuged at 20,000 x g for 15 minutes at 4°C. The pellet was discarded and the supernatant was pre-cleared with 20 μ l of thoroughly re-suspended sepharose protein A (A/G) beads by incubating for 3 hours at 4°C with constant gentle shaking. After pre-clearing, the beads were pelleted down by spinning at 610 x g for 5 minutes and the supernatant was carefully pipetted out into another tube. The supernatant was incubated with corresponding antibodies or Ig control overnight at 4°C with constant mixing. Precipitation of the antibodies was performed with sepharose beads (5 hours at 4°C) followed by washing 4 times with ice-cold RIPA buffer and once with ice-cold PBS. The samples were analysed by immunoblotting after addition of SDS sample buffer and boiling at 100°C for 10 minutes.

IV.2.5 Cell culture of primary neurons

2.5.1 Preparation and cultivation of dissociated cerebellar granule cells

Dissociated cerebellar neurons were prepared using a procedure as described in Chen et al. (1999) and Loers et al. (2005). Cerebella of 6-7 days old mice were quickly isolated from decapitated mice and placed into petri dishes containing cold HBSS. The meninges along with blood vessels were removed under a dissecting microscope using a fine forceps. The cerebella were cut into 3 pieces and transferred in a laminar flow hood to a 15 ml plastic centrifugation tube in which all the subsequent procedures were performed. Then tissue from a maximum of 3 cerebella was incubated in 1 ml of 1% trypsin and 0.05% DNase solution for 12 minutes at room temperature. The tissue pieces were washed thrice with 5 ml of ice cooled HBSS and re-suspended in 1 ml of 0.05% DNase solution. The tissue pieces were then triturated by passing through fire polished Pasteur pipettes of narrowing bores, about 5-8 passes through each of the 1 mm diameter bore pipette followed by a 0.5 mm and then a 0.1-0.2mm bore pipettes. The cells were suspended in 5 ml of cold HBSS and placed on ice for 5 minutes to allow remaining tissue clumps to settle. The suspension without the clumps was carefully transferred to a new centrifuge tube and centrifuged for 10 minutes at 4 °C at 100 x g. The cell pellet was re-suspended in 5 ml of X-1 medium (equilibrated to 37°C, 5% CO₂ and 90% relative humidity) (Chen et al., 1999) using Neurobasal A instead of BME medium. Cell concentrations and viability of cells were simultaneously determined using 10 µl of this cell suspension mixed with 10 µl of a 0.4% Trypan blue solution and cells were counted in a hemocytometer.

2.5.2 Neuritogenesis of cerebellar granule cells

Neurite outgrowth assay is a functional study showing the effects of different biological compounds on the length of neurites. For measuring of neurite

outgrowth, the cerebellar primary granule cells were seeded at a density of $1-2 \times 10^5$ cells/ml into 48-well plates (Nunc). Previously wells were pre-treated with 0.01% poly-L-lysine (PLL) for overnight at 4°C, washed twice with water, and air-dried under UV light. Then proteins of interest were coated above PLL overnight in different concentrations and plates were washed with phosphate buffer saline (PBS) prior use. The cells were added to the coated wells and cultured in chemically defined serum-free medium (as described above). In order to investigate the effect of soluble compounds they were added in different concentrations 1 hour after the cell seeding to avoid an influence on cell attachment.

In brief Histone H1 and laminin were substrate-coated at a concentration of 10 µg/ml onto the dried PLL surfaces for overnight at 4 °C. The plates were washed twice with PBS, and neurons were plated at a density of $1-2 \times 10^5$ cells/well in 300 µl of chemically defined serum free medium. For antibody blocking experiments, rabbit polyclonal antibodies against human Histone H1 at a concentration of 10 µg/ml were added to the wells 1 hour after cells had been seeded. At the same time, cells were treated with soluble Histone H1 and/or soluble colominic acid (10 µg/ml). After 24 hours culturing at 37°C with 5% CO₂ in a humidified atmosphere, cells were fixed by the gentle addition of 25% glutaraldehyde to a final concentration of 2.5% (Agar Scientific, Stansted, UK). After fixation, cultures were washed 3 times with distilled water and stained with 1% methylen blue/toluidine blue (Sigma) in 1% borax for 1 hour at RT. Morphological parameters were quantified with the Axiovert microscope and the AxioVision image analysis system 4.6 (Carl Zeiss Micro Imaging, Göttingen, Germany). For morphometric analysis, only cells without contact with other cells were evaluated. Neurites were defined as those processes with a length of at least one cell body diameter. To determine the total neurite length per cell, 50 cells in each of two wells were analyzed per experiment. The data were analyzed by analysis of t-test, with

$p < 0.05$ being considered significant.

2.5.3 Cell surface biotinylation on cerebellar granule cells

Dissociated cerebellar granule cells were seeded into 48-well plastic plates (Nunc) at a density of 10^6 cells/ml. The cells were cultured in chemically defined serum-free medium as described above. Wells were previously coated with PLL (10 $\mu\text{g/ml}$) overnight, washed with distilled water and treated under UV light during 10 minutes. Cells were cultured for 37°C with 5% CO_2 in a humidified atmosphere before surface biotinylation was started. Cells surface biotinylation was performed using sulfo-NHS-LS-biotin (Pierce). Cells taken from the 37°C incubator were put on ice and washed twice with cold PBS-2+. Then the cells were incubated with sulfo-NHS-LS-biotin freshly dissolved in PBS-2+ for 10 minutes on ice. Part of the cells was incubated in PBS-2+ without sulfo-NHS-LS-biotin for the negative control. The reaction of sulfo-NHS-LS-biotin with surface proteins was quenched during 5 minutes on ice with quenching buffer. Then the cells were carefully washed with PBS-2+ and 250 μl of lysis buffer were added to each well. Lysis of cells occurred at 4°C during 20 minutes with shaking. Cells were scratched from plastic using cell scrapers. Cell lysates were centrifuged for 10 minutes with 1,000 g at 4°C to remove DNA and cell debris. Streptavidin-coupled magnetic beads were added to the lysates and these mixtures were incubated overnight at 4°C in order to precipitate all biotinylated proteins. Afterwards, magnetic beads were washed twice with lysis buffer and boiled in 20 μl SDS-loading buffer. Samples were then subjected to SDS-PAGE and biotinylated proteins were detected using Western blot with either neutrAvidin-conjugated with HRP or Histone H1 specific antibodies.

2.5.4 Preparation and cultivation of dissociated hippocampal neurons

One to two days old wild-type mice were used for preparation. After cutting of the head, brains were removed from the skull and put into ice cold dissection solution.

The brains were cut along the midline. Each half was fixed with glass needles and hippocampi were extracted, cut into 1 mm pieces and transferred into a 15 ml falcon tube. Tissue pieces were washed thrice with dissection solution, and 5 ml of Hank's balanced salt solution was applied. During this time 6 µg of trypsin and 1.5 µg of DNase I per each hippocampus were dissolved in digestion solution, filtered and applied to the tissue. The falcon tube was warmed in the hands during 1 minute and then stayed for 5 minutes at RT to allow the trypsin cleavage. After trypsinization the tissue was washed thoroughly three times with dissection solution. 4 µg of trypsin inhibitor were dissolved in 4 ml of dissection solution and filtered. 2.5 ml of trypsin inhibitor were applied to the hippocampi for 5 minutes, removed and the rest 1.5 ml were added for 5 minutes. 1 mg of DNase I was dissolved in 2.5 ml of dissection solution and subjected to the tissue which was re-suspended into separate cells using rounded Pasteur pipettes with decreasing diameter of aperture. At least 3 volumes of dissection solution were added to the cell suspension and centrifuged for 15 minutes at 900 x g and 4°C to remove dead cells and cell debris. The pellet was diluted with an appropriate amount of Neurobasal A medium with supplements. The number of cells was counted in a Neubauer cell chamber. The hippocampal primary neurons were seeded into 48-well plastic plates (Nunc), pre-coated with poly-L-lysine (PLL; 10 µg/ml) overnight, washed with distilled water and treated under UV light during 10 minutes. A cell density of 10⁶ cells/ml was seeded for immunocytochemistry.

2.5.5 Schwann cell culture and analysis of process elongation

Mouse Schwann cells were isolated from dorsal root ganglia (DRG) of 7-days-old C57BL/6J mice. Tissues were removed, washed once with ice-cooled Ham's F-12 (PAA Laboratories, Cölbe, Germany), and then incubated with 0.25% trypsin and 0.1% collagenase (Sigma-Aldrich, Steinheim, Germany) at 37°C for 30 minutes. After enzymatic digestion, tissues were washed twice with ice-cooled Ham's F-12

medium and then suspended in 1 ml Ham's F-12 medium containing 0.01% DNase (Sigma). Mechanical digestion was performed using fire-polished Pasteur pipettes, and cells were suspended in 5 ml Ham's F-12 medium, added on top of a 5 ml 4% bovine serum albumin (BSA, fraction V, PAA Laboratories) cushion and centrifuged for 10 minutes at 4°C and 500 x g. Finally, Schwann cells were suspended in fresh pre-warmed (37°C) medium and seeded on 48-well plates (Nunc), that were pre-treated with 0.01% PLL and coated with different substrates like laminin (10 µg/ml, Sigma) and different concentrations of purified Histone H1 (Upstate, CA, USA). The medium used for Schwann cell culture contained DMEM high glucose/Ham's F-12 (1:1) (PAA Laboratories), 60 ng/ml progesterone (Sigma), 16 µg/ml putrescine (Sigma), 5 µg/ml insulin (Sigma), 0.4 µg/ml L-thyroxine (Sigma), 160 ng/ml sodium selenite (Sigma), 10.1 ng/ml triiodothyronine (Sigma), 38 ng/ml dexamethasone (Sigma), 100 U/ml penicillin (PAA Laboratories), 100 µg/ml streptomycin (PAA Laboratories) and 2 mM L-glutamine (PAA Laboratories). Schwann cells were seeded at a density of 50,000 cells/ml. Cells were treated with soluble Histone H1 and/or soluble colomonic acid (10 µg/ml) 1 hour after cells had been seeded. Cells were cultured for 24 hours at 37°C, 5% CO₂ in a humidified chamber, fixed with 2.5% glutaraldehyde and stained with 1% methylen blue/toluidine blue in 1% borax. The length of processes was measured by using the Axiovert microscope and the AxioVision image analysis system 4.6 for morphometric analysis. Only cells without contact with other cells were evaluated. Processes were defined as those processes with a length of at least one cell body diameter. To determine the total neurite length per cell, 50 cells in each of two wells were analyzed per experiment. The data were analyzed by analysis of t-test, with $p < 0.05$ being considered significant.

2.5.6 Schwann cell proliferation

Schwann cells were seeded at a density of 250,000 cells/ml onto 12-well plates (Nunc), containing 12 mm glass cover slips pre-treated with 0.01% PLL and coated with different substrates like laminin and purified Histone H1 at a concentration of 10 µg/ml. The cells were cultured in the presence of neuroregulin (12 ng/ml, ImmunoTools, Friesoythe, Germany). Four hours after seeding, 20 µM BrdU (Sigma) was added to the culture. Cells were treated with soluble Histone H1 and/or soluble colominic acid at a concentration of 10 µg/ml 1 hour after BrdU treatment and then cultured for additional 48 hours. Cells were washed shortly with PBS and fixed with 4% formaldehyde in 0.1 M phosphate buffer, pH 7.3. After incubation for 30 minutes with 2 N HCl at 37°C, cells were washed, blocked with normal goat serum and incubated overnight with mouse primary antibodies G3G4 against BrdU (1:100 dilution). Appropriate secondary antibodies coupled to fluorescent dye Cy3 were applied to the cells in the dilution 1:200 for 1 hour at room temperature in the dark. The cover slips were finally washed and mounted with Fluoromount-G (Southern Biotech, Birmingham, UK). To estimate the number of proliferating cells, 10 photographs per treatment were taken from different areas of the cover slip using an Axiophot 2 microscope (Zeiss) and a 20x objective. Each area was photographed using phase contrast and epifluorescence. The two digital images were then overlaid using the Image J software (<http://rsbweb.nih.gov/ij/download.html>) and Image Tool 2.0 software (University of Texas, San Antonio, TX, USA, <http://ddsdx.uthscsa.edu/dig/>) was used to count proliferating (BrdU-positive) Schwann cells and total number of Schwann cells. Schwann cells in culture have a long spindle-shaped cell body and two processes in opposite directions (**Figure 18**), which makes them easily distinguishable from other contaminating cells (DRG neurons and fibroblasts). We counted approximately 1,000 cells for each experimental value.

2.5.7 Preparation and passage of neural stem cells

A pregnant mouse at the specified gestational age of 13.5 days (E13.5) was sacrificed by cervical dislocation. Immediately the uteri were aseptically removed and transferred to 70% ethanol, PBS and to a Petri dish containing sterile Dulbecco's phosphate-buffer saline (PBS, Invitrogen) in order. The amniotic sac was gently removed and each embryo was transferred to a new Petri dish containing fresh pre-cold PBS kept on ice. Embryos were decapitated, mid-dissection-embryo brain skin was exposed and skull peeled away. Ganglionic eminence were dissected and transferred to serum-free medium and then mechanically dissociated by pipetting up and down with three fire-polished Pasteur pipettes with sequentially smaller diameters. After dissociation the neurospheres were centrifuged at 91 x g for 1 minute at room temperature, re-suspended with 0.5 ml of accutase (Invitrogen) and incubated at 37°C for 10 minutes. 0.5 ml of neural stem cell medium was applied to the cells and pipetted up and down for 15 to 20 times to make single cells. After centrifuging at 91 x g for 5 minutes at RT, cells were re-suspended in 5 ml of neural stem cell medium and diluted to 10⁵ cells/ml of neural stem cell medium.

2.5.8 Neurosphere migration assay

After 10 to 15 days cultured *in vitro* in neurosphere-formation medium, the cell migration assay was performed according to the previously described procedure (Decker et al., 2000). Briefly, the non-adherent neurospheres were seeded in 10 µl droplets on glass cover slips pre treated with 0.02% PLL followed by 10 µg/ml laminin or Histone H1 as substrate. Neurospheres were then incubated at 37°C for 20 minutes and after transferred in culture dishes containing 1 ml neurosphere-formation medium (without FGF-2 and EGF) per well with 10 µg/ml soluble colominic acid and/or Histone H1/MARCKS. After 24 hours, migration was

assessed by measurement of the distance from the edge of the sphere to the leading cell of outgrowth. If this distance was more than the diameter of the neurosphere or the neurosphere was completely dispersed, this sphere was evaluated as a migrating neurosphere. (n = 20 per group) using an Axiovert microscope and the AxioVision image analysis system 4.6. The data were analyzed by analysis of Student's t-test, with $p < 0.05$ being considered significant.

IV.2.6 Immunocytochemistry

For immunocytochemistry, dissociated hippocampal/cerebellar neurons or Schwann cells were seeded onto coverslips (d = 12 mm) at the density $2-5 \times 10^5$ cells/ml. Coverslips were first cleaned by extensive washing with acetone and sonification. Then they were washed thoroughly 20-30 times with distilled water and air-dried. Coverslips were then treated with 0.01% PLL overnight at 4°C followed by 2 washes with water, and air-dried under UV light. The cells were cultured in chemically defined serum-free medium for 1-5 days before staining.

2.6.1 Immunocytochemistry of living cells

In order to show cell surface localization/expression of proteins using immunocytochemistry staining of living cells was performed. One hour before the experiment the medium was exchanged to fresh serum free medium. Primary antibodies were added in appropriate concentrations (1:700 in case of anti PSA mouse monoclonal 735 antibodies, 1:3000 in case of anti MARCKS rabbit polyclonal antibodies, 1:50 in case of anti Histone H1 rabbit polyclonal antibodies) to the cells just taken out from the incubator. The cells were immediately put back and incubated with antibodies for 15 minutes at 37°C. Then the cells were carefully washed 3 times with warm PBS and 4% paraformaldehyde (PF) was added for 60 minutes to fix the cells. In order to prevent the exocytosis of cytoplasmic proteins and their non-specific binding to the membrane a part of cells was put on ice for 15

minutes before application of primary antibodies. Then the cells were incubated with primary antibodies of appropriate concentrations during 40 minutes on ice, washed 3 times with cold PBS and fixed in cold 4% PF. Afterwards, the fixing solution was washed out 3 times with PBS. Blocking solution containing 0.1% Triton X-100 was subjected to the fixed cells for 10 minutes at RT with the additional aim to permeabilise cell membranes. Appropriate secondary antibodies coupled to a fluorescent dye (Cy2 or Cy3) were applied to the cells in a dilution of 1:100 for 30 minutes at RT in the darkness and then cells were washed 3 times with PBS. Coverslips with fixed stained cells were put on microscopic slides and embedded into Fluoromount-G (Southern Biotech, Birmingham, UK).

2.6.2 Immunocytochemistry of fixed cells

The medium was removed from the coverslips, the cells were washed with PBS and fixed with 4% PF for 60 minutes at RT. The fixing solution was removed and cells were washed 3 times with PBS. Blocking solution was applied to the fixed cells for 15 minutes and then primary antibodies were added in appropriate concentrations (1:700 in case of anti PSA mouse monoclonal 735 antibodies, 1:3000 in case of anti MARCKS rabbit polyclonal antibodies, 1:50 in case of anti Histone H1 rabbit polyclonal antibodies) for 30 minutes at RT. After washing with PBS appropriate secondary antibodies coupled to a fluorescent dye (Cy2 or Cy3) were applied to the cells in the dilution 1:100 for 30 minutes at RT and then washed 3 times with PBS. Coverslips with fixed stained cells were put on microscopic slides and embedded into Fluoromount-G (Southern Biotech).

2.6.3 Immunocytochemistry of neurospheres

Neurospheres were allowed to settle for 10 minutes after culturing in neurosphere-formation medium [DMEM/F12 (1:1) without L-Glutamine, 1x B27 supplement (Invitrogen), 0.02% sodium bicarbonate (Invitrogen),, 0.5M HEPES (Sigma),, 16.6 mM Glucose (Sigma), 100 mM ,L-glutamine (Invitrogen), 20 ng/ml EGF (company), 20 ng/ml FGF-2 (company)] for 4-5 days. After washing for 3 times in pre-cold-PBS, neurospheres were fixed with 4% PFA in cacodylate buffer at 4°C for 1 hour and dehydrated with 30% sucrose in cacodylate buffer at 4°C for 4 hours. The neurospheres were embedded in tissue-tag, frozen at -30°C and sectioned at 14 µm on a cryostat (Leica CM 3050). Neurosphere sections were blocked with 10% v/v normal goat serum and 0.1% Triton X-100 at room temperature for 1 hour before incubation with the primary antibodies against PSA and Histone H1 (concentration, in with buffer) at 4°C overnight. After washing for 3 times with PBS, appropriate secondary antibodies coupled to fluorescent dye Cy3 and Cy 2 were applied to the cells in a dilution of 1:200 for 1 hour at room temperature in the dark. Next, neurosphere sections were washed 3 times with PBS, labeled with bisbenzimidazole (diluted 1:105, Sigma) for nuclei staining and mounted with Fluoromount-G after additional washes in PBS. Images were taken with an Olympus Fluoview 1000 microscope (Olympus, Hamburg, Germany).

2.6.4 Confocal laser-scanning microscopy

All images of dissociated primary neurons/Schwann cells were obtained with a Zeiss LSM510 argon krypton confocal laser-scanning microscope equipped with a 60x oil-immersion objective lens. Images were scanned with a resolution of 512x512. Detector gain and pinhole were adjusted to give an optimal signal to noise ratio.

IV.2.7 Femoral nerve injury and morphology

2.7.1 Animals

C57BL/6J female mice at the age of 3-4 months were obtained from the central animal facility of the Universitätsklinikum Hamburg-Eppendorf. Animals were kept under standard laboratory conditions. All experiments were conducted in accordance with the German and European Community laws on protection of experimental animals. The procedures used were approved by the responsible committee of The State of Hamburg. Numbers of animals studied in different experimental groups and at different time periods after surgery are given in the text and figures. All animal treatments, data acquisition and analyses were performed in a blinded fashion.

2.7.2 Femoral nerve injury and Histone H1 application

Animals were anaesthetized by intraperitoneal injections of 0.4 mg kg⁻¹ fentanyl (Fentanyl-Janssen, Janssen-Cilag GmbH, Neuss, Germany), 10 mg * kg⁻¹ droperidol (Dehydrobenzperidol, OTL Pharma, Paris, France) and 5 mg * kg⁻¹ diazepam (Ratiopharm, Ulm, Germany). The right femoral nerve was exposed and nerve transection performed at a distance of approximately 3 mm proximal to the bifurcation of the nerve into motor and sensory branches (**Figure 12A, B**). A polyethylene tubing (3 mm length, 0.58 mm inner diameter; Becton Dickinson, Heidelberg, Germany) was placed between the two nerve stumps (**Figure 12C**) and filled with PBS containing Histone H1 (with a concentration of 200 µg/ml) that forms a gel matrix support (0.5% PuraMatrix Peptide Hydrogel, 3D, BD Biosciences, USA), or PBS. The cut ends of the 20 nerve were inserted into the tube and fixed with single epineural 11-0 nylon stitches (Ethicon, Norderstedt, Germany) so that a 2 mm gap was present between the proximal and distal nerve

stumps. Finally, the skin wound was closed with 6-0 sutures (Ethicon). At least 8 animals were operated for each group.

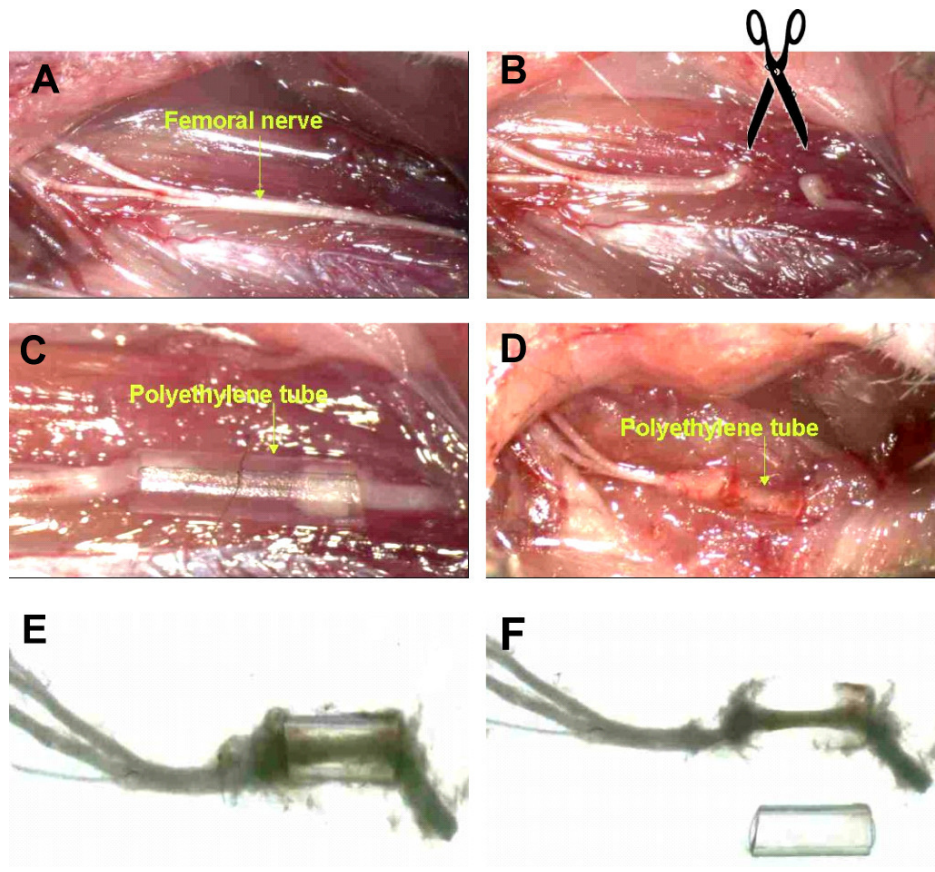


Figure 12. Femoral nerve surgery and regeneration.

(A) An intact femoral nerve (arrow) with its two major branches (on left hand side): the thicker quadriceps (motor) branch (upper one in A) and the thin saphenous (sensory) branch. Transection of the femoral nerve was performed proximal to the bifurcation (B) followed by surgical repair using a polyethylene tube (C). Panels D-F show the macroscopic appearance of a regenerated nerve 3 months after surgery in situ (D) and after dissection (E, F). Figures were taken with a "Stemi 2000-C Stereo Microscope" from Zeiss, with the program "Second32". Picture taken from Mehanna A. (Regeneration in peripheral and central nervous systems after injury and application of glycomimetics. Study in *Mus musculus*, Linnaeus-1758, Hamburg, 2009)

2.7.3 Analysis of motor function

Functional recovery was assessed by single-frame motion analysis (Irintchev et al., 2005; Ahlborn et al., 2007) to evaluate quadriceps muscle function during ground locomotion. Prior to operation, mice were trained to perform a beam-walking test in which the animal walks unforced from one end of a horizontal beam (length 1000 mm, width 38 mm) towards its home cage located at the other end of the beam. A rear view of one walking trial per animal was captured prior to the operation with a high-speed camera (A602fc, Basler, Ahrensburg, Germany) at 100 frames per second and stored on a personal computer in Audio Video Interleaved (AVI) format. The recordings were repeated 1, 2, 4, 8, 12 and 16 weeks after nerve transection. The video sequences were examined using SIMI-Motion 7.0 software (SIMI Reality Motion Systems, Unterschleissheim, Germany). Selected frames in which the animals were seen in defined phases of the step cycle were used for measurements of two parameters as described previously (Irintchev et al., 2005): the foot-base angle (FBA) and the heels-tail angle (HTA). The analysis was performed with UTHSCSA Image Tool 2.0 software (University of Texas, San Antonio, TX, USA, <http://ddsdx.uthscsa.edu/dig/>). Both parameters are directly related to the ability of the quadriceps muscle innervated by the motor branch of the femoral nerve to keep the knee joint extended during contralateral swing phases. As a relative measure of functional recovery at different time-point after nerve injury, the stance recovery index was calculated, which is a mean of the recovery index (RI) for the HTA and the FBA. The index for each angle is calculated in percent as: $RI = [(X_{reinn} - X_{den}) / (X_{pre} - X_{den})] \times 100$, where X_{pre} , X_{den} and X_{reinn} are values prior to operation, during the state of denervation (7 days after injury), and at any given time-point during reinnervation, respectively. A third parameter, the limb protraction length ratio (PLR), was evaluated from video recordings of voluntary pursuit movements of the mice. The mouse, when held by its tail and allowed to grasp a pencil with its fore paws, tries to catch the object with its hind paws and extends simultaneously both hind limbs. In intact animals the

relative length of the two extremities, as estimated by lines connecting the most distal mid-point of the extremity with the anus, is approximately equal and the PLR (ratio of the right to left limb length) is close to 1. After unilateral injury, the denervated limb cannot extend maximally and the PLR increases significantly above 1.

2.7.4 Retrograde labelling and evaluation of motoneuron number and soma size

Following the last video recording, mice were re-operated for retrograde labelling. Under fentanyl/droperidol/diazepam anaesthesia, the two nerve branches were transected ~5 mm distal to the bifurcation, and two fluorescent dyes, Fast Blue (EMS-Chemie, Großumstadt, Germany) and Fluoro-Gold (Fluorochrome, Denver, CO, USA), were applied to the motor and sensory branches, respectively. One week later, the animals were perfused with 4% formaldehyde (Sigma-Aldrich) in 0.1 M sodium cacodylate buffer, pH 7.3, and spinal cords and femoral nerves were dissected for morphological analyses. After overnight fixation, the lumbar part of the spinal cord was cut transversely (serial sections of 50 µm thickness) on a Leica vibratome VT1000S (Leica). The sections were examined under a fluorescence microscope (Axiophot 2, Zeiss) with appropriate filter sets. All cell profiles labelled with one of the dyes or with both tracers are distributed within a stack of 35–45 serial cross-sections. Each section, containing typically 2–5 labelled cell profiles, was examined using a 40x objective by focusing through the section thickness starting from the top surface. All profiles except those visible at the top surfaces of sections were counted (Simova et al., 2006). The application of this simple stereological principle prevents double counting of labelled cells and allows an unbiased evaluation of cell numbers, which does not rely on assumptions or requires corrections. The same sections were used for measurements of soma size using Neurolucida software-controlled computer system (MicroBrightField Europe, Magdeburg, Germany).

2.7.5 Analysis of degree of myelination

After fixation with formaldehyde, femoral nerves were post-fixed in 1% osmium tetroxide in 0.1 M sodium cacodylate buffer, pH 7.3, for 1 hour at room temperature, dehydrated and embedded in resin according to standard protocols. Transverse 1 μm -thick sections from the motor and sensory nerve branches were cut (Ultramicrotome, Leica) at a distance of ~ 3 mm distal to the bifurcation and stained with 1% toluidine blue/1% borax in distilled water. Axonal and nerve fibre diameters were measured in a random sample from each section using a 100x oil objective and a grid with a line spacing of 30 μm projected into the visual field of an Axioskop microscope (Zeiss) equipped with a motorized stage and Neurolucida software. Selection of the reference point (zero coordinates) of the grid was random. For all myelinated axons crossed by or attaching the vertical grid lines through the sections, mean orthogonal diameters of the axon (inside the myelin sheath) and of the nerve fibre (including the myelin sheath) were measured. The mean orthogonal diameter is calculated as a mean of the line connecting the two most distal points of the profile (longest axis) and the line passing through the middle of the longest axis at right angle. The degree of myelination was estimated by the ratio axon to fibre diameter (g-ratio).

V Results

V.1 Histone H1 is a potential binding partner of PSA

Immunoaffinity chromatography with PSA-mimicking anti-idiotypic scFv antibody was used to identify novel PSA binding partners previously in our institute (von der Ohe). First, scFv antibodies that bind to PSA antibodies were isolated. Therefore, phage scFv library was screened for phages binding to immobilized PSA antibody. Next, ELISA and surface plasmon resonance (SPR) were performed to determine whether the binding of scFv antibodies deriving from the selected phages was PSA-specific. The binding of the scFv antibodies to immobilized PSA antibody was inhibited by the bacterial homolog of PSA, colominic acid, in a concentration-dependent manner in both assays, while other negatively charged polymers such as chondroitin sulfate A and C or heparin showed no inhibition of the binding. Furthermore, the scFv antibodies did not bind to substrate coated HNK-1 antibody. These results indicate that the selected scFv antibodies mimic PSA. The purified scFv antibodies were used for affinity chromatography using brain fractions. A 33 kD and a 45 kD protein were eluted from the scFv column when a fraction which was enriched in membrane-associated proteins that were removed from the membranes by alkaline treatment was used, while a 70 kDa and a 50 kD protein were isolated from a fraction consisting of soluble brain proteins. Mass spectrometry identified Histone H1 in the 33 kD band, Myristoylated Alanine Rich C Kinase Substrate (MARCKS) in the 70 kD band, NAP22 in the 50 kDa and IgG in the 45 kD band. This result suggested that Histone H1 and MARCKS and NAP22 are binding partners of PSA.

To verify the direct interaction between Histone H1 and PSA, an ELISA with purified colominic acid was performed using purified Histone H1 from calf thymus

as substrate coat and GAPDH a negative control substrate coat. PSA directly binds in a concentration dependent manner to Histone H1, but not to GAPDH (**Figure 13**) indicating that Histone H1 and PSA can interact directly with each other.

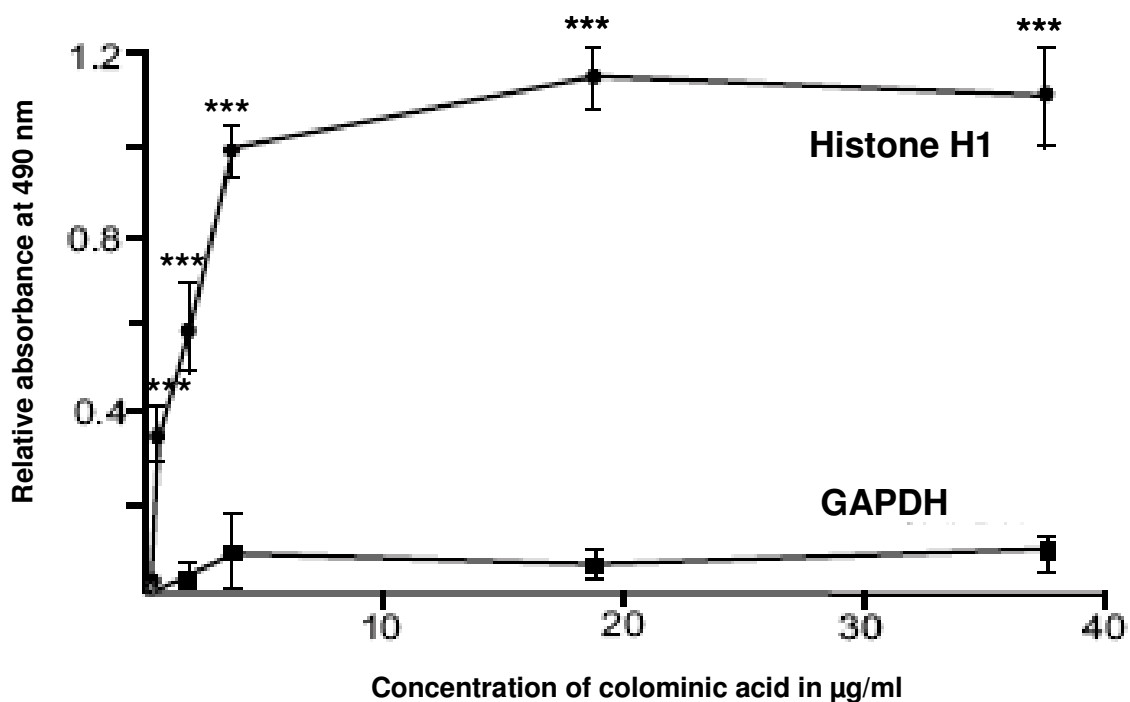


Figure 13. Histone H1 directly binds to colomic acid in a concentration dependent manner. Binding of colomic acid to substrate-coated Histone H1 and GAPDH (negative control) was tested using monoclonal 735 antibodies against colomic acid. Wells were coated with 10 µg/ml of Histone H1 and GAPDH, washed, blocked and incubated with 0-38 µg/ml colomic acid. After washing, wells were incubated with anti-PSA antibody (5 µg/ml), washed again and horseradish peroxidase conjugated secondary antibodies were used for detection. Mean values ± standard deviations are from one representative experiment out of three independent experiments carried out in triplicates. Triple asterisks denotes $p < 0.001$, two-tailed t test.

V.2 Histone H1 is present at the surface of cultured cerebellar neurons

Since polysialylation of NCAM occurs only extracellularly, proteins able to interact to PSA should be present -temporary or constantly- at the surface of neuronal cells. To test, whether Histone H1 is present at the outer surface of neuronal cells, cerebellar granule cells were subjected to surface biotinylation. Biotinylated proteins were isolated using streptavidin magnetic beads and separated by SDS-PAGE. Western blot analysis with polyclonal α -Histone H1 antibodies showed that a dimeric form of Histone H1 (**Figure 14**) could be isolated from cerebellar granule cells as biotinylated surface protein. Detection using NeutrAvidin-horse radish peroxidase (HRP) confirmed that proteins with an apparent molecular weight of 62 kDa (dimeric Histone H1) were indeed biotinylated (**Figure 14**).

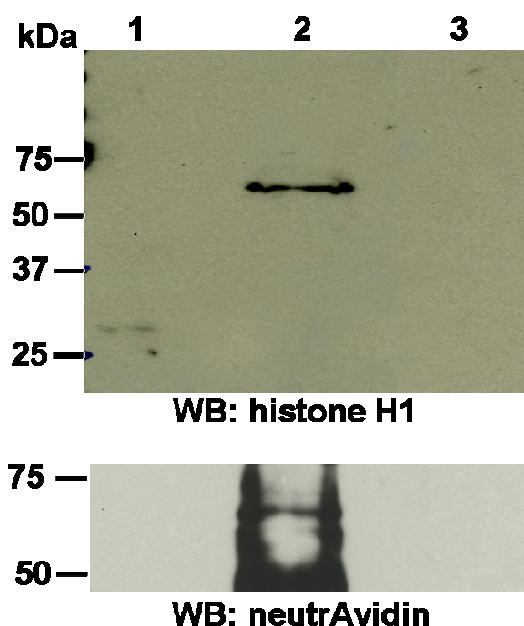


Figure 14. Histone H1 is present at the surface of cultured cerebellar granule cells.

Cerebellar granule cells were isolated, seeded on PLL coated 6-well plates and grown in defined serum free medium for 24 hours. Then cells were treated with biotinylation reagent (lane 2) or mock treated (without biotinylation reagent; lane 1 and 3) for 10 minutes and lysed with lysis buffer. Biotinylated surface proteins were precipitated by streptavidin beads (lane 2 and 3) and subjected to SDS-PAGE. Cell lysates (lane 1) were used as input control. Western blot (WB) analysis using either polyclonal α -Histone H1 antibodies or NeutrAvidin-HRP demonstrated that Histone H1 is localized at the outer surface of neuronal cells.

To further corroborate the notion that Histone H1 interacts with PSA, live immunocytochemical staining was performed to test whether Histone H1 and PSA co-localize at the surface of cultured cerebellar neurons. Confocal microscopic analysis using a polyclonal Histone H1 antibody and a monoclonal PSA antibody showed Histone H1 (**Figure 15B**) and PSA (**Figure 15C**) immunoreactivity both at the surface and neurites of neuronal cell bodies. Superimposed images (**Figure 15D**) demonstrated that a significant portion of Histone H1 co-localizes with PSA. The co-localization of Histone H1 and PSA at the cell surface of live neural cells suggests that both molecules associate *in vivo* in brain.

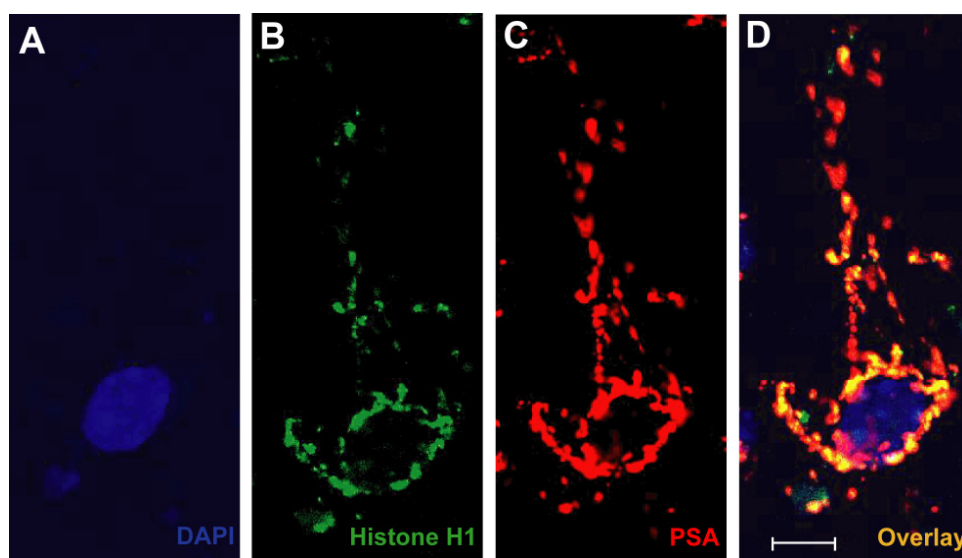


Figure 15. Histone H1 and PSA co-localize on the surface of cultured cerebellar granular cells.

Primary cultures of cerebellar granular cells were grown in defined serum free medium for 24 hours and live staining with Histone H1 (B) and PSA specific (C) antibodies was performed to make sure that only surface components are stained. Afterwards, cells were fixed and appropriate fluorescent secondary antibodies were applied. Microscopic evaluation revealed that the cerebellar granular cells expressed PSA and Histone H1 at the cell surface and on processes. (Scale bar, 10 μ m).

V.3 Histone H1 alters PSA induced neurite outgrowth of cerebellar neurons

To determine the functional consequences of the interaction between PSA and Histone H1 it was analysed if binding of Histone H1 to PSA influences PSA induced neurite outgrowth was analysed (**Figure 16**). Therefore, cerebellar neurons were grown on substrate-coated PLL or PLL with Histone H1 in the absence or presence of soluble PSA. In parallel, neurons were grown on PLL in the presence of soluble PSA and polyclonal Histone H1 antibody to block endogenous Histone H1 and its effect on neurite outgrowth. Neurite outgrowth on substrate coated Histone H1 was enhanced approximately 3 fold when compared to that seen on PLL substrate and reached values obtained for the positive control substrate laminin. Similarly, neurite outgrowth on PLL increased approximately 3 fold when soluble PSA was present, while a 2 fold increase in neurite outgrowth was observed in the presence of soluble Histone H1 indicating that soluble PSA and Histone H1 individually trigger neurite outgrowth. However, in the concomitant presence of soluble Histone H1 and PSA neurite outgrowth was only slightly affected, indicating that soluble Histone H1 and PSA interact and are no longer able to trigger neurite outgrowth. Addition of soluble Histone H1 antibody significantly blocked the neurite outgrowth promoting effect of soluble PSA, while the antibody had no significant effect on neurite outgrowth in the absence of PSA. These results indicate that interaction between Histone H1 and PSA play a crucial role in neurite outgrowth.

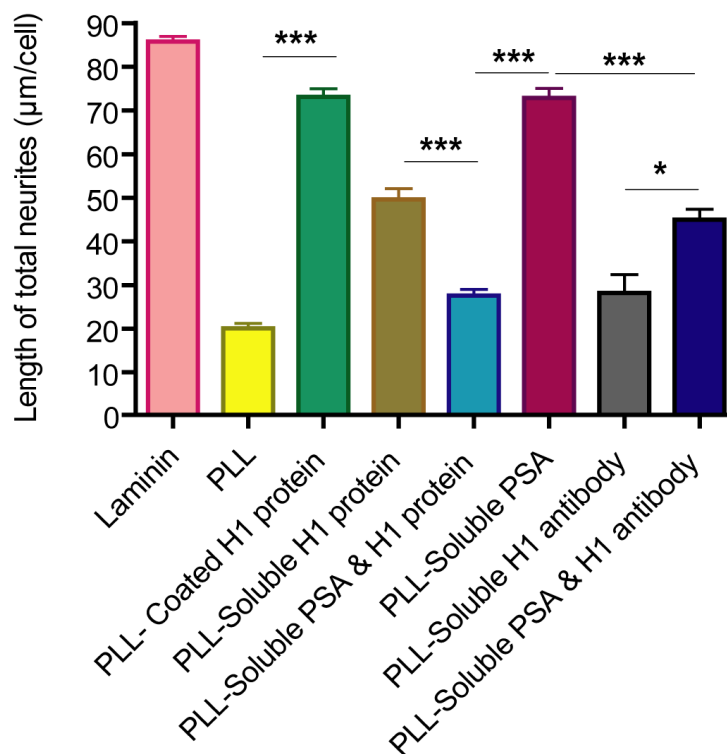


Figure 16. Histone H1 stimulates outgrowth of cerebellar neurons in a PSA dependent manner.

Neurons from wild type mice were seeded (2×10^5) as single cell suspensions on 48-well PLL-treated tissue culture plates coated with or without Histone H1. Soluble Histone protein, anti Histone H1 antibody, PSA peptide and a combination of PSA peptide with either Histone H1 protein or anti Histone H1 antibody were applied 1 hour after seeding and cells were cultured for additional 24 hours. Afterwards cells were fixed and stained and neurite outgrowth effect of Histone H1 and PSA was determined. Bars marked by asterisks and triple asterisks denotes $p < 0.05$ and $p < 0.001$ respectively, two-tailed t test; $n > 100$ neurons in three independent experiments.

V.4 Histone H1 and PSA influence process formation and proliferation of Schwann cells *in vitro*

It has been shown that a PSA mimicking peptide improves myelination by Schwann cells *in vivo* (Mehanna et al., 2009). These findings suggested that Histone H1 and PSA have a possible effect on Schwann cell process formation. But before going to analyse the functional consequence, expression of both

Histone H1 and PSA on the surface of Schwann cells was checked by live immunocytochemical staining. Confocal microscopic analysis using a polyclonal Histone H1 antibody and a monoclonal PSA antibody showed Histone H1 (**Figure 17B**) and PSA (**Figure 17C**) immunoreactivity at the surface of Schwann cells. Superimposed images (**Figure 17D**) demonstrated that a significant portion of Histone H1 co-localizes with PSA.

To test the assumption that Histone H1 and PSA have a possible effect on Schwann cell process formation, Schwann cells from dorsal root ganglia of early postnatal mice were cultured on substrate coated PLL or Histone H1 or in the presence of soluble Histone H1 protein or soluble PSA and the lengths of Schwann cell processes were measured. Morphometric analysis of Schwann cell process length revealed an increase of process length on substrate coated Histone H1 relative to PLL substrate and also in the presence of soluble PSA or soluble Histone H1 (**Figure 17E**). The concomitant presence of soluble PSA and Histone H1 led to a neutralization of the promotional affect seen with the PSA and Histone H1 when applied individually.

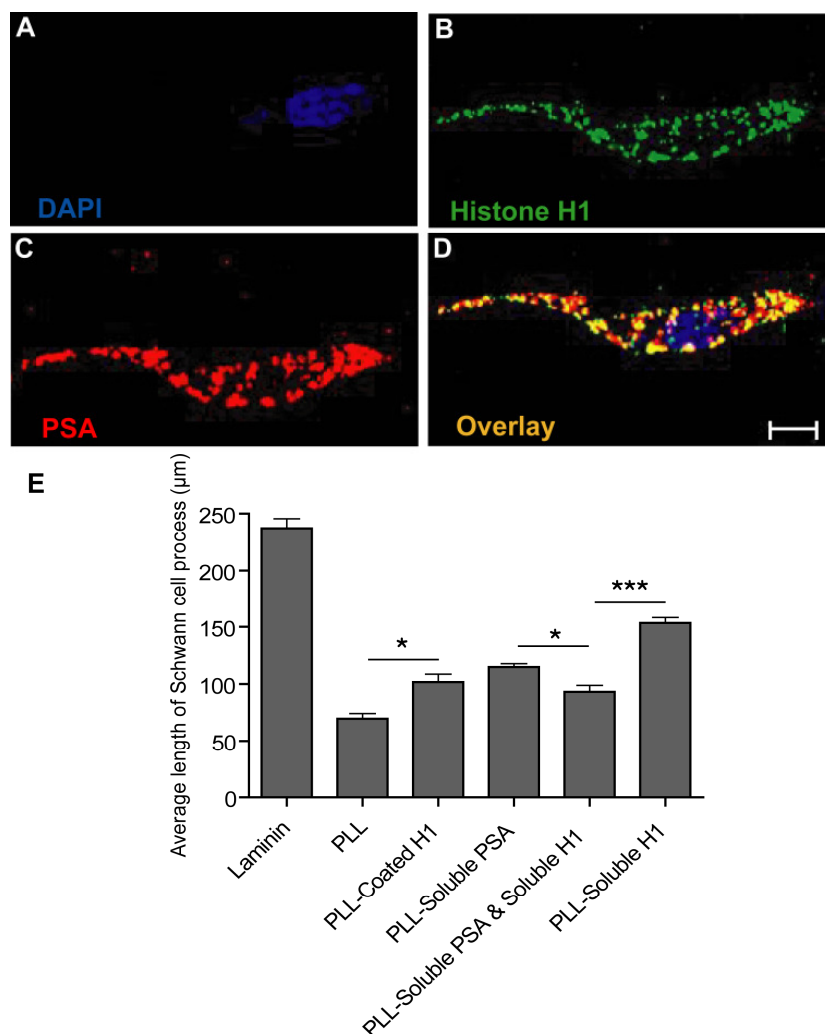


Figure 17. Histone H1 and PSA are present at the surface of Schwann cells and Histone H1 and PSA stimulate Schwann cell process formation.

Primary cultures of Schwann cells were stained with (A) DAPI, (B) Histone H1 and (C) PSA specific antibodies. Schwann cells express PSA and Histone H1 at the cell surface and on processes (scale bar, 10 µm). (E) Schwann cells isolated from dorsal root ganglia of wild type mice were seeded (50,000 cells/well) as single cell suspensions on 48 well PLL-treated tissue culture plates coated with or without Histone H1. Soluble Histone protein, PSA and a combination of soluble PSA with or without Histone H1 protein were used to investigate the effect of Histone H1 on process outgrowth of Schwann cells in presence or absence of PSA. Error bars indicate S.D. from at least three independent experiments. Bars marked by asterisks and triple asterisks denotes $p < 0.05$ and $p < 0.001$ respectively, two-tailed t test; $n > 100$ cells in three independent experiments.

In addition, the effect of the Histone H1 and PSA on Schwann cell proliferation was

also tested by analysis of BrdU incorporation and results showed that Schwann cell proliferation was enhanced by at least 184% and 123% in the presence of soluble Histone H1 and soluble PSA, respectively, when compared to proliferation in the absence of PSA and Histone H1. The mixture of soluble Histone H1 and soluble PSA decreased the proliferation (**Figure 18A, B**).

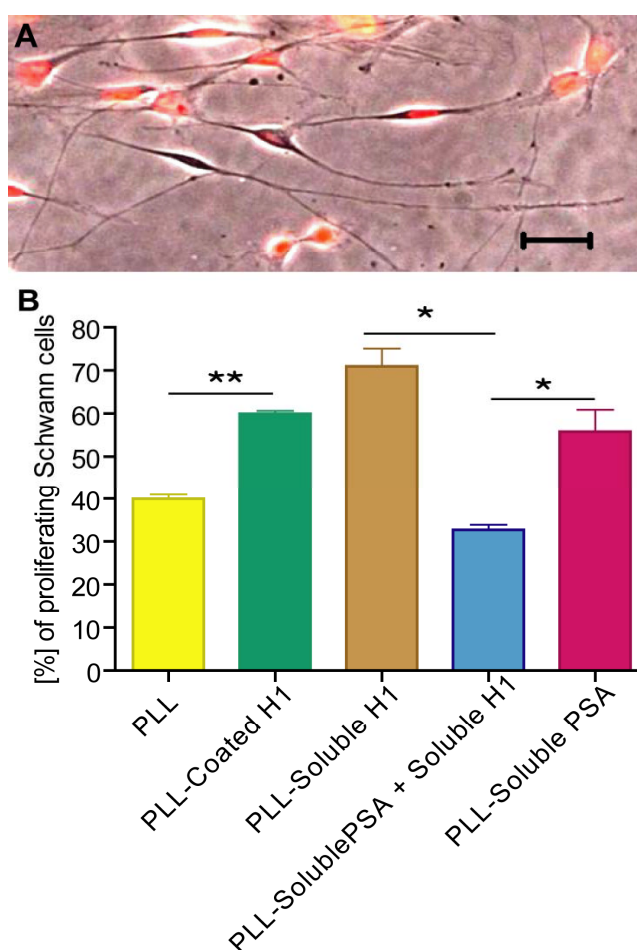


Figure 18. Analysis of Schwann cell proliferation *in vitro*.

(A) Representative picture of Schwann cells isolated from dorsal root ganglia of wild type mice. Schwann cells were treated 4 hours after seeding with 20 μM BrdU for 48 hours to label proliferating cells. Schwann cells were identified by phase contrast microscopy as elongated bipolar cells (scale bar, 20 μm). (B) Schwann cells seeded (200,000 cells/well) as single cell suspensions on 10 mm glass cover slips pre-treated with 0.01% PLL followed by substrate coating with or without Histone H1. Soluble Histone protein, PSA and a combination of soluble PSA with or without Histone H1 protein were used to investigate the effect of Histone H1 on Schwann cell proliferation

in presence or absence of PSA. Error bars indicate S.D. from at least two independent experiments. Bars marked by asterisks and double asterisks denotes $p < 0.05$ and $p < 0.01$ respectively, two-tailed t test; $n > 1000$ cells in two independent experiments.

V.5 Histone H1 and PSA alter migration of neural precursor cells *in vitro*

Previous studies have suggested that PSA is required for tangential migration of neural precursors toward the olfactory bulb (Chazal et al., 2000; Hu, 2000). Based on these studies, the possible effect of Histone H1 on neural precursor cell migration *in vitro* was investigated by using substrate coated Histone H1, soluble Histone H1 or soluble PSA. As seen on the positive control substrate laminin, migration of neural stem cells was enhanced either when soluble PSA, substrate coated or soluble Histone H1 was applied. A mixture of PSA and Histone H1 had only a slight effect on neural precursor migration. On PLL, the progenitor cells did not migrate out of the neurosphere, while neural progenitor cells migrated out of the neurosphere when grown on laminin or Histone H1 (**Figure 19**). The migration of neural progenitor cells ceased when a mixture of soluble Histone H1 and PSA was applied to the medium. This finding indicates that both Histone H1 and PSA are important for neural progenitor cell migration *in vitro*.

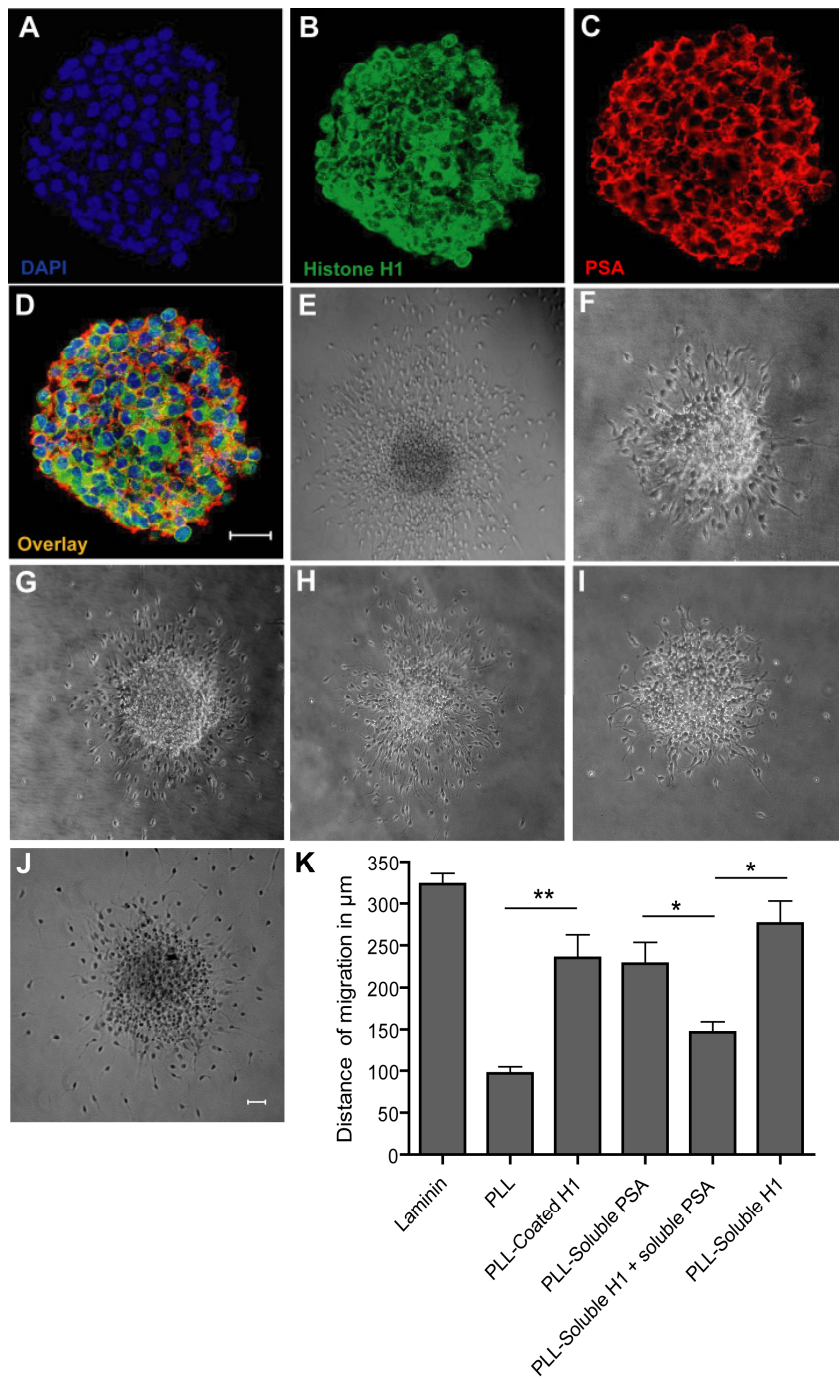


Figure 19. Histone H1 and PSA are expressed on neurospheres and Histone H1 and PSA alter migration of neural precursors.

Neurospheres were fixed with cacodylate buffer followed by dehydration with 30% sucrose.

Afterwards neurospheres were embedded in tissue-tag, frozen at -30°C and sectioned into $14\ \mu\text{m}$ thick slices and were stained with (A) DAPI (B) Histone H1 and (C) PSA specific antibodies (scale bar, $10\ \mu\text{m}$). To determine Histone H1 and PSA dependent migration of neurospheres derived from mouse E13.5, neurospheres were plated on cover glass pre-treated with 0.02% PLL and coated with (E) $10\ \mu\text{g/ml}$ laminin or (F) without laminin (PLL) (G) $10\ \mu\text{g/ml}$ Histone H1 (H) $10\ \mu\text{g/ml}$ soluble PSA (I) $10\ \mu\text{g/ml}$ Histone H1 and same concentration of soluble PSA and (J) $10\ \mu\text{g/ml}$ soluble Histone H1. Cell migration was assessed. Data are the SD of at least three independent experiments (bar $20\ \mu\text{m}$.) (K) The effect of Histone H1 and PSA on the migration of neurospheres is quantitated as a mean distance travelled by migrating neurospheres \pm SD ($n = 20$ per group). Bars marked by asterisks and double asterisks denotes $p < 0.05$, and $p < 0.01$ respectively, two-tailed t test; $n = 20$, in three independent experiments.

V.6 Histone H1 promotes functional recovery after femoral nerve injury in adult mice

Since PSA enhances regeneration after injury of the peripheral nervous system of adult mice (Mehanna et al., 2009) and since we have observed that Histone H1 has beneficial effects on Schwann cells and neurons, we addressed the question whether Histone H1 also enhances regeneration after femoral nerve injury. Function of the quadriceps muscle in mice was evaluated after treated with Histone H1 or PBS during a 4 months period after surgery. Femoral nerve injury in mice induces changes in gait which can be precisely evaluated by two parameters, the heels-tail angle (HTA) and the foot-base angle (FBA) evaluated during beam walking (**Figure 20 A, H**). Changes in gaits are caused by impaired extensor function of the quadriceps muscle leading to abnormal external rotation of the ankle (**Figure 20 A, D**) and high heel position (**Figure 20 E, H**) at defined gait cycle phases. We used these parameters to evaluate the effect of Histone H1 on locomotor recovery. Superior functional recovery after Histone H1 treatment was apparent when the stance recovery index was calculated for both angles on an individual animal basis. Stance recovery index is a measure of the individual degree of recovery and reflects the degree of post-operative normalization of the quadriceps extensor function during ground locomotion. The recovery index

reached 100% at 4 months in animals treated with Histone H1, which was not statistically different from the pre-operative values (100%; $p > 0.05$, analysis of variance [ANOVA] and Tukey's post hoc test) indicates complete functional recovery. At the same time recovery from the control group of mice was calculated as 62%; $p > 0.05$, compared with the preoperative index of 100%, ANOVA and Tukey's post hoc test. One week after injury, the degree of functional impairment, as evaluated by the increase of the foot-base angle (**Figure 20B**) and decrease of the heels-tail angle (**Figure 20F**) compared with the pre-operative values and found to be similar between groups of mice treated with Histone H1 and PBS (negative control) .

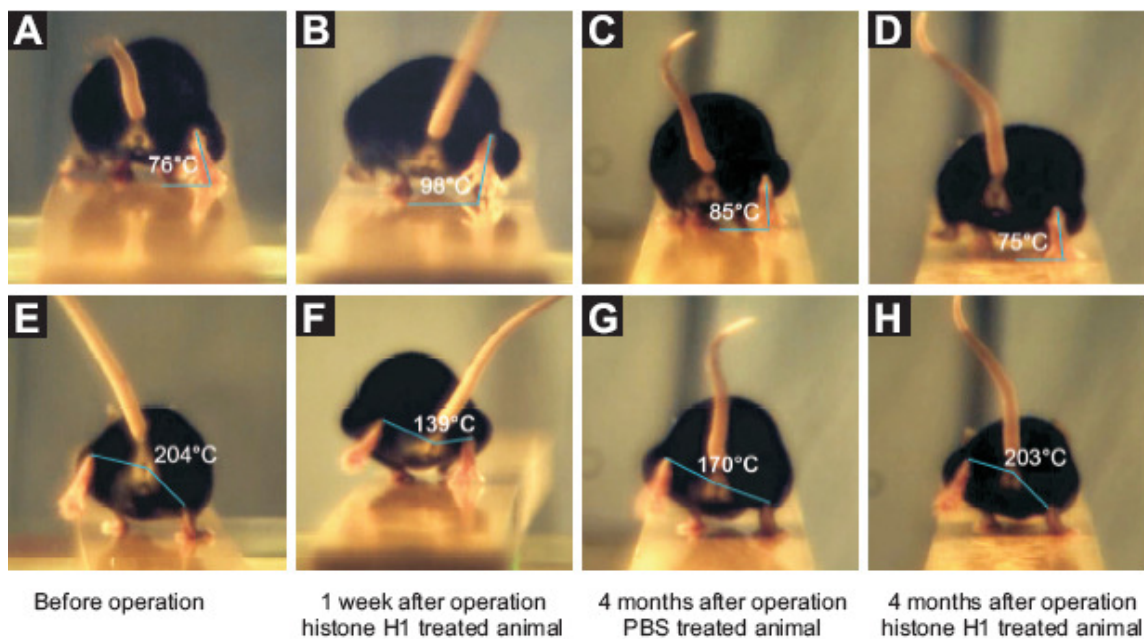


Figure 20. Analysis of motor function in the mouse after femoral nerve lesion and application of Histone H1.

Single video frames from recordings of beam walking (A-H) of C57BL/6J mice prior to (day 0, panels A, E), one week (panels B, F) and three months (panels C, D, G, H) after surgical repair of the right femoral nerve. Animal showed in panel C and G are treated with PBS (negative control) and animal showed in panel B, F, D and H are treated with Histone H1. Panels A-D show video frames in which the right paws of the mouse is at take-off position. Such frames were used for measuring the foot-base angle shown by lines drawn in the panels. Quadriceps muscle dysfunction causes an abnormal external rotation of the heel (panels B-D) resulting in a larger angle compared with the angle prior to operation (A). In panels E-H the mouse is seen at mid-stance of the right hind limb and maximum altitude of the contralateral swing. Such video frames were used to measure the

heels-tail angle as shown by the lines drawn in all the panels. Note the decrease of the angle after operation (panels F-H) resulting from higher position of right heel in all the panels compared with E.

Better functional improvement was observed in Histone H1-treated mice compared to the control groups at 12 and 16 weeks after injury. (**Figure 21C, D**). As estimated by the outcome of femoral nerve repair, at 4 months after injury significantly better in Histone H1-treated mice than in mice treated with PBS ($p < 0.05$, ANOVA with Tukey's *post-hoc* test, Figure 21 C). Thus, the overall results show that Histone H1 treatment leads to a superior functional outcome.

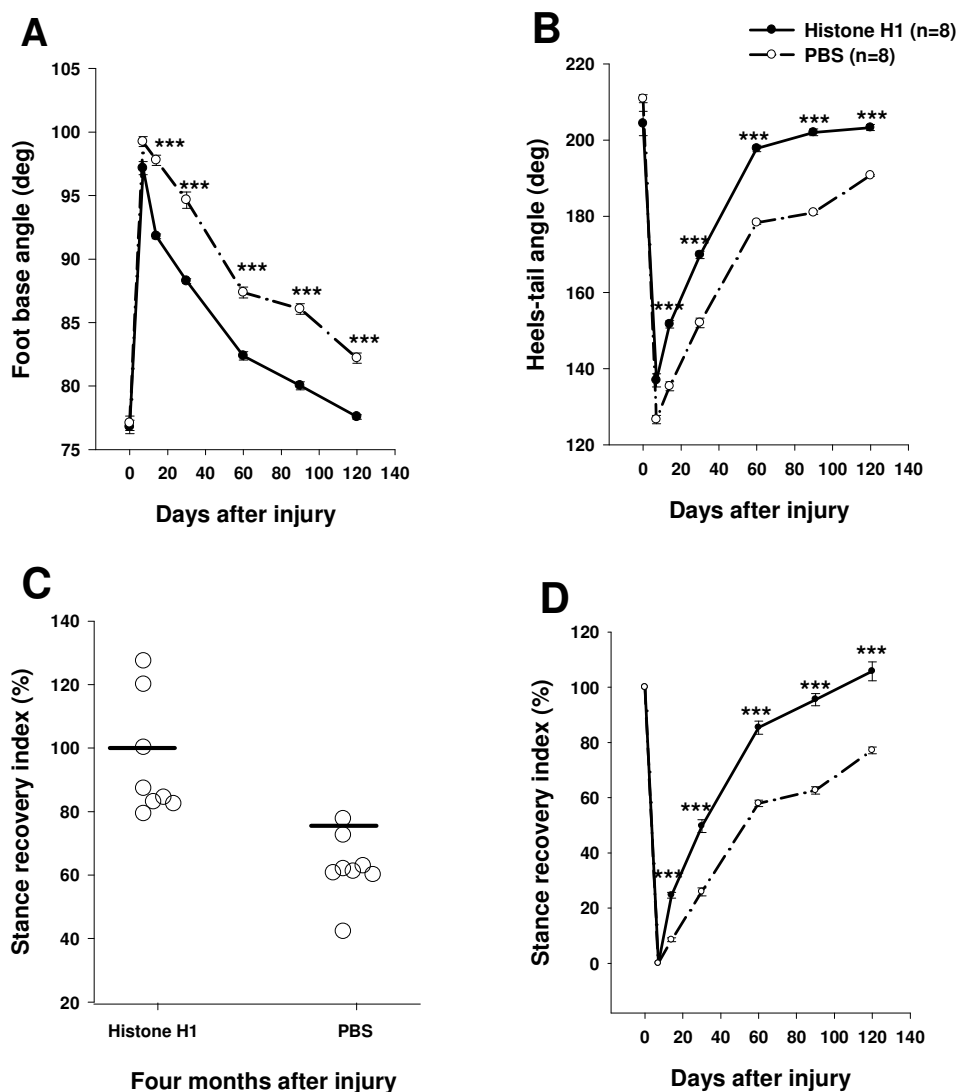


Figure 21. Application of Histone H1 to the lesioned femoral nerve of mice enhances functional recovery.

(A-B) Shown are mean values \pm SEM of foot-base angles (A) and heels-tail angles (B) at different time-points after femoral nerve injury and application of Histone H1 or PBS. Pre-operative values are plotted at day 0. Numbers of animals studied per group are indicated in panel B. Panel C shows individual animal values (circles) and group mean values (horizontal lines) of the stance recovery index calculated for the heels-tail and the foot-base angles at 4 months after injury. A recovery index of 100% indicates complete recovery. n indicates the number of animals operated per group. (D) Comparison of motor recovery in mice treated with Histone H1 and PBS. Shown are mean values \pm SEM of stance recovery indices at different time points after femoral nerve transection and application of Histone H1 or PBS. Asterisks indicate significant differences ($p < 0.05$, one-way ANOVA with Tukey's post-hoc test) between the Histone H1-treated group and the control groups at the given time points.

V.7 Histone H1 promotes survival, regrowth and reinnervation of motoneurons

To search for structural correlates of the superior functional recovery after application of Histone H1, retrograde labelling of regenerated motoneurons was performed in animals after analyzing the functional recovery. The number of motoneurons back-labelled through the motor (quadriceps) which represent correctly projected regrown motoneurons significantly increased in animals to which Histone H1 has been applied relative to PBS treated animals (**Figure 22A**). At the same time, the number of back-labelled motoneurons through the sensory (saphenous) branch representing incorrectly projecting neurons decreased in animals treated with Histone H1 in comparison to animals treated with PBS (**Figure 22A**). The small number of motoneurons back-labelled through both branches of the femoral nerve as well as the total number of labelled neurons was similar in Histone H1 or vehicle treated mice (**Figure 22A**). Since number of retrogradely labelled motoneurons reflect the extent of motoneuron survival (de la Cruz et al., 1994; Waters et al., 1998; Asahara et al., 1999), we can conclude that treatment with Histone H1 reduces motoneuron death, a characteristic feature of the femoral nerve injury paradigm in mice (Simova et al., 2006). On the other hand Histone H1 application improves motoneuron survival and also increases the number of regenerated motoneurons projecting to the appropriate motor nerve branch and thus increases preferential motor reinnervation, which is a characteristic feature of the femoral nerve regeneration (Brushart, 1988; Al-Majed et al., 2000; Franz et al., 2008). In conclusion, our results show that better functional recovery in Histone H1 treated mice attributed to better motoneuron regeneration, since motoneuron loss was reduced and precision of motor reinnervation was improved as compared with control mice. Since a significant correlations between recovery index and motoneuron size have been found 4 months after femoral nerve injury (Simova et al., 2006; Ahlborn et al., 2007), we

measured soma size of motoneurons regrowing their axons correctly and found a significant increase in soma size of correctly projecting motoneurons in Histone H1 treated animals in comparison to PBS treated animals, while no difference in soma size of incorrectly projecting motoneurons was observed among the groups (**Figure 22B**). Therefore, we can attribute better functional recovery in Histone H1-treated mice to larger motoneuron size, which is an indicator of a better functional state of regenerated motoneurons (Simova et al., 2006; Ahlborn et al., 2007). We next analyzed regenerated nerves morphometrically to assess the degree of myelination evaluated by the g-ratio (axon- to fibre-diameter ratio) and found no significant similarity between frequency distributions of the g-ratio for axons of intact and Histone H1 or PBS treated injured nerves (**Figure 22C**), indicating that Histone H1 does not effect myelination during regeneration.

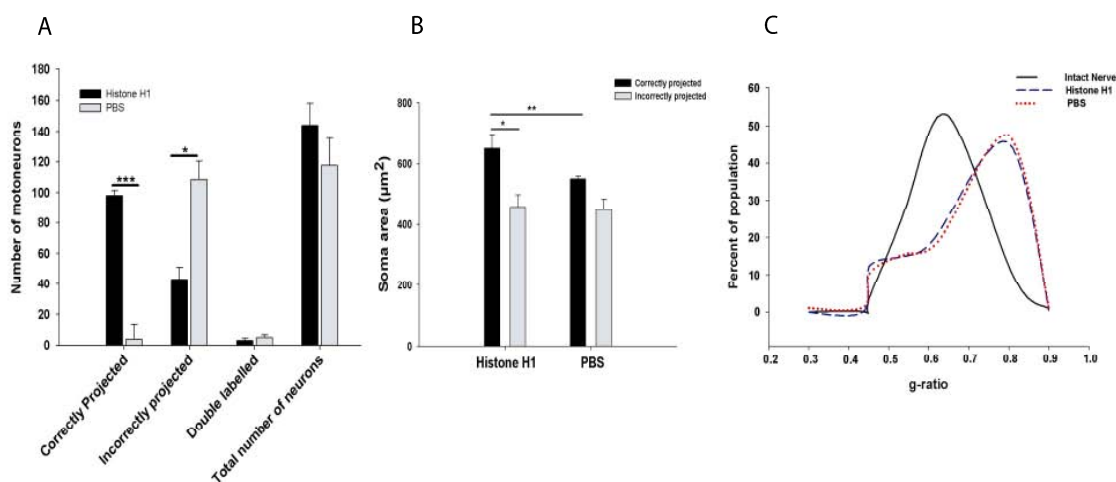


Figure 22. Analysis of regrowth of motoneuron axons after injury.

Four months after femoral nerve injury and application of Histone H1 or vehicle (PBS), animals were subjected to retrolabelling of motoneurons. (A) Mean numbers \pm SEM of motoneurons labelled through the motor branch representing correctly projecting neurons (correct), through the sensory branch representing incorrectly projecting neurons (incorrect), through both branches (mixed) and the sum of labelled neurons (total number) are shown. (B) Morphometric analysis of soma size of regenerated motoneurons was performed. Mean values \pm SEM of soma area of correctly and incorrectly projecting motoneurons after application of Histone H1 or PBS are shown. (A, B)

Significant differences between the groups of eight animals were found ($p > 0.05$, one-way ANOVA with Tukey's *post hoc* test). (C) Analysis of myelinated nerve fibres in regenerated and intact nerves. Shown are normalized frequency distributions of g-ratios (axon/fibre diameter) in the motor nerve branches of the femoral nerve of intact mice (intact) and mice treated with Histone H1 or vehicle (PBS) after femoral nerve injury. Regenerated nerves were studied 4 months after injury.

V.8 Cloning, expression and purification of MARCKS

To verify the interactions of MARCKS with PSA by ELISA experiments it was necessary to obtain purified MARCKS. A recombinant approach was used to express MARCKS with a carboxy terminal His tag and purify this recombinant protein using Ni-NTA affinity chromatography.

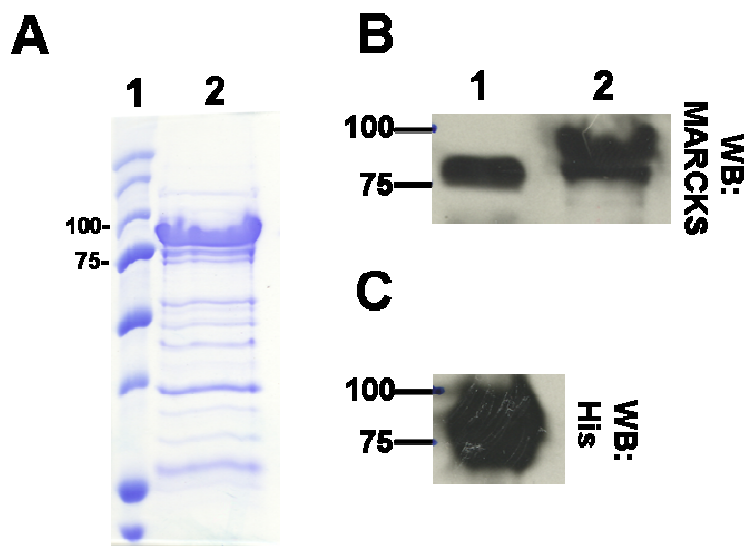


Figure 23. Affinity chromatography using Ni-NTA to purify His-tagged MARCKS from *E. coli*. (A) Lane 1: Protein ladder, Lane 2: purified MARCKS as shown by coomassie blue staining. (B) Western blot showing purified MARCKS protein as detected by polyclonal anti-MARCKS antibody. Lane 1: total brain homogenate, Lane 2: His-tagged MARCKS eluted from the Ni-NTA matrix. (C) His-tagged MARCKS eluted from the Ni-NTA matrix as detected by anti-His antibody.

V.9 Characterization of binding of MARCKS and PSA

To verify the direct interaction between MARCKS and PSA, ELISA with purified colominic acid was performed using purified MARCKS as substrate coat and GAPDH a negative control substrate coat. Histone H1 was taken as positive control as we have already confirmed its tight association with PSA. PSA directly binds to Histone H1, but neither to MARCKS nor to GAPDH, in a concentration dependent manner (**Figure 24**), indicating that MARCKS and PSA do not interact directly.

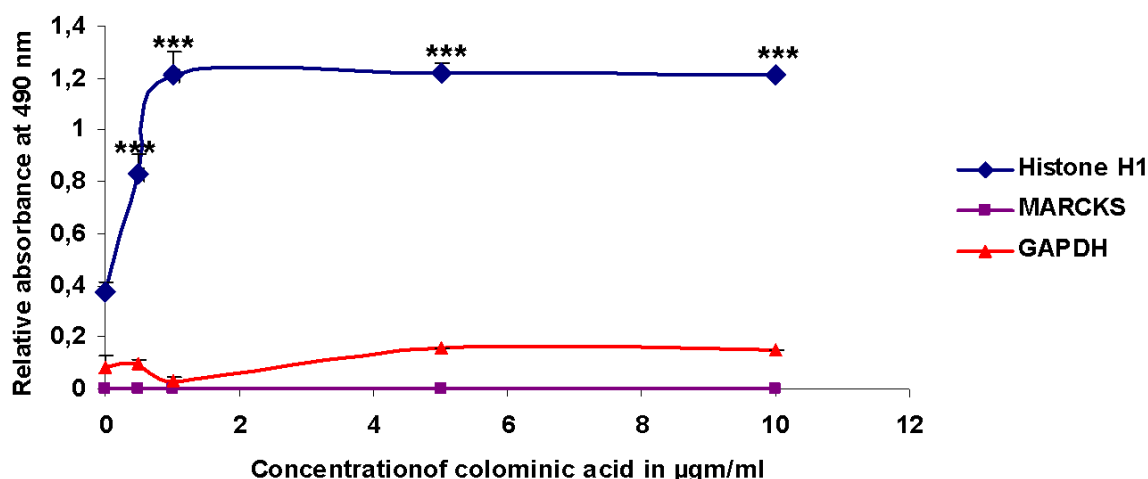


Figure 24. MARCKS does not bind to PSA directly.

Binding of colominic acid to substrate-coated purified MARCKS, Histone H1 and GAPDH (negative control) was tested using monoclonal 735 antibodies against colominic acid. Horseradish peroxidase conjugated secondary antibodies were used for detection. Mean values \pm standard deviations are from one representative experiment out of three independent experiments carried out in triplicates. Triple asterisks denotes $p < 0.001$, two-tailed t test.

V.10 Co-immunoprecipitation of MARCKS and PSA from brain homogenate

Immunoprecipitation of MARCKS from brain homogenate from PSA wild type, endo-N treated and endo N non-treated brain homogenate was performed in order to observe the association between PSA and MARCKS. For this purpose polyclonal MARCKS antibodies were coupled to Protein A/G magnetic beads. After incubation with brain homogenates from endo-N treated and endo N non-treated brain homogenate. Co-precipitated proteins were applied for Western blot analysis using monoclonal α -PSA antibody (**Figure 25**) which demonstrated the co-precipitation of MARCKS from homogenate not treated with endoN, but not from endoN treated sample.

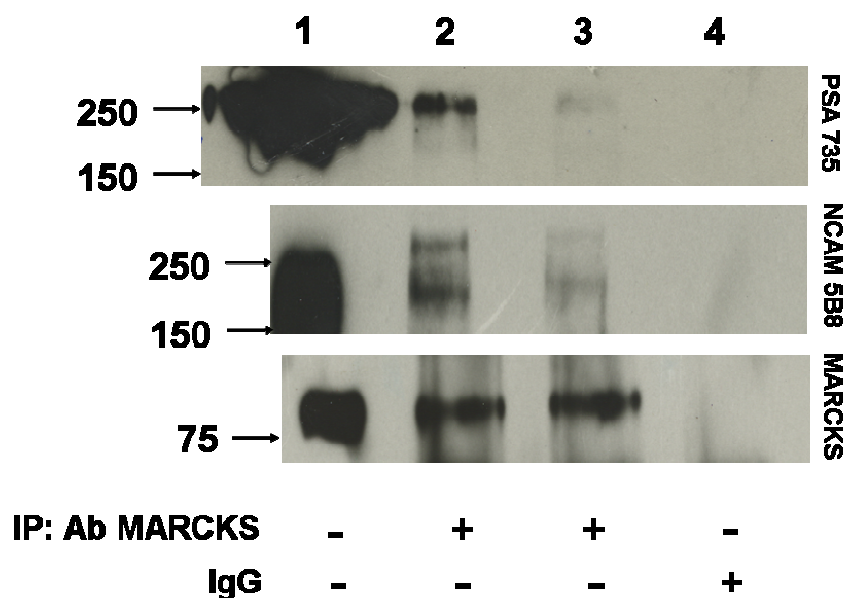


Figure 25. Co-immunoprecipitation of MARCKS and PSA from brain homogenate.
 Lane 1: crude brain homogenate; Lane 2: MARCKS was precipitated using polyclonal α -MARCKS antibodies immobilized on the Protein A/G magnetic beads from homogenate of endo-N non-treated sample; Lane 3: MARCKS was precipitated using polyclonal α -MARCKS antibodies immobilized on

the Protein A/G magnetic beads from homogenate of endo N non-treated samples; Lane 4: MARCKS was precipitated using non-specific rabbit antibodies (negative control) immobilized on the Protein A/G magnetic beads from homogenate of endo-N non-treated sample and subjected for Western blot (WB) analysis using monoclonal α -PSA antibody (IP – immunoprecipitation).

V.11 Confirmation of intracellular localization of MARCKS and colocalization of MARCKS and PSA using immunocytochemistry of live and fixed hippocampal neurons

To observe intracellular localization of MARCKS and also to investigate colocalization of MARCKS and PSA, polyclonal α -MARCKS antibodies were used for immunocytochemical analysis of live and fixed hippocampal neurons. Primary neurons were cultivated in chemically defined serum-free medium for 4-5 days. α -MARCKS polyclonal antibodies were applied to living cells and incubated with antibody during 15 minutes at 37°C. According this procedure only MARCKS associated with the outer membrane (if there) could be labelled. Confocal microscopic analysis revealed no specific MARCKS labelling in this case. This confirms the absence of MARCKS on cell surface. After fixation and permeabilisation of cell membrane the neurons were stained with α -PSA monoclonal antibodies. PSA staining showed the typical surface distribution in neurons (**Figure 26A**, red). Then the subcellular localization of MARCKS in fixed hippocampal neurons was examined using immunofluorescence confocal microscopy. Primary cultured hippocampal neurons were co-stained with MARCKS and PSA after fixation and permeabilization (**Figure 26F**) and shows a significant amount of MARCKS partially co-localize with PSA along neurites and indicates that these two molecules have chance to interact with each other.

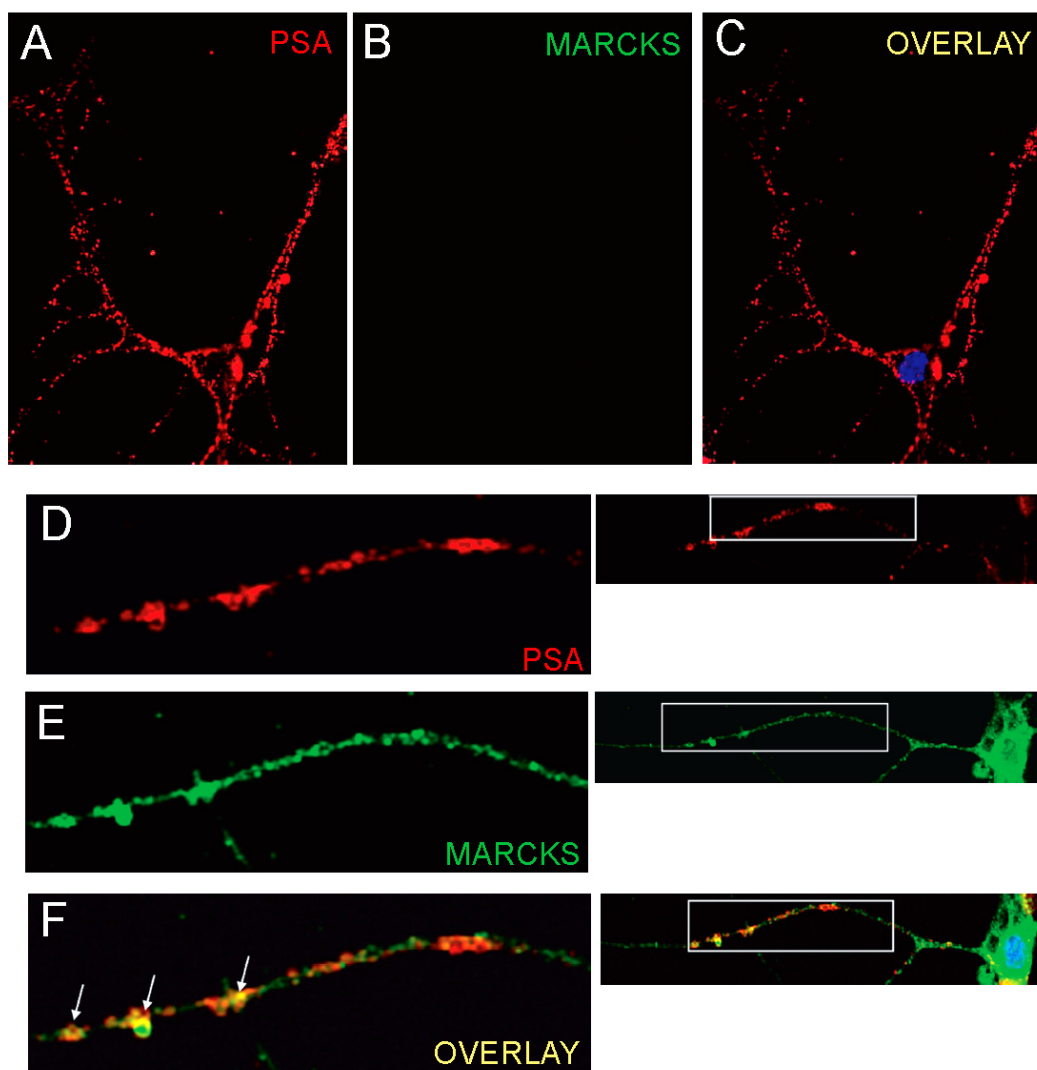


Figure 26. Partial co-localization of MARCKS and PSA in primary hippocampal neuron. Three days-old cultured hippocampal neurons were immunostained with MARCKS rabbit polyclonal antibody (green) and PSA mouse monoclonal antibody (red). Nucleus was stained with DAPI. Images of a representative neuron are shown here. Note that MARCKS partially co-localized with PSA along neurites. Scale bar: 20 μ m.

V.12 MARCKS and PSA alter neurosphere migration *in vitro*

Previous studies have suggested that PSA is required for tangential migration of neural precursors toward the olfactory bulb (Angata, K et al., 2000; Chazal, G et al., 2000; Hu H, 2000) Based on these studies, possible effect of MARCKS on neural precursor cell migration was investigated by using substrate coated MARCKS, soluble MARCKS or soluble PSA *in vitro*. As seen on the positive control substrate laminin, migration of neural stem cells was enhanced either when soluble PSA, substrate coated or soluble MARCKS was applied. A mixture of PSA and MARCKS had only a slight affect on migration. On PLL, the progenitor cells did not migrate out of the neurosphere, while neural progenitor cells migrated out of the neurosphere when grown on laminin or MARCKS (**Figure 27**). The migration of neural progenitor cells ceased when a mixture of soluble MARCKS and PSA were applied to the medium. This finding indicates that both MARCKS and PSA are important for neural progenitor cell migration *in vitro*.

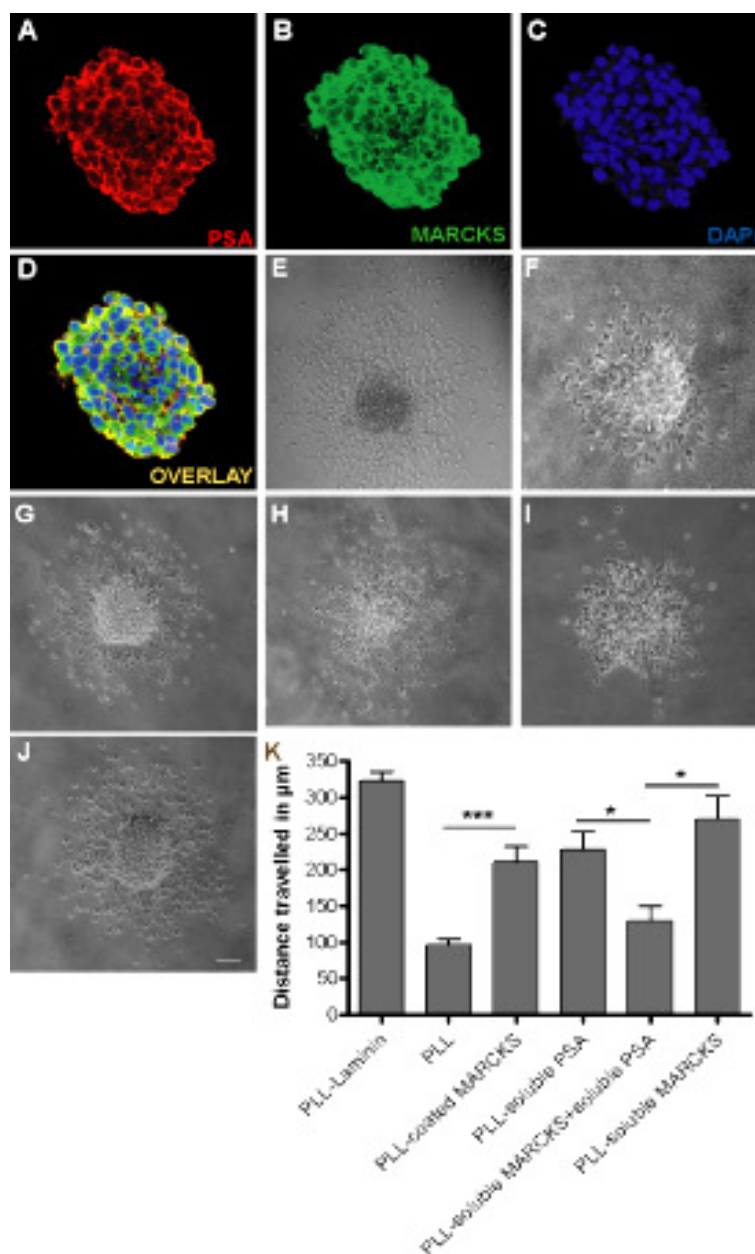


Figure 27. Expression of MARCKS and PSA on neurospheres and effect of MARCKS and PSA on migration of neurospheres.

Neurospheres were fixed with cacodylate buffer followed by dehydration with 30% sucrose. Afterwards neurospheres were embedded in tissue-tag, frozen at -30°C and sectioned into $14\ \mu\text{m}$ thick slices and were stained with (A) PSA (B) MARCKS and (C) DAPI specific antibodies (scale bar, $10\ \mu\text{m}$). To determine MARCKS and PSA dependent migration of neurospheres derived from mouse E13.5, neurospheres were plated on cover glass pre-treated with 0.02% PLL and coated with (E) $10\ \mu\text{g/ml}$ laminin or (F) without laminin (PLL) (G) $10\ \mu\text{g/ml}$ MARCKS (H) $10\ \mu\text{g/ml}$ soluble

PSA (I) 10µg/ml MARCKS and same concentration of soluble PSA and (J) 10µg/ml soluble MARCKS. Cell migration was assessed as described in *Materials and Methods*. Data are the SD of at least three independent experiments (bar 20 µm.) (K) The effect of MARCKS and PSA on the migration of neurospheres is quantitated as a mean distance travelled by migrating neurospheres ± SD (n = 20 per group). Bars marked by asterisks and double asterisks denotes p< 0.05, and p<0.01 respectively, two-tailed *t* test; n =20, in three independent experiments.

VI. Discussion

This project mainly focuses on potential binding partners of PSA. Main goal of the project was functional characterization of association between PSA and its identified potential binding partners, i.e. Histone H1 and MARCKS and the application of Histone H1 on the treatment of peripheral nerve injuries.

VI.1 Histone H1 is a novel binding partner of PSA

In this study few hints were obtained that indicates Histone H1 is involved in the development and regeneration of the nervous system via its interaction with PSA. PSA is involved in processes that are important during development of the nervous system, such as neural cell migration, neuritogenesis and synaptogenesis (for review see Rutishauser, 2008; Kleene and Schachner, 2004). In early steps of development PSA is highly expressed, whereas the expression decreases to low levels in later stages. In the adulthood, PSA plays an important role in nervous system function and in synaptic plasticity. The functional and developmental defects observed upon ablation of PSA in mouse mutants lacking the main PSA carrier NCAM or the polysialyltransferases essential for the synthesis of PSA underscore the functional importance of PSA. In addition, the effects observed upon application of endoneuraminidase N which specifically degrades PSA further documented the functional plasticity of PSA. Although much is known about the functions of PSA which have been intensively studied, only a few possible binding partners have been described so far: BDNF (Muller et al. 2000), heparan sulfate proteoglycans (Storms and Rutishauser 1998), AMPA receptors (Vaithianathan et al., 2004), NR2B subunit containing NMDA receptors (Hammond et al., 2006) and estradiol (Garcia-Segura et al., 1995). BDNF is a neurotrophic factor that shows a direct binding to PSA *in vitro* (Kanato et al., 2008) and promotes neuronal survival

and differentiation during development (Sofroniew et al., 2001). Heterophilic binding of PSA-NCAM to the heparan sulfate proteoglycans has a positive effect on cell adhesion (Storms and Rutishauser 1998). The interaction between PSA and AMPA receptors results in age-dependent potentiation of AMPA receptor which might modulate signalling via AMPA receptors in immature neurons and thereby affecting their development (Vaithianathan et al., 2004), while the interaction of PSA with NR2B subunit containing NMDA receptors prevents excitotoxicity (Hammond et al., 2006). The interaction of PSA with estradiol appears to participate in the estradiol-induced changes of glial cells with a polygonal shape to process-bearing cells (Garcia-Sequra et al., 1995).

In this thesis Histone H1 is identified as a direct interaction partner of PSA by Maren von der Ohe. . The results presented here provide evidence that an extranuclear pool of Histone H1 is present extracellularly at the cell surface of neural cells. Here it is showed that extracellular Histone H1 associates with PSA which is presented extracellularly. Previously it has been reported that immunohistochemistry revealed a staining of Histone H1 at neuronal cell bodies of cultured primary mouse cortical neurons, suggesting that Histone H1 was located at the cell surface of neurons (Bolton and Perry, 1997). However, an extracellular localization of Histone H1 was yet not proven for neuronal cells. Nevertheless, extracellular histones, among them Histone H1 have been detected at the surface of human monocytes (Holers and Kotzin, 1985), activated human peripheral blood lymphocytes (Watson et al., 1995) and cultured T-cells (Watson et al., 1995; Watson et al., 1999) as well as macrophage cell line where it interacts with thyroglobulin and may mediate thyroglobulin endocytosis (Brix et al., 1998). The trafficking of Histone proteins from the nucleus to the cytoplasm, cell surface or extracellular environment is not known yet, but since penetration of extracellular Histone through the plasma membrane and into the cell has been demonstrated (Hariton-Gazal et al., 2003) it may be possible that a similar pathway may exist for

the export of Histones. Extracellular Histones including H1 have been shown to bind to cell surface heparan sulfate proteoglycans (Watson et al., 1999) and lipopolysaccharide (LPS) (Hampton et al., 1988; Bolton and Perry, 1997) which up-regulate the expression of Histones on the cell surface of monocytes (Emlen et al., 1992). In addition, extracellular Histones, in particular Histone H1, have also been reported to exhibit antibacterial activity (Hirsch, 1958; Hiemstra et al., 1993) which is antagonized by acid polysaccharides like heparin. There are also indications that Histone H1 binds to amyloid precursor protein (Potempska et al., 1993) and amyloid-like motifs, such as β -amyloid and α -synuclein (Duce et al., 2006) and it was found associated with amyloid plaques (Duce et al.; 2006). It has also been discussed that it binds to the pathogenic scrapie form of the prion protein and it has been shown that Histone H1 is up-regulated in brains of mice showing clinical sign of scrapie and an increased immunostaining of Histone H1 was observed in region of pathology (Bolton et al., 1999). These observations suggest that Histone H1 might play a subtle role in the development of Alzheimer's disease and/or other neurodegenerative diseases. It is noteworthy to mention that prion protein as well as amyloid precursor protein binds to heparan sulfate proteoglycans which play a role in the pathogenesis of both diseases (van Horssen, 2003; Horonchik et al., 2005) and which bind to PSA-NCAM and Histone H1. Histone H1 has been localized on the plasma membrane or in the extracellular matrix of skeletal muscle cells and the level of extracellular Histone H1 increases during muscle differentiation (Henriquez et al., 2002). The extracellular pool of Histone H1 colocalizes with heparan sulfate proteoglycan perlecan in the extracellular matrix of myotube cultures and in regenerating skeletal muscle. In addition, Histone H1 was identified as endogenous extracellular ligand for muscle cell heparan sulfate proteoglycans which regulate skeletal muscle differentiation. Extracellular Histone H1 strongly stimulated myoblast proliferation via a heparan-sulfate-dependent mechanism, suggesting that extracellular Histone H1 in conjunction with heparan sulfate proteoglycans plays a functional role during skeletal muscle development

and regeneration. The role of extracellular Histone H1 in regulating cell proliferation and differentiation is also supported by its anti-proliferative effects on cancer cells (Vani et al., 2006). Interestingly, it has effects on estrogen receptor status of human breast cancer cells (Vani and Devi, 2005); suggesting that it together with PSA which is a putative binding partner of estradiol regulates estrogen-induced effects on proliferation.

VI.2 Improvement of motor function by Histone H1

This is the first report that provides functional evidence that application of Histone H1 has positive impact on peripheral nerve regeneration. Since Histone H1 can alter PSA induced cellular functions and PSA or PSA mimetics are known to promote functional recovery after femoral nerve injury (Mehnanna et al., 2009), possible similar effect of Histone H1 was evaluated on 3 months old mice. Lack of effect of PBS control (hence endogenous Histone H1) is one argument in favour of externally administered Histone H1 related specificity. Of the observed effects, the improved functional outcome of nerve repair is of greatest interest from a clinical point of view. The evidence for better recovery of function was obtained using an objective video-based analysis of three parameters directly related to the quadriceps muscle function that has proved to be reliable and sensitive (Irintchev et al., 2005; Eberhardt et al., 2006; Simova et al., 2006; Ahlborn et al., 2007). Therefore, better recovery of functional parameters after Histone H1 treatment, observed is convincing evidence for functional improvement related to the treatment.

Another issue is how a single intra-operative application of a protein can produce late-appearing and long-lasting effects. Although a fibrin coat is formed around a nerve-guide chamber after 24 to 48 hours preventing leakage of the guide's

contents (Hekimian et al., 1995) and a gel-forming matrix was used to immobilize Histone H1, its local availability is most likely limited to hours or at best days, because of degradation by peptidases originating from the damaged tissue and infiltrating proteolytically active immune cells. We favour the explanation that the Histone H1 causes priming of the injured femoral nerve, both at and around the lesion site, in the sense that early cellular and molecular responses to injury are modulated so that the subsequent regeneration process is favourably influenced over weeks. Considering our *in vitro* data on the enhanced proliferation and process elongation by Schwann cells, we propose that Histone H1 stimulates the early response of these cells to injury *in vivo*. The idea of priming the nerve at and around the lesion site is supported by previous observations of long-lasting positive effects after a single intra-operative application of a PSA mimicking peptide to the severed femoral nerve of adult mice (Mehanna et al., 2009). In that case, it was proposed that priming is achieved by activation of the RAGE (receptor for advanced glycation end-products) signalling pathway (Chou et al., 2004). Another example for strikingly long-lasting effects of a short-term post-operative treatment is brief low-frequency electrical stimulation (1 hour, 20 Hz) of the proximal nerve stump of the femoral nerve immediately after nerve transection and surgical repair. This treatment significantly shortens the period of asynchronous -and staggered over weeks- axonal regrowth after femoral nerve lesion in rats (Al Majed et al., 2000a; Brushart et al., 2002) and accelerated functional recovery after femoral nerve lesion in mice (Ahlborn et al., 2007). These beneficial effects are associated with an accelerated and enhanced up-regulation in expression of brain-derived neurotrophic factor (BDNF) and its tyrosine kinase B (TrkB) receptor in motoneurons which results from the depolarization of motoneuron cell bodies during the one-hour stimulation period (Al Majed et al., 2000b, 2004).

The diverse and, importantly, long-lasting effects of the Histone H1 treatment suggest its involvement of basic signalling mechanisms which are either PSA-

dependent or PSA-independent. PSA is associated with NCAM and act as a positive modulator of NCAM functions by inhibiting the cis-interactions of NCAM and making more NCAM available for trans-interactions for instance with heparan sulfate proteoglycans which promote axonal growth and synaptic plasticity. On the other hand, Histone H1 may bind to PSA-NCAM and trigger its diverse functions via NCAM-mediated signal transduction and/or it may bind to other binding partners such as heparan sulfate proteoglycans and trigger PSA- and NCAM-independent signal pathways. Interaction of Histone H1 with NCAM binding partners, such as heparan sulfate proteoglycans and prion protein may modulate the interaction with PSA and its binding partners like BDNF and further influence PSA-dependent signal transduction pathways. Since neurite outgrowth was promoted by Histone H1, it was assumed that the regeneration of injured nerve by Histone H1 is accompanied by an enhanced axon regrowth *in vivo*. This notion was confirmed by retro-labelling of motoneurons showing that survival of motoneurons, axon regrowth and precision of reinnervation was significantly enhanced, while myelination was not improved. These results are different from those obtained for a PSA-mimicking peptide (Mehanna et al., 2009), which improves myelination but has no effect on motoneuron survival and regrowth. This difference may indicate that Histone H1 and PSA effect different signal pathways. The diverse functions of Histone H1 in different tissues or cell types and its interaction with different binding partners may be an indication that it plays a central role in modulating, modifying, orchestrating or integrating various interactions and processes associated with cell survival, proliferation and regeneration in a PSA-dependent or -independent manner.

VI.3 Identification of MARCKS as a possible binding partner of PSA

Identification of potential binding partners of PSA using anti-idiotypic approach (von der Ohe, unpublished data) has provided the information about structural, but not charge dependent, interaction of PSA to other proteins. In the present study, the characterization of MARCKS and Histone H1 as putative binding partners of PSA were performed using different approaches in order to prove the interaction and possibly highlight the mechanisms of PSA-mediated functions in the nervous system. Initial distribution analysis of identified putative binding partners of PSA in membrane subfractions has demonstrated that MARCKS presents in Triton X-100 soluble membrane subfractions in fewer amounts compare to insoluble fraction and postsynaptic densities (PSD) whereas Histone H1 is presenting in insoluble subfractions and PSD [Tatiana Makhina, "Identification, characterization and functional analysis of novel protein binding partners of the cell recognition molecule L1 and the polysialylated neural cell adhesion molecule in mouse (*Mus musculus L.*, 1758) Hamburg, 2009]. PSD is an electron-dense structure in which neurotransmitter receptors and associated signalling molecules (for instance, protein kinase C) are tightly clustered (Nonaka et al., 2006). So far MARCKS is described as soluble proteins temporary associating with membrane and appeared to be a substrate for protein kinase C, the detection of MARCKS in those membrane structures is quit expectable. Although PSA was also detected in these membrane subfractions, no further confirmation for direct interaction between PSA-NCAM and MARCKS were obtained but interaction between PSA-NCAM and MARCKS was detected using co-immunoprecipitation experiment. Co-localization of MARCKS and PSA-NCAM along the length of hippocampal neurons was a promising indication for potential interaction between PSA-NCAM and MARCKS, but it seems to be either indirect or required further strong modification of biochemical protocols.

VI.4 Proposed working model indicating possible interaction between MARCKS and PSA

To conclude, we predict a model based on the results obtained and discussed in this study (Figure 25 and 26).

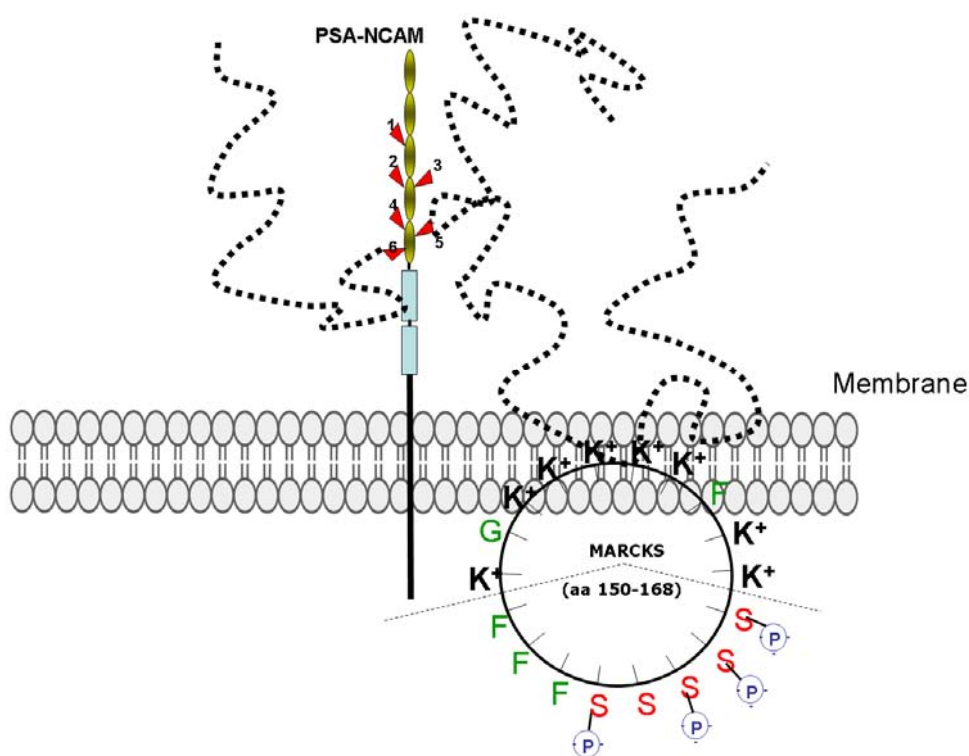


Figure 28. Helical wheel representation of effector domain (residues: 150-168) showing amphipathicity and proposed model showing MARCKS and PSA interaction in the membrane.

Helical wheel representations of the effector domain shows phenylalanine residues that contribute to the amphipathic structure (F), lysine residues that form the calmodulin and actin binding sites (^+K) and serine residues that are phosphorylated by PKC (^+K). The electrostatic interaction of the basic effector domain with acidic lipids in the plasma membrane promotes a charge dependent interaction with highly negatively charged polysialic acid that translocates into the membrane and changes the membrane properties.

We propose that PSA carrying a free carboxyl group on each unit can accept positively-charged amino groups from MARCKS. Furthermore, PSA is known to form extensive helical regions recognized by anti-PSA antibodies (Mühlenhoff M et al., 1998) and might provide additional interactions between MARCKS and PSA molecules holding them together. The helical models of PSA, proposed by Samuel et al., (2004) have several important features in common. Most significantly, in each model the negatively charged carboxylic acid groups face the interior of the helix with a repeat distance of 5-8 Å⁰ while the N-acetyl groups face the exterior of the helix. This means that for any of the models, over one turn of the helix, one end of the oligomer would present the negatively charged carboxylic acid groups to the binding site on the protein while the midpoint of the oligomer would present the relatively uncharged but protruding N-acetyl groups. When we tried to investigate colocalization of MARCKS and PSA on live and fixed hippocampal neurons, no specific MARCKS labelling was detected on live hippocampal neurons, which confirms the absence of MARCKS on cell surface. After fixation and permeabilisation of cell membrane the neurons were stained with α-PSA monoclonal antibodies as well as α-MARCKS polyclonal antibodies. In this case a significant amount of MARCKS partially co-localize with PSA along neurites. This indicates that these two molecules have chance to interact with each other. From this observation we speculate that *in vivo* interaction of both PSA and MARCKS is possible only when both the molecule meet each-other in the membrane.

VII. References

Acheson A, Sunshine JL, Rutishauser U (1991) NCAM PSA can regulate both cell-cell and cell-substrate interactions. *J Cell Biol* 114: 143-153.

Aderem AA, Albert KA, Keum MM, Wang JKT, Greengard P Cohn ZA (1988) Stimulus-dependent myristoylation of a major substrate for protein kinase C. *Nature* 332: 362-364.

Ahlborn P, Schachner M, Irintchev A (2007) One hour electrical stimulation accelerates functional recovery after femoral nerve repair. *Exp Neurol* 208: 137-144.

Albach C, Damoc E, Denzinger T, Schachner M, Przybylski M, Schmitz B (2004) Identification of N-glycosylation sites of the murine neural cell adhesion molecule NCAM by MALDI-TOF and MALDI-FTICR mass spectrometry. *Analytical and Bioanalytical Chemistry* 378: 1129-1135.

Albert KA, Nairn AC, Greengard P (1987) The 87-kDa protein, a major specific substrate for protein kinase C: purification from bovine brain and characterization. *Proc Natl Acad Sci U S A* 84: 7046-7050.

Alberts, Johnson A, Lewis J (2002b) Basic Genetic Mechanisms, in *Molecular Biology of The Cell*: 212.

Allen LA, Aderem A (1995) Protein kinase C regulates MARCKS cycling between the plasma membrane and lysosomes in fibroblasts. *EMBO J* 14: 1109-1121.

Al-Majed AA, Neumann CM, Brushart TM, Gordon T (2000a) Brief electrical stimulation promotes the speed and accuracy of motor axonal regeneration. *J Neurosci* 20: 2602-2608.

Angata K, Suzuki M, Fukuda M (1998) Differential and cooperative polysialylation of the neural cell adhesion molecule by two polysialyltransferases, PST and STX. *J*

Biol Chem 273: 28524-28532.

Angata K, Suzuki M, Fukuda M (2002) ST8Sia II and ST8Sia IV polysialyltransferases exhibit marked differences in utilizing various acceptors containing oligosialic acid and short PSA. The basis for cooperative polysialylation by two enzymes. J Biol Chem 277: 36808-36817.

Angata K, Suzuki M, McAuliffe J, Ding Y, Hindsgaul O, Fukuda M (2000) Differential biosynthesis of PSA on neural cell adhesion molecule (NCAM) and oligosaccharide acceptors by three distinct alpha 2,8-sialyltransferases, ST8Sia IV (PST), ST8Sia II (STX), and ST8Sia III. J Biol Chem 275: 18594-18601.

Appel F, Holm J, Conscience JF, Schachner M (1993) Several extracellular domains of the neural cell adhesion molecule L1 are involved in neurite outgrowth and cell body adhesion. J Neurosci 13: 4764-4775.

Arbuzova A, Schmitz AA, Vergères G (2002) Cross-talk unfolded: MARCKS proteins. Biochem J 362: 1-12.

Asahara T, Lin M, Kumazawa Y, Takeo K, Akamine T, Nishimura Y (1999) Long-term observation on the changes of somatotopy in the facial nucleus after nerve suture in the cat: morphological studies using retrograde labeling. Brain Res Bull 49: 195-202.

Ausrubel FM (1996) Current Protocols in Molecular Biology: Brooklyn, New York: Grene Publishing Associates, Inc.

Becker CG, Artola A, Gerardy SR, Becker T, Welzl H, Schachner M (1996) The PSA modification of the neural cell adhesion molecule is involved in spatial learning and hippocampal long-term potentiation. J Neurosci Res 45: 143-152.

Bhatnagar RS, Schall OF, Jackson-Machelski E, Sikorski JA, Devadas B, Gokel

GW, Gordon JI (1997) Titration calorimetric analysis of AcylCoA recognition by myristoylCoA: protein N-myristoyltransferase. *Biochemistry* 36: 6700-6708.

Bhatnagar RS, Gordon JI (1997) Understanding covalent modifications of proteins by lipids: where cell biology and biophysics mingle. *Trends Cell Biol* 7: 14-21.

Bliss JM, Garon CF, Silver RP (1996) PSA export in *Escherichia coli* K1: the role of KpsT, the ATP-binding component of an ABC transporter in chain translocation. *Glycobiology* 6: 445-452.

Bliss JM, Silver RP (1996) Coating the surface: a model for expression of capsular polysialic acid in *Escherichia coli* K1. *Mol Microbiol* 21: 221-231.

Bliss TV, Collingridge GL (1993) A synaptic model of memory: long-term potentiation in the hippocampus. *Nature* 361: 31-39.

Bolton SJ, Perry VH (1997) Histone H1; A neuronal protein that binds bacterial lipopolysaccharide. *J Neurocytol* 26: 823-831.

Bolton SJ, Russelakis-Carneiro M, Betmouni S, Perry VH (1999) Non-nuclear Histone H1 is up-regulated in neurons and astrocytes in prion and Alzheimer's diseases but not in acute neurodegeneration. *Neuropathol Appl Neurobiol* 25: 425-432.

Bonfanti L (2006) PSA-NCAM in mammalian structural plasticity and neurogenesis. *Prog Neurobiol* 80: 129-164.

Boulnois GJ, Roberts IS, Hodge R, Hardy KR, Jann KB, Timmis KN (1987) Analysis of the K1 capsule biosynthesis genes of *Escherichia coli*: Definition of three functional regions for capsule production. *Mol Gen Genet* 208: 242-246.

Brisson JR, Baumann H, Imberty A, Perez S, Jennings HJ (1992) Helical epitope of the group B meningococcal alpha (2,8)-linked sialic acid polysaccharide. *Biochemistry* 31: 4996-5004.

Brix K, Summa W, Lottspeich F, Herzog V (1998) Extracellularly occurring Histone H1 mediates the binding of thyroglobulin to the cell surface of mouse macrophages. *J Clin Invest* 102: 283-293.

Brümmendorf T, Rathjen FG (1995) Cell adhesion molecules 1: immunoglobulin super family. *Protein Profile* 2: 963-1108.

Brusés JL, Rutishauser U (2001) Roles, regulation, and mechanism of polysialic acid function during neural development. *Biochimie* 83: 635-643.

Brushart TM, Hoffman PN, Royall RM, Murinson BB, Witzel C, Gordon T (2002) Electrical stimulation promotes motoneuron regeneration without increasing its speed or conditioning the neuron. *J Neurosci* 22: 6631-6638.

Brushart TM (1988) Preferential reinnervation of motor nerves by regenerating motor axons. *J Neurosci* 8: 1026–1031.

Casey PJ (1995) Protein lipidation in cell signaling. *Science* 268: 221-225.

Chazal G, Durbec P, Jankovski A, Rougon G, Cremer H (2000) Consequences of Neural Cell Adhesion Molecule Deficiency on Cell Migration in the Rostral Migratory Stream of the Mouse. *J Neurosci* 20: 1446-1457.

Chen S, Mantei N, Dong L, Schachner M (1999) Prevention of neuronal cell death by neural cell adhesion molecule L1 and CHL1. *J Neurobiol* 38: 428–439.

Chothia C, Jones EY (1997) The molecular structure of cell adhesion molecules, *Annu Rev Biochem* 66: 823-862.

Chou DK, Zhang J, Smith FI, McCaffery P, Jungalwala FB (2004) Developmental expression of receptor for advanced glycation end products (RAGE), amphoterin and sulfoglucuronyl (HNK-1) carbohydrate in mouse cerebellum and their role in neurite outgrowth and cell migration. *J Neurochem* 90: 1389-1401.

Cole GJ, Loewy A, Glaser L (1986) Neuronal cell cell adhesion depends on interactions of N-CAM with heparin-like molecules. *Nature* 320: 445-447.

Damour D, Barreau M, Blanchard JC, Burgevin MC, Doble A, Herman F, Pantel G, James-Surcouf E, Vuilhorgne M, Mignani S, Poitout L, Le Merrer Y, Depezay JC (1996) Design, synthesis and binding affinities of novel non-peptide mimics of somatostatin/sandostatin. *Bioorg Med Chem Lett* 6: 1667-1672.

Datta AK, Paulson JC (1995) The sialyltransferase "sialylmotif" participates in binding the donor substrate CMP-NeuAc. *J Biol Chem* 270: 1497-1500.

de la Cruz RR, Pastor AM, Delgado-García JM (1994) Effects of target depletion on adult mammalian central neurons: morphological correlates. *Neuroscience* 58: 59–79.

Decker L, Avellana-Adalid V, Nait-Oumesmar B, Durbec P, Baron-Van Evercooren A (2000) Oligodendrocyte Precursor Migration and Differentiation: Combined Effects of PSA Residues, Growth Factors, and Substrates. *Mol Cell Neurosci* 16: 422-439.

Doherty P, Walsh FS (1992) Cell adhesion molecules, second messengers and axonal growth. *Curr Opin Neurobiol* 2: 595-601.

Doherty P, Walsh FS (1996) CAM-FGF Receptor Interactions. A model for axonal growth. *Mol Cell Neurosci* 8: 99-111.

Duce JA, Smith DP, Blake RE, Crouch PJ, Li QX, Masters CL, Trounce IA (2006)

Linker Histone H1 binds to disease associated amyloid-like fibrils. *J Mol Biol* 361: 493-505.

Eberhardt KA, Irintchev A, Al-Majed AA, Simova O, Brushart TM, Gordon T (2006) BDNF/TrkB signalling regulates HNK-1 carbohydrate expression in regenerating motor nerves and promotes functional recovery after peripheral nerve repair. *Exp Neuro* 198: 500-510.

Eckhardt M, Mühlenhoff M, Bethe A, Koopman J, Frosch M, Gerardy-Schahn R (1995) Molecular characterization of eukaryotic polysialyltransferase-1. *Nature* 373: 715-718.

Elangbam CS, Qualls CW Jr, Dahlgren RR (1997) Cell adhesion molecules-update. *Vet Pathol* 34: 61-73.

Emlen W, Holers VM, Arend WP, Kotzin B (1992) Regulation of nuclear antigen expression on the cell surface of human monocytes. *J Immunol* 148: 3042-3048.

Finne J, Finne U, Deagostini-Bazin H, Goridis C (1983) Occurrence of alpha 2-8 linked polysialosyl units in a neural cell adhesion molecule. *Biochem Biophys Res Commun* 112: 482-487.

Finne J, Makela H (1985) Cleavage of the polysialosyl units of brain glycoproteins by a bacteriophage endosialidase. *J Biol Chem* 260: 1265-1270.

Franz CK, Rutishauser U, Rafuse VF (2008) Intrinsic neuronal properties control selective targeting of regenerating motoneurons. *Brain* 131: 1492–1505.

Fujimoto I, Bruses JL, Rutishauser U (2001) Regulation of cell adhesion by PSA. Effects on cadherin, immunoglobulin cell adhesion molecule, and integrin function and independence from neural cell adhesion molecule binding or signaling activity. *J Biol Chem* 276: 31745-31751.

Gagneux P, Varki A (1999) Evolutionary considerations in relating oligosaccharide diversity to biological function. *Glycobiology* 9: 747-755.

Gaiarsa JL, Caillard O, Ben-Ari Y (2002) Long-term plasticity at GABAergic and glycinergic synapses: mechanisms and functional significance. *Trends Neurosci* 25: 564-570.

Galuska SP, Geyer R, Gerardy-Schahn R, Mühlenhoff M, Geyer H (2008) Enzyme-dependent variations in the polysialylation of the neural cell adhesion molecule (NCAM) *in vivo*. *J Biol Chem* 283: 17-28.

Galuska SP, Oltmann-Norden I, Geyer H, Weinhold B, Kuchelmeister K, Hildebrandt H, Gerardy-Schahn R, Geyer R, Mühlenhoff M (2006) PSA profiles of mice expressing variant allelic combinations of the polysialyltransferases ST8SialI and ST8SialIV. *J Biol Chem* 281: 31605–31615.

Garcia-Segura LM, Cañas B, Parducz A, Rougon G, Theodosis D, Naftolin F, Torres-Aleman I (1995) Estradiol promotion of changes in the morphology of astroglia growing in culture depends on the expression of polysialic acid of neural membranes. *Glia* 13: 209-216.

Gascon E, Vutskits L, Jenny B, Durbec P, Kiss JZ (2007) PSA-NCAM in postnatally generated immature neurons of the olfactory bulb: a crucial role in regulating p75 expression and cell survival. *Development* 134: 1181-1190.

Graff JM, Young TN, Johnson JD, Blackshear PJ (1989) Phosphorylation-regulated calmodulin binding to a prominent cellular substrate for protein kinase C. *J Biol Chem* 264: 21818-21823.

Griffiths AD, Williams SC, Hartley O, Tomlinson IM, Waterhouse P, Crosby WL, Kontermann RE, Jones PT, Low NM, Allison TJ (1994) Isolation of high affinity human antibodies directly from large synthetic repertoires. *EMBO J* 13: 3245-3260.

Hall AK, Rutishauser Urs (1985) Phylogeny of a neural cell adhesion molecule. *Developmental Biology* 110: 39-46.

Hammond MS, Sims C, Parameshwaran K, Suppiramaniam V, Schachner M, Dityatev A (2006) Neural cell adhesion molecule-associated polysialic acid inhibits NR2B-containing N-methyl-D-aspartate receptors and prevents glutamate-induced cell death. *J Biol Chem* 281: 34859-34869.

Hampton RY, Golenbock DT, Raetz CR (1988) Lipid A binding sites in membranes of macrophage tumor cells. *J Biol Chem* 263: 14802-14807.

Hariton-Gazal E, Rosenbluh J, Graessmann A, Gilon C, Loyter A (2003) Direct translocation of histone molecules across cell membranes. *J Cell Sci* 116: 4577-4586.

Hartwig JH, Thelen M, Rosen A, Janmey PA, Nairn AC, Aderem A (1992) MARCKS is an actin filament cross linking protein regulated by protein kinase C and calcium-calmodulin. *Nature* 356: 618-622.

Häyrinen J, Jennings H, Raff HV, Rougon G, Hanai N, Gerardy-Schahn R, Finne J (1995) Antibodies to PSA and its N-propyl derivative: binding properties and interaction with human embryonal brain glycopeptides. *J Infect Dis* 171: 1481-1490.

He HT, Barbet J, Chaix JC, Goridis C (1986) Phosphatidylinositol is involved in the membrane attachment of NCAM-120, the smallest component of the neural cell adhesion molecule. *EMBO J* 5: 2489-2494.

Hekimian KJ, Seckel BR, Bryan DJ, Wang KK, Chakalis DP, Bailey A (1995) Continuous alteration of the internal milieu of a nerve-guide chamber using an osmotic pump and internal exhaust system. *J Reconstr Microsurg* 11: 93-98.

Henriquez JP, Casar JC, Fuentealba L, Carey DJ, Brandan E (2002) Extracellular matrix Histone H1 binds to perlecan, is present in regenerating skeletal muscle and stimulates myoblast proliferation. *J Cell Sci* 115: 2041-2051.

Hiemstra PS, Eisenhauer PB, Harwig SS, van den Barselaar MT, van Furth R, Lehrer RI (1993) Antimicrobial proteins of murine macrophages. *Infect Immun* 61: 3038-3046.

Hildebrandt H, Mühlenhoff M, Gerardy-Schahn R (2008) Polysialylation of NCAM. *Neurochem Res.* 2008 May 7 [Epub ahead of print].

Hinkle CL, Diestel S, Lieberman J, Maness PF (2006) Metalloprotease-induced ectodomain shedding of neural cell adhesion molecule (NCAM). *J Neurobiol* 66: 1378-1395.

Hirsch JG (1958) Bactericidal action of histone. *J Exp Med* 108: 925-944.

Holers VM, Kotzin BL (1985) Human peripheral blood monocytes display surface antigens recognized by monoclonal antinuclear antibodies. *J Clin Invest* 76: 991-998.

Horonchik L, Tzaban S, Ben-Zaken O, Yedidia Y, Rouvinski A, Papy-Garcia D, Barritault D, Vlodaysky I, Taraboulos A (2005) Heparan sulfate is a cellular receptor for purified infectious prions. *J Biol Chem* 280: 17062-17067.

Hu H (2000) PSA Regulates Chain Formation by Migrating Olfactory Interneuron Precursors. *J Neurosci Res* 61: 480-492.

Inoue H, Nojima H, Okayama H (1990) High efficiency transformation of *Escherichia coli* with plasmids. *Gene* 96: 23-28.

Inoue S, Lin SL, Inoue Y (2000) Chemical analysis of the developmental pattern of polysialylation in chicken brain. Expression of only an extended form of polysialyl

chains during embryogenesis and the presence of disialyl residues in both embryonic and adult chicken brains. *J Biol Chem* 275: 29968-29979.

Irintchev A, Simova O, Eberhardt KA, Morellini F, Schachner M (2005) Impacts of lesion severity and tyrosine kinase receptor B deficiency on functional outcome of femoral nerve injury assessed by a novel single-frame motion analysis in mice. *Eur J Neurosci* 22: 802-808.

James WM, Agnew WS (1987) Multiple oligosaccharide chains in the voltage-sensitive Na channel from *Electrophorus electricus*: evidence for alpha-2, 8-linked PSA. *Biochem Biophys Res Commun* 148: 817-826.

Janas T, Janas T, Krajiński H (2000) Membrane transport of polysialic acid chains: modulation of transmembrane potential. *Eur Biophys J* 29:507-514.

Johnson CP, Fragneto G, Konovalov O, Dubosclard V, Legrand JF, Leckband DE (2005) Structural studies of the neural-cell-adhesion molecule by X-ray and neutron reflectivity. *Biochemistry* 44: 546-554.

Kabat EA, Liao J, Osserman EF, Gamian A, Michon F, Jennings HJ (1988) The epitope associated with the binding of the capsular polysaccharide of the group B meningococcus and of *Escherichia coli* K1 to a human monoclonal macroglobulin, IgMNOV. *J Exp Med* 168: 699-711.

Kadmon G, Kowitz A, Altevogt P, Schachner M (1990) Functional cooperation between the neural adhesion molecules L1 and N-CAM is carbohydrate dependent. *J Cell Biol* 110: 209-218.

Kalus I, Bormann U, Mzoughi M, Schachner M, Kleene R (2006) Proteolytic cleavage of the neural cell adhesion molecule by ADAM17/TACE is involved in neurite outgrowth. *J Neurochem* 98: 78-88.

Kanai Y (2003) The role of non-chromosomal histones in the host defense system.

Microbiol Immunol 47: 553-556.

Kanato Y, Kitajima K, Sato C (2008) Direct binding of PSA to a brain-derived neurotrophic factor depends on the degree of polymerization. Glycobiology 18: 1044–1053.

Karlsson R, Michaelsson A, Mattsson L (1991) Kinetic analysis of monoclonal antibody-antigen interactions with a new biosensor based analytical system. J Immunol Methods 145: 229–240.

Kelm S, Schauer R (1997) Sialic acids in molecular and cellular interactions. Int Rev Cytol 175: 137-240.

Kiss JZ, Rougon G (1997) Cell biology of PSA. Current Opinion in Neurobiology 7: 640-646.

Kitajima K, Inoue Y, Inoue S (1986) Polysialoglycoproteins of salmonidae fish eggs. Complete structure of 200-kDa polysialoglycoprotein from the unfertilized eggs of rainbow trout (*Salmo gairdneri*). J Biol Chem 261: 5262-5269.

Kitazume-Kawaguchi S, Kabata S, Arita M (2001) Differential biosynthesis of polysialic or disialic acid Structure by ST8Sia II and ST8Sia IV. J Biol Chem 276: 15696-156703.

Kleene R, Schachner M (2004) Glycans and neural cell interactions. Nat Rev Neurosci 5: 195-208.

Kojima N, Kono M, Yoshida Y, Tachida Y, Nakafuku M, Tsuji S (1996) Biosynthesis and expression of PSA on the neural cell adhesion molecule is predominantly directed by ST8Sia II/STX during in vitro neuronal differentiation. J Biol Chem 271: 22058-22062.

Kojima N, Yoshida Y, Tsuji S (1995) A developmentally regulated member of the sialyltransferase family (ST8Sia II, STX) is a PSA synthase. FEBS Lett 373: 119-122.

Kurosawa N, Yoshida Y, Kojima N, Tsuji S (1997) PSA synthase (ST8Sia II STX) mRNA expression in the developing mouse central nervous system. *J Neurochem* 69: 494–503.

Landmesser L, Dahm L, Schultz K, Rutishauser U (1988) Distinct roles for adhesion molecules during innervation of embryonic chick muscle. *Dev Biol* 130: 645-670.

Lennox RW, Cohen LH (1983) The Histone H1 complements of dividing and Non-dividing cells of the mouse. *J Biol Chem* 258: 262-268.

Liedtke S, Geyer H, Wuhrer M, Geyer R, Frank G, Gerardy-Schahn R, Zähringer U, Schachner M (2001) Characterization of N-glycans from mouse brain neural cell adhesion molecule. *Glycobiology* 11: 373-384.

Lin DM, Goodman CS (1994) Ectopic and increased expression of Fasciclin II alters motoneuron growth cone guidance. *Neuron* 13: 507-523.

Loers G, Chen S, Grumet M, Schachner M (2005) Signal transduction pathways implicated in neural recognition molecule L1 triggered neuroprotection and neuritogenesis. *J Neurochem*: 92:1463-1476.

Lois C, Alvarez-Buylla A (1994) Long-distance neuronal migration in the adult mammalian brain. *Science* 264: 1145-1148.

McLaughlin S, Aderem A (1995) The myristoyl-electrostatic switch: a modulator of reversible protein-membrane interactions. *Trends Biochem Sci* 20: 272-276.

Mehanna A, Mishra B, Kurschat N, Schulze C, Bian S, Loers G, Irintchev A, Schachner M (2009) PSA glycomimetics promote myelination and functional recovery after peripheral nerve injury in mice. *Brain* 132: 1449-1462.

Mendoza HL, Faye I (1999) Physiological aspects of the immunoglobulin

superfamily in invertebrates, *Dev Comp Immunol* 23: 359-374.

Michon F, Brisson J, Jennings H (1987) Conformational differences between linear alpha (2-8)-linked homosialooligosaccharides and the epitope of the group B meningococcal polysaccharide. *Biochemistry* 26: 8399–8405.

Milev P, Meyer-Puttlitz B, Margolis RK, Margolis RU (1995) Complex-type asparagine-linked oligosaccharides on phosphacan and protein-tyrosine phosphatase-zeta/beta mediate their binding to neural cell adhesion molecules and tenascin. *J Biol Chem* 270: 24650-24653.

Mühlenhoff M, Eckhardt M, Gerardy-Schahn R (1998) Polysialic acid: three dimensional structure, biosynthesis and function. *Curr Opin Struct Biol* 8: 558–564.

Mühlenhoff M, Eckhardt M, Bethe A, Frosch M, Gerardy-Schahn R (1996) Autocatalytic polysialylation of polysialyltransferase-1. *EMBO J* 15: 6943-6950.

Muller D, Djebbara-Hannas Z, Jourdain P, Vutskits L, Durbec P, Rougon G, Kiss JZ (2000) Brain-derived neurotrophic factor restores long-term potentiation in polysialic acid-neural cell adhesion molecule-deficient hippocampus. *Proc Natl Acad Sci U S A* 97: 4315-4320.

Muller D, Wang C, Skibo G, Toni G, Cremer H, Calaora V, Rougon G, Kiss JZ (1996) PSA-NCAM is required for activity-induced synaptic plasticity. *Neuron* 17: 413-422.

Murray D, Ben-Tal N, Honig B, McLaughlin S (1997) Electrostatic interaction of myristoylated proteins with membranes: simple physics, complicated biology. *Structure* 5: 985-989.

Nadja P, Aronoff B, Wu F, Schacher S (1994) Decrease in growth cone-neurite fasciculation by sensory or motor cells in vitro accompanies down regulation of

Aplysia cell adhesion molecules by neurotransmitters. *J Neurosci* 14: 1413-1421.

Nakata D, Troy FA (2005) Degree of polymerization (DP) of PSA (polySia) on neural cell adhesion molecules (N-CAMS): development and application of a new strategy to accurately determine the DP of polySia chains on N-CAMS. *J Biol Chem* 280: 38305-38316.

Nakayama J, Fukuda MN, Fredette B, Ranscht B, Fukuda M (1995) Expression cloning of a human polysialyltransferase that forms the polysialylated neural cell adhesion molecule present in embryonic brain. *Proc Natl Acad Sci U S A* 92: 7031-7035.

Nelson RW, Bates PA, Rutishauser U (1995) Protein determinants for specific polysialylation of the neural cell adhesion molecule. *J Biol Chem* 270: 17171-17179.

Nonaka M, Doi T, Fujiyoshi Y, Takemoto-Kimura S, Bito H (2006) Essential contribution of the ligand-binding beta B/beta C loop of PDZ1 and PDZ2 in the regulation of postsynaptic clustering, scaffolding, and localization of postsynaptic density-95. *J Neurosci* 26: 763-774.

Ohmori S, Sakai N, Shirai Y, Yamamoto H, Miyamoto E, Shimizu N, Saito N (2000) Importance of protein kinase C targeting for the phosphorylation of its substrate, myristoylated alanine-rich C-kinase substrate. *J Biol Chem* 275: 26449-26457.

Oltmann-Norden I, Galuska SP, Hildebrandt H (2008) Impact of the polysialyltransferases ST8SialII and ST8SialIV on PSA synthesis during postnatal mouse brain development. *J Biol Chem* 283: 1463-1471.

Ono K, Tomasiewicz H, Magnuson T, Rutishauser U (1994) N-CAM mutation inhibits tangential neuronal migration and is phenocopied by enzymatic removal of PSA. *Neuron* 13: 595-609.

Ouimet CC, Wang JK, Walaas SI, Albert KA, Greengard P (1990) Localization of

the MARCKS (87 kDa) protein, a major specific substrate for protein kinase C, in rat brain. *J Neurosci* 10: 1683-1698.

Pavelka MS Jr, Hayes SF, Silver RP (1994) Characterization of KpsT, the ATP-binding component of the ABC-transporter involved with the export of capsular polysialic acid in *Escherichia coli* K1. *J Biol Chem* 269: 20149–20158.

Pavelka MS Jr, Wright LF, Silver RP (1991) Identification of two genes, *kpsM* and *kpsT*, in region 3 of the polysialic acid gene cluster of *Escherichia coli* K1. *J Bacteriol* 173: 4603–4610.

Potempska A, Ramakrishna N, Wisniewski HM, Miller DL (1993) Interaction between the beta-amyloid peptide precursor and histones. *Arch Biochem Biophys* 304: 448-453.

Probstmeier R, Bilz A, Schneider-Schaulies J (1994) Expression of the neural cell adhesion molecule and PSA during early mouse embryogenesis. *J Neurosci Res* 37: 324–335.

Reichhart R, Zeppezauer M, Jornvall H (1985) Preparations of homeostatic thymus hormone consist predominantly of histones 2A and 2B and suggest additional histone functions. *Proc Natl Acad Sci U S A* 82: 4871-4875.

Retzler C, Göhring W, Rauch U (1996) Analysis of neurocan structures interacting with the neural cell adhesion molecule N-CAM. *J Biol Chem* 271: 27304-27310.

Rieger F, Grumet M, Edelman GM (1985) N-CAM at the vertebrate neuromuscular junction. *J Cell Biol* 101: 285-293.

Rosen A, Keenan KF, Thelen M, Nairn AC, Aderem A (1990) Activation of protein kinase C results in the displacement of its myristoylated, alanine-rich substrate from punctate structures in macrophage filopodia. *J Exp Med* 172: 1211-1215.

Roth J, Kempf A, Reuter G, Schauer R, Gehring WJ (1992) Occurrence of sialic acids in *Drosophila melanogaster*. *Science* 256: 673-675.

Rutishauser U (1998) PSA at the Cell Surface: Biophysics in Service of Cell Interactions and Tissue Plasticity. *J Cell Biochem* 70: 304–312.

Rutishauser U (2008) Polysialic acid in the plasticity of the developing and adult vertebrate nervous system. *Nat Rev Neurosci* 9: 26-35.

Rutishauser U, Acheson A, Hall AK, Mann DM, Sunshine J (1988) The neural cell adhesion molecule (NCAM) as a regulator of cell-cell interactions. *Science* 240: 53-57.

Rutishauser U, Hoffman S, and Edelman GM (1982) Binding properties of a cell adhesion molecule from neural tissue. *Proc Natl Acad Sci U S A* 79: 685-689.

Rutishauser U, Thiery JP, Brackenbury R, Sela BA, Edelman GM (1976) Mechanisms of adhesion among cells from neural tissues of the chick embryo. *Proc Natl Acad Sci U S A* 73: 577-581.

Sadoul R, Hirn M, Deagostini-Bazin H, Rougon G, Goridis C (1983) Adult and embryonic mouse neural cell adhesion molecules have different binding properties. *Nature* 304: 347-349.

Saiki RK, Gelfand DH, Stoffel S, Scharf SJ, Higuchi R, Horn GT, Mullis KB, Erlich HA (1988) Primer-directed enzymatic amplification of DNA with a thermostable DNA polymerase. *Science* 239: 487-491.

Sambrook J, Fritsch EF, Maniatis T (1989) Molecular cloning: A Laboratory Manual. (Cold Spring Harbor: Cold Spring Harbor Laboratory).

Samuel J, Bertozzi CR (2004) Chemical tools for the study of PSA. Trends in Glycoscience and Glycotechnologies 16: 305-318.

Scheidegger EP, Sternberg LR, Roth J, Lowe JB (1995) A human STX cDNA confers PSA expression in mammalian cells. J Biol Chem 270: 22685-22688.

Seki T, Arai Y (1993) Distribution and possible roles of the highly polysialylated neural cell adhesion molecule (NCAM-H) in the developing and adult central nervous system. Neurosci Res 17: 265-290.

Silver RP, Finn CW, Vann WF, Aaronson W, Schneerson R, Kretchmer PJ, Garon CF (1981) Molecular cloning of the K1 capsular polysaccharide genes of *E. coli*. Nature 289: 696–698.

Simova O, Irintchev A, Mehanna A, Liu J, Dihné M, Bächle D, Sewald N, Loers G, Schachner M (2006) Carbohydrate mimics promote functional recovery after peripheral nerve repair. Ann Neurol 60: 430-437.

Smith AN, Boulnois GJ, Roberts IS (1990) Molecular analysis of the *Escherichia coli* K5 *kps* locus: identification and characterization of an inner-membrane capsular polysaccharide transport system. Mol Microbiol 4:1863–1869.

Sofroniew MV, Howe CL, Mobley WC (2001) Nerve growth factor signaling, neuroprotection, and neural repair. Annu Rev Neurosci 24: 1217-1281.

Soroka V, Kolkova K, Kastrup JS, Diederichs K, Breed J, Kiselyov VV, Poulsen FM, Larsen IK, Welte W, Berezin V, Bock E, Kasper C (2003) Structure and interactions of NCAM Ig1-2-3 suggest a novel zipper mechanism for homophilic adhesion. Structure 11: 1291-1301.

Storms SD, Kim AC, Tran BH, Cole GJ, Murray BA (1996) NCAM-mediated adhesion of transfected cells to agrin. *Cell Adhes Commun* 3: 497-509.

Storms SD, Rutishauser UA (1998) Role for PSA in neural cell adhesion molecule heterophilic binding to proteoglycans. *J Biol Chem* 273: 27124–27129.

Swierczynski SL, Blackshear PJ (1995) Membrane association of the myristoylated alanine-rich C kinase substrate (MARCKS) protein. Mutational analysis provides evidence for complex interactions. *J Biol Chem* 270: 13436-13445.

Tang J, Landmesser L, Rutishauser U (1992) PSA influences specific path finding by avian motoneurons. *Neuron* 8: 1031-1044.

Taniguchi H (1999) Protein myristoylation in protein-lipid and protein-protein interactions. *Biophys Chem* 82: 129-137.

Troy FA, Vijay IK, McCloskey MA, Rohr TE (1982) Synthesis of capsular polymers containing PSA in *Escherichia coli* 07-K1. *Methods Enzymol* 83: 540-548.

Vaithianathan T, Matthias K, Bahr B, Schachner M, Suppiramaniam V, Dityatev A, Steinhäuser C (2004) Neural cell adhesion molecule-associated PSA potentiates AMPA receptor currents. *J Biol Chem* 279: 47975-47984.

van Horssen J, Wesseling P, van den Heuvel LP, de Waal RM, Verbeek MM (2003) Heparan sulphate proteoglycans in Alzheimer's disease and amyloid-related disorders. *Lancet Neurol* 2: 482-492.

Vani G, Devi CS (2005) Effect of Histone H1 on estrogen receptor status of human breast cancer MCF 7 cells. *Mol Cell Biochem* 272: 151-155.

Vani G, Vanisree AJ, Shyamaladevi CS (2006) Histone H1 inhibits the proliferation of MCF 7 and MDA MB 231 human breast cancer cells. *Cell Biol Int* 30: 326-331.

Varki A (1993) Biological roles of oligosaccharides: All of the theories are correct. *Glycobiology* 3: 97-130.

Vergères G, Manenti S, Weber T, Stürzinger C (1995) The myristoyl moiety of myristoylated alanine-rich C kinase substrate (MARCKS) and MARCKS-related protein is embedded in the membrane. *J Biol Chem* 270: 19879-19887.

Vogel U, Claus H, Heinze G, Frosch M (1997) Functional characterization of an isogenic meningococcal alpha-2, 3-sialyltransferase mutant: the role of lipooligosaccharide sialylation for serum resistance in serogroup B meningococci. *Med Microbiol Immunol* 186: 159-166.

von Der Ohe M, Wheeler SF, Wuhrer M, Harvey DJ, Liedtke S, Mühlenhoff M, Gerardy-Schahn R, Geyer H, Dwek RA, Geyer R, Wing DR, Schachner M (2002) Localization and characterization of PSA-containing N-linked glycans from bovine NCAM. *Glycobiology* 12: 47-63.

Walmod PS, Kolkova K, Berezin V, Bock E (2004) Zippers Make Signals: NCAM-mediated molecular interactions and signal transduction. *Neurochemical Research* 29: 2015–2035.

Walsh FS, Doherty P (1992) Second messengers underlying cell-contact-dependent axonal growth stimulated by transfected N-CAM, N-cadherin or L1. *Cold Spring Harb Symp Quant Biol* 57: 431-440.

Walsh FS, Parekh RB, Moore SE, Dickson G, Barton CH, Gower HJ, Dwek RA, Rademacher TW (1989) Tissue specific O-linked glycosylation of the neural cell adhesion molecule (N-CAM). *Development* 105: 803-811.

Waters HJ, Barnett G, O'Hanlon GM, Lowrie MB (1998) Motoneuron survival after

References

neonatal peroneal nerve injury in the rat-evidence for the sparing effect of reciprocal inhibition. *Exp Neurol* 152: 95-100.

Watson K, Edwards RJ, Shaunak S, Parmelee DC, Sarraf C, Gooderham NJ, Davies DS (1995) Extra-nuclear location of histones in activated human peripheral blood lymphocytes and cultured T-cells. *Biochem Pharmacol* 50: 299-309.

Watson K, Gooderham NJ, Davies DS, Edwards RJ (1999) Nucleosomes Bind to Cell Surface Proteoglycans. *J Biol Chem* 274: 21707-21713.

Widom J (1988) Chromatin structure: Linking structure to function with Histone H1. *Curr Biol* 8: 788-791.

Winter G, Griffiths AD, Hawkins RE, Hoogenboom HR (1994) Making antibodies by phage display technology. *Annu Rev Immunol* 12: 433-455.

Yang P, Major D, Rutishauser U (1994) Role of charge and hydration in effects of PSA on molecular interactions on and between cell membranes. *J Biol Chem* 269: 23039-23044.

Yang P, Yin X, Rutishauser U (1992) Intercellular space is affected by the polysialic acid content of NCAM. *J Cell Biol* 116: 1487-1496.

VIII. Appendix

VIII.1 Oligonucleotides

<u>Name</u>	<u>Sequence</u>
MARCKS 5' primer	AAAACATATGGGTGCCCAGTTCTCCAAG
MARCKS 3' primer	TTTCTCGAGCTCTGCCGCCTCCGCTGGGGGGGCTTCT

VIII.2 Abbreviations

x g	g-force
°C	Degree celcius
μ	Micro (10 ⁻⁶)
A	Adenosine
Ab	Antibody
AD	Alzheimer's disease
ADP	Adenosine biphosphate
Amp	Ampicillin
AMP	Adenosine monophosphate
AMPA	α-Amino-3-hydroxy-5-methylisoxazole-4- propionic acid receptor
ANT	Adenine nucleotide transporter
APP	Amyloid precursor protein
APS	Ammoniumpersulphate
ATP	Adenosine triphosphate
BDNF	Brain derived neurotrophic factor

BLAST	Basic Local Alignment Search Tool
BME	Basal Medium Eagle
bp	Base pairs
BrdU	Bromodeoxyuridine
BSA	Bovine serum albumin
C	Cytosine
Ca	Calcium
CAMs	Cell adhesion molecules
cDNA	Complementary deoxyribonucleic acid
CHAPS	3-[(3-Cholamidopropyl) dimethylammonio]-1 propanesulfonate
ChAT	Choline acetyltransferase
CL	Cross-linking
CM	Catalase-MBS
CMF-HBSS	Ca ²⁺ -Mg ²⁺ free Hank's buffered salt solution
CNS	Central nervous system
Da	Dalton
dH₂O	Distilled water
DMEM	Dulbecco's modified Eagle medium
DMSO	Dimethylsulfoxide
DNA	deoxyribonucleic acid
DNase	Deoxyribonuclease
DRG	Dorsal root ganglia
E. coli	Escherichia coli
EC	Extracellular
ECL	Enhanced chemiluminescence
ECM	Extracellular matrix
EDTA	Ethylene diamine tetra acetic acid
EGF	epidermal growth factor

EGTA	Ethylene glycol-bis(beta-aminoethyl ether)-N,N,N',N'-tetraacetic acid
ELISA	Enzyme-linked ImmunoSorbant Assay
EM	Electron Microscope
Endo H	Endoglycosidase H
endo-N	Endosialidase N
F	Phenylalanine
f.c.	Final concentration
FBA	Foot-base angle
FCS	Fetal calf serum
FGFR	Fibroblast growth factor receptor
Fn	Fibronectin
FNIII	Fibronectin III
g	Gram
G	Guanosine
GABA γ-	Aminobutyric acid
GAPDH	Glyceraldehyde-3-phosphate dehydrogenase
GFP	Green fluorescent protein
GPI	Glycosylphosphatidylinositol
GST	Glutathione S transferase
H	Histidine
HBSS	Hank's buffered sodium chloride solution
HEPES	2-(4-(2-Hydroxyethyl)-piperzino)-ethansulfonic acid
HNK-1	Human natural killer cell glycan
HRP	Horseradish peroxidase
HS	Horse serum
HTA	Heels-tail angle
IC	immunocytochemistry

ICD	Intracellular domain
Ig	Immunoglobulin
IgCAM	Immunoglobulin cell adhesion molecule
IgG	Immunoglobulin subclass G
IP	immunoprecipitation
IPTG	Isopropyl- β -D-thiogalactoside
kb	Kilo base pairs
l	Liter
LB	Luria Bertani
LTP	Long term potentiation
m	Milli (10^{-3})
MARCKS	Myristoylated alanine-rich C kinase substrate
MEM	Minimal essential medium
Mg	Magnesium
Mn	Manganese
mRNA	Messenger ribonucleic acid
n	Nano (10^9), number
NaAc	Sodium acetate
NAD	Nicotinamine adenine dinucleotide
NAP-22	neuronal tissue-enriched acidic protein
NCAM	Neural Cell Adhesion Molecule
NMDA	N-methyl-D-aspartate
NP-1	Neuropillin-1
OD	Optical density
OD_x	Optical density at x
OPD	O-phenylenediamine dihydrochloride
p	Statistical significance
p pico	(10^{-12})

P	Proline
PBS	Phosphate buffered saline
PCR	Polymerase chain reaction
PEG/NaCl	Polyethylene glycol/sodium chloride
PFA	Paraformaldehyde
PKC	Protein kinase C
PLL	Poly-L-lysine
PLR	Protraction length ratio
PMR	Preferential motor reinnervation
PMSF	Phenyl methyl sulfonyl fluoride
PSA	Polysialic Acid
PSD	Postsynaptic densities
RER	Rough endoplasmic reticulum
RNA	Ribonucleic acid
RNase	Ribonuclease
rpm	Rotations per minute
RT	Room temperature
scFv	Single chain variable fragment
SDS-PAGE	Sodium dodecyl sulphate poly acrylamide gel electrophoresis
Ser	Serine
ssDNA	Single-stranded DNA
syn	Synaptosome
T	Thymine
TE	Tris EDTA
TEMED	N,N,N',N'-tetraethylenamine
Tet	Tetracycline
Thr	Threonine
Thy-1	Thymus cell antigen

TM	Trade Mark
Tris	tris (-hydroxymethyl)-aminomethane
U	Unit (enzymatic)
V	Volts
V/v	Volume per volume
W	Tryptophan
W/v	Weight per volume
WB	Western blot
X-gal	5-bromo-4-chloro-3-indolyl- beta-D-galactopyranoside
Y	Tyrosine
ZMNH	Zentrum für Molekulare Neurobiologie Hamburg
α	anti

IX. Publications

The present thesis is mainly based on the following articles.

1. Mehanna A, **Mishra B**, Kurschat N, Schulze C, Bian S, Loers G, Irintchev A, Schachner M (2009). PSA glycomimetics promote myelination and functional recovery after peripheral nerve injury in mice. *Brain* 132: 1449-1462.
2. **Mishra B**, Von Der Ohe M, Schulze C, Bian S, Makhina T, Loers G, Kleene R and Schachner M. Functional role of the interaction between PSA and extracellular Histone H1. Submitted.

X.Acknowledgements

This study has been performed in the Institute of Biosynthesis of Neuronal Structures of the Center for Molecular Neurobiology (ZMNH) at the University of Hamburg. With great pleasure I want to acknowledge many people for their contribution to my PhD thesis and experience.

First and foremost I would like to extend an enormous thanks to Prof. Dr. Melitta Schachner, for giving me an opportunity to work in her esteemed Laboratory with an international working atmosphere and providing facilities for scientific investigations. Her fruitful discussions, support and guidance throughout these years have helped to develop my knowledge and skill in the field of molecular neurosciences. I appreciate her keen interest in my personal development with her suggestions on being a good speaker. I am highly thankful and glad to have been a part of her lab for my PhD. She has always inspired me to achieve excellence in my work area. Her valuable suggestions and inputs have made my PhD thesis and my research experience more meaningful.

I cannot forget to extend my heartiest acknowledgement to Dr. Gabriele Loers and Dr. Ralf Kleene for introducing me to this interesting project, for their excellent supervision, the inspiring and fruitful discussions and ideas and for their endless support during these years. The suggestions and the valuable time that they have rendered for my seminars and discussions were of immense help. It would be very difficult for me to complete my PhD thesis without the sincere efforts and care taken by Drs. Gabriele Loers and Ralf Kleene.

I would like to thank our collaborator Dr. Christian Schulze for performing the BIACORE experiments. I am grateful to Dr. Iris Oezen, Dr. Nuray Akyüz and Peggy

Acknowledgements

Putthoff for helping me a lot with cloning experiments. Special thanks to Dr. Ali Mehanna for sharing his valuable time and suggestions for *in vivo* experiments. Same time I would like to thank Nicole Karl and Dr. Meifang Xiao for their valuable suggestions from time to time during my PhD project. I am also thankful to Achim Dahmann, Joseph Thorairajoo, Fritz Kutschera and Torsten Renz for their technical assistance. I sincerely thank Ellen Bryssnick, our librarian for her help in providing even the rarest literature. Thanks to all the administrative staff, who have always helped me with smiling face.

Last but never the least my heart always thanks my parents for what I am today. Their love, care and selfless attitude is valuable to me. My father and mother had been a constant support to me while coming to a far off land, to lead my life independently. I feel special when I thank my dearest wife Gunjan for being with me all the time when I needed a support, for the encouragement and the strength she has given me. Her idea of perfectionism, obedience, sincerity and moral in life amazes me all the time. Lastly I cannot miss to thank my parents in law for giving me such a wonderful wife and for the love and care they have rendered.